

CONTENTS

CHAPTER 4

THE MAPS

4.1 THE LARGE SCALE FEATURES	4.1
Some interesting features towards the Galactic centre direction	4.4
Some spurious features	4.4
4.2 NOISE IN THE MAPS	4.6
Dynamic range of the maps	4.9
REFERENCES	4.11

Chapter 4

THE MAPS

This chapter contains the results of the survey in the form of contour maps in the equatorial (Right Ascension and Declination) coordinate system. Since an all-sky survey with similar resolution already exists at 408 MHz (Haslam et al. 1982) we felt that it would be useful to give our maps in the same format, size and 1950 coordinate system as the 408 MHz maps. We have used the NOD2 system to display our data in the form of contour maps. However, it must be borne in mind that the present 34.5 MHz survey has a resolution of $21' \times 34' \text{sec}(\delta - 14^\circ.1)$ whereas the 408 MHz survey has a resolution of $51' \times 5'$. The NOD2 plot library has a provision for indicating absorption and emission regions unambiguously. Arrows on the contours pointing clockwise indicate absorption and those which are counter-clockwise indicate emission (right hand cork screw notation). Wherever contours are labelled by numbers we have not shown the arrows. But the labels are also written in the same sense as the arrows. An example is given below :



Ambiguities regarding numbers like 6 or 9 can be solved by looking at the adjacent contours.

4.1 THE LARGE SCALE FEATURES

An important aspect of this survey is that it includes short

spacings all the way down to zero. This has enabled us to **map** the brightness temperature at all angular scales. Before proceeding to give the detailed maps at the full resolution we would like to present a low resolution map of the entire region of the sky that is not aliased (all the **24** hours of **R.A.** in the dec. range of -36° to $+64^\circ$). This will give an overall impression of the sky at **34.5** MHz. Figure **4.1** shows such a map which has been convolved to a resolution of 2° . The numbers on the contours are in units of **5722** K (full beam brightness temperature) above absolute zero. The absolute levels of the contours are accurate to within **5 %** - the accuracy to which the flux of Cygnus A, our calibrator, is known (Baars et al. **1977**). The steps in the contour level are as follows:

1 to 5	every 0.25 unit, but labelled every 1 unit
5 to 10	every 0.5 unit, but labelled every 2 units
10 to 20	every 1.0 unit, but labelled every 4 units
20 to 32	every 1.5 unit, but labelled every 6 units.

For the purpose of comparison we give a map of the sky at **408** MHz also convolved to 2° (Fig. **4.2**). In this figure the labels on the contours are in units of **10** K. The steps in the contour level are as described above. Both figures **4.1** and **4.2** were prepared using the **NOD2** library.

Some of the large scale features that have been identified earlier (Large et al. **1962**; Quigley and **Haslam 1965**; Berkhuijsen et al. **1971**; Berkhuijsen **1971** and Milogradov-Turin and **Smith 1973**) and which can be seen clearly in the 408 MHz map (Fig. **4.2**) are listed in Table **4.1**. These include the North Polar Spur and

Table 4.1 Some large scale features that can be seen on both the 34.5 MHz 408 MHz maps and their temperature spectral indices (β) where (temperature \propto frequency ^{β}).

	position (α, δ) (hour, deg.)	Spectral index between 34.5 MHz and 408 MHz
Loop II (Cetus arc)	2.5, +30 to 21 , -5	Varies from -2.6 to -2.8 as one moves from 2.5 ^h , +30 ^o to 21 ^h , -5 ^o
Loop III	3 , +45	-2.55
Loop IV	5 , +15	-2.55
Loop III	5 , +60 8 , +15	-2.5 ; more pronounced at 5 ^h , +50 ^o not seen clearly
Loop I (North polar spur)	17 , +10	Base of the spur is at more like 18 ^h , 0 ^o . Spectral index varies from -2.7 at the base to -2.4 at the tip (13 ^h , +15 ^o)
Loop III	19 , +55	not seen clearly
Loop V	22 , +20	-2.7
Loop III	22.5, +40	-2.7

the Cetus Arc. A comparison between figures 4.1 and 4.2 shows that all but one of the well known features are clearly seen in the 34.5 MHz map. The exception is the feature at 8^{h} , $+15^{\circ}$. Table 4.1 also gives the temperature spectral indices, β (temperature \propto frequency $^{\beta}$), of these features between 34.5 MHz and 408 MHz. It is conceivable that the spur at 8^{h} , $+15^{\circ}$ does not stand out against the background at 34.5 MHz because it has a somewhat flatter spectral index than the other spurs.

As mentioned earlier the 38 MHz survey of Milogradov-Turin and Smith (1973) had a declination coverage very similar to ours (-25° to $+75^{\circ}$). Since this survey was done with a single dish telescope it would be very useful to compare their maps with ours obtained with a synthesis telescope. With this in mind, we convolved our data to a resolution of 8^{a} (comparable to that of the Milogradov-Turin and Smith (1973) survey). Although we have not included these maps in this thesis we wish to point out that there was good agreement between them - both qualitative as well as quantitative. It might be mentioned that all the temperatures quoted on the Jodrell Bank maps were consistently lower than our value by about 16%. Since the temperatures quoted by Milogradov-Turin and Smith were based on a calibration against a noise source switched in at the antenna output (as opposed to calibrating against the absolute flux density of, say, Cygnus A) it is likely that the discrepancy in the temperature scales is due to the aperture efficiency of the Jodrell Mark I telescope.

4.1.1 Some interesting features towards the Galactic centre direction

We wish to draw attention to the following three features:

The $l = 0^\circ$ feature: An arc starting at $17^{\text{h}} 20^{\text{m}}, -25^\circ$ and extending upto $16^{\text{h}}, -22^\circ$ can be clearly seen in emission on the 34.5 MHz maps. This feature can also be seen clearly on the 408 MHz map. We estimate the average temperature spectral index of this arc to be -2.45 . Recently Sofue et al. (1988) have suggested that this may be a jet emanating from the Galactic centre. They estimate the spectral index to be -2.6 between 408 MHz and 2.3 GHz. It is not yet clear whether one should attribute significance to the different spectral index derived by us.

The $l = 355^\circ$ feature: This structure starting at $16^{\text{h}} 40^{\text{m}}, -25^\circ$ and going towards 16^{h} and -30° is not as pronounced in the 408 MHz map as at 34.5 MHz. However, the estimated average spectral index is -2.45 .

The $l = 345^\circ$ feature: This ridge between $15^{\text{h}} 40^{\text{m}}, -25^\circ$ and $15^{\text{h}}, -30^\circ$ is again not seen as clearly in the 408 MHz map. Its spectral index is again -2.45 .

Without further study it is difficult to tell whether these features are related to one another or not.

4.1.2 Some spurious features

The above inter-comparisons between the various maps gives us some confidence in interpreting the large scale features seen on our maps. However, there are some features which we believe are spurious and wish to draw attention to them.

The blobs of extended emission centered around $\alpha = 17^{\text{h}} 40^{\text{m}}$, $\delta = +42^{\circ}$ and at $\alpha = 17^{\text{h}}$, $\delta = +30^{\circ}$, as well as the adjacent region of lower intensity ($\alpha = 17^{\text{h}} 40^{\text{m}}$, $\delta = +60^{\circ}$) are unlikely to be of astronomical origin. For one thing they are not present in the 38 MHz map made with a **single** dish (Milogradov-Turin and Smith 1973). Further, they are aligned in R.A. with the brightest portion of the Galactic plane. These regions are $\approx 10^{\circ}$ in extent and have an average flux of 25 Jy.

Another feature we wish to draw attention to is the ridge of emission at -15° declination which extends from 20^{h} to 5^{h} .

What could these spurious **features** be due to ?

From the geometry of these features and the fact that they repeat at the same **sidereal** time one can conclude that they are not due to any interference even from a satellite.

Since they are also present in the raw maps they could not be artefacts introduced in the **CLEANing** procedure.

As mentioned above the common aspect of all these features is their large angular size. This immediately forces one to seek explanation in terms of the measured visibilities in the short baselines. It may be recalled from the discussions in Chapter 3 that we have not removed the offsets, if any, present in the short spacing (**<50 m**) visibilities since it was not possible to separate the contribution of the sky background from the possible offsets in these baselines. The ridge of emission at -15° declination running parallel to R.A. may be due to this. However, it is unlikely that the other features are due to this. They may be due to the peculiarities in the **illumination** pattern

of the short spacing S-array elements which may also be a function of the zenith angle. Interaction between the short spacing S array elements and the EW antenna could lead to such effects. This has been noted previously by Jones and **Finlay** (1974) in their survey at **29.9** MHz from Fleurs. If such peculiarities are indeed present, then, given an intense broad emission region near the Galactic centre one would expect to see its '**sidelobes**'. An attempt was made to correct for this by using several point sources at different zenith angles (such as Cyg A, Cas A, Tau A, Vir A and Hyd A) but without success. Since there is no strong source with a declination similar to the Galactic centre region, it is not possible to test this hypothesis. Nevertheless, at the moment we believe this to be the most plausible explanation. It should be pointed out that the spurious features under discussion are at the level of $\approx 5\%$ of the intensity of the Galactic centre region. Hence, if the above explanation is the right one then one does not expect to see similar features elsewhere since there are no extended bright emissions comparable to the Galactic centre anywhere else in the sky.

4.2 NOISE IN THE MAPS

We have given in this section the full resolution maps at 34.5 MHz obtained from our survey. The numbers on the contours are in units of **5722** K (full beam brightness temperature). The steps in the contour levels are as follows:

- 1 to **5** every 0.5 unit, but labelled every 1 unit
- 5** to 10 every 1 unit, but labelled every 2 unit

10 to 20 every 2 unit, but labelled every 4 unit
 20 to 32 every 3 unit, but labelled every 6 unit
 32 to Max. every 4 unit, but labelled every 8 unit.

The convention for indicating emission and absorption regions are as described before in this Chapter.

We wish to discuss here the noise in these maps. There are two factors which are expected to contribute to the random fluctuations (over the size of the beam) in the map : system noise and confusion. The system noise at Gauribidanur is almost entirely due to the sky noise and is expected to be ≈ 1.6 Jy for an antenna temperature of 10^4 K (Chapter 2)

The confusion level of a telescope refers to that value of the flux at which statistically there is typically one source within the beam of the telescope. So, wherever the telescope is pointed, if it is confusion limited, it will record fluctuations of the order of the confusion level. Even though the system noise might be much smaller, the minimum detectable flux for a point source will be decided by the confusion. One source per main beam of the GEETEE implies 4.3×10^3 sources per steradian. The confusion limit can be estimated from the $\log(N)$ vs. $\log(S)$ plot. Since such a plot is not available at 34.5 MHz, we have used the $\log(N)$ vs. $\log(S)$ plot at 408 MHz (Shaver and Pierre 1988), and assumed a spectral index of -0.8, to estimate the confusion limit at 34.5 MHz. This turns out to be 3.2 Jy. Since this is almost twice the system noise, it follows that our maps are confusion limited (at least in those regions where the antenna temperature is $\lesssim 10^4$ K),

It is possible to actually obtain the system noise and the confusion limit from the maps themselves. Take the raw map of the given region of the sky. If it is convolved with a **sinc** function of resolution corresponding to the antenna, then all spatial variations over scales smaller than the resolution will be smoothed. A subtraction of the convolved map from the raw map leaves contribution only due to the system noise.

To estimate the confusion, we can find the difference between every point on the map and the average value of the map one resolution away. The average value of this difference over the region of interest will then give us an estimate which includes both the confusion and system noise. Since the two sources of noise are uncorrelated we can write $\sigma^2 = \sigma_{sys}^2 + \sigma_{conf}^2$ (where σ is the **r.m.s.** fluctuation on the **map**, σ_{sys} the contribution due to the system and σ_{conf} is the contribution due to confusion). Using σ_{sys} obtained from the difference map (above paragraph) one can now estimate σ_{conf} . An analysis of this kind was done on a cold region and a hot region of the sky. The region of sky in the range of $12^h 30^m$ to $13^h 30^m$ of RA and -36° to $+64^\circ$ declination was divided into regions of $5^\circ \times 5^\circ$ size and in each block σ_{sys} and σ were determined. The average value of $\sigma_{sys} = 1.4$ Jy and $\sigma = 3.9$ Jy. This gives $\sigma_{conf} = 3.6$ Jy. A similar analysis done on $17^h 30^m$ to $18^h 30^m$ and $-3d$ to $+64^\circ$ gave values of $\sigma_{sys} = 3$ Jy and $\sigma = 4.8$ Jy implying $\sigma_{conf} = 3.7$ Jy. These numbers appear very reasonable. The increase of system noise from 1.4 Jy in the colder region to 3 Jy in the hotter region is to be expected as the antenna temperatures of both the EW and the S array rows increase by a factor of 2 as one goes from the

colder region to the hotter region (the system noise will increase in proportion to the system temperature, T_{sys} , provided all other parameters are the same. In a correlation telescope, $T_{\text{sys}} = \sqrt{T_{\text{sys}1} T_{\text{sys}2}}$ where the subscripts 1 and 2 refer to the two telescopes whose outputs are multiplied - in our case it is the EW antenna and any of the S array rows). As far as the variation of the total noise on the map is concerned it is very small - varying from 4 Jy in colder regions to 4.8 Jy towards hotter regions.

4.2.1 Dynamic range of the maps

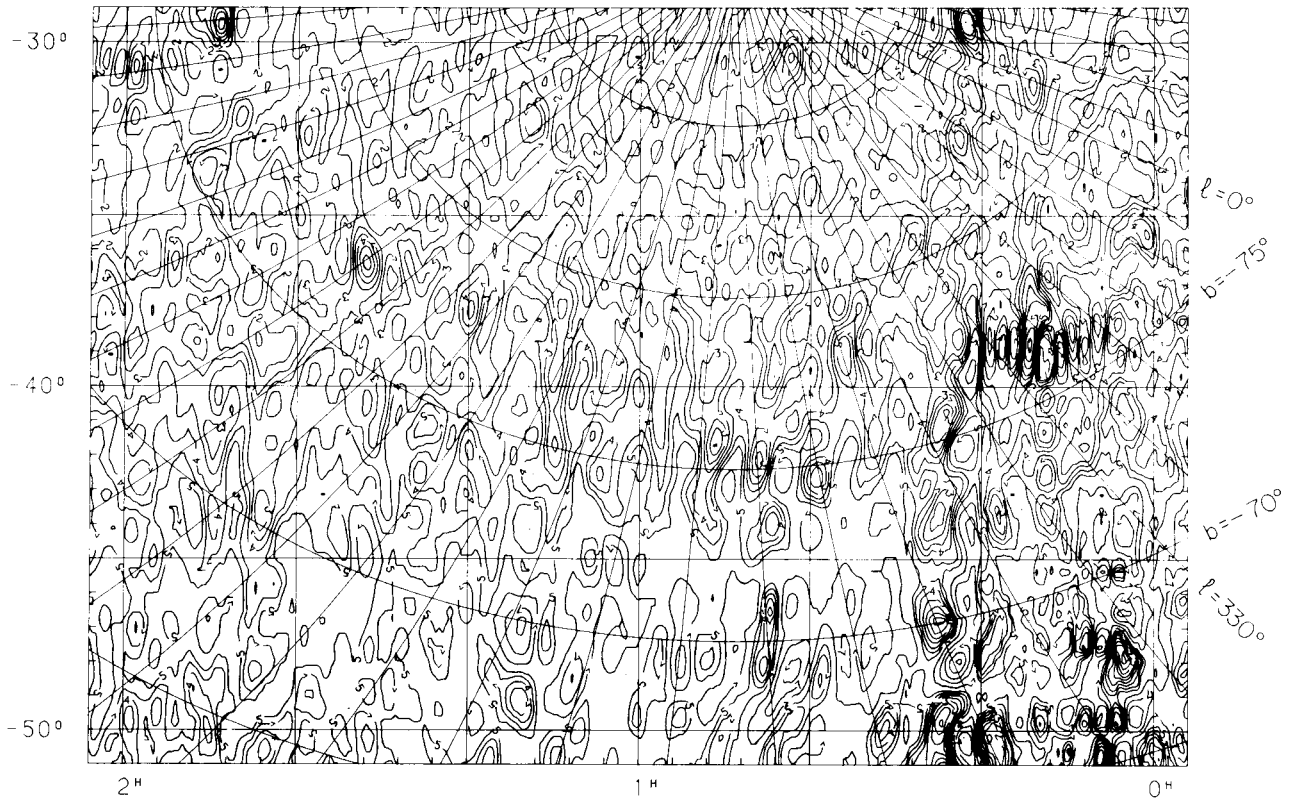
The dynamic range is the ratio of the fluxes of the weakest and the strongest source in a given region. Clearly, this will depend upon how close or far away one is from a strong source. In addition, in the present case it also depends upon the 'direction'. In the R.A. and **Dec.** directions, for example, the residual **sidelobe** levels of a point source are 0.2 to 0.5 % of the peak value. This implies a dynamic range of 16 to 20 dB in these directions. The 'diagonal' directions are much cleaner. Except around Cyg A and Cas A, the noise in the diagonal direction is essentially the noise inherent to the map and is not relevant to the discussion of the dynamic range of the map.

Since we have chosen Cygnus A to generate the Point Spread Function, the region around Cygnus A naturally has the **maximum** apparent dynamic range and in the cleaned map it is ≈ 27 dB.

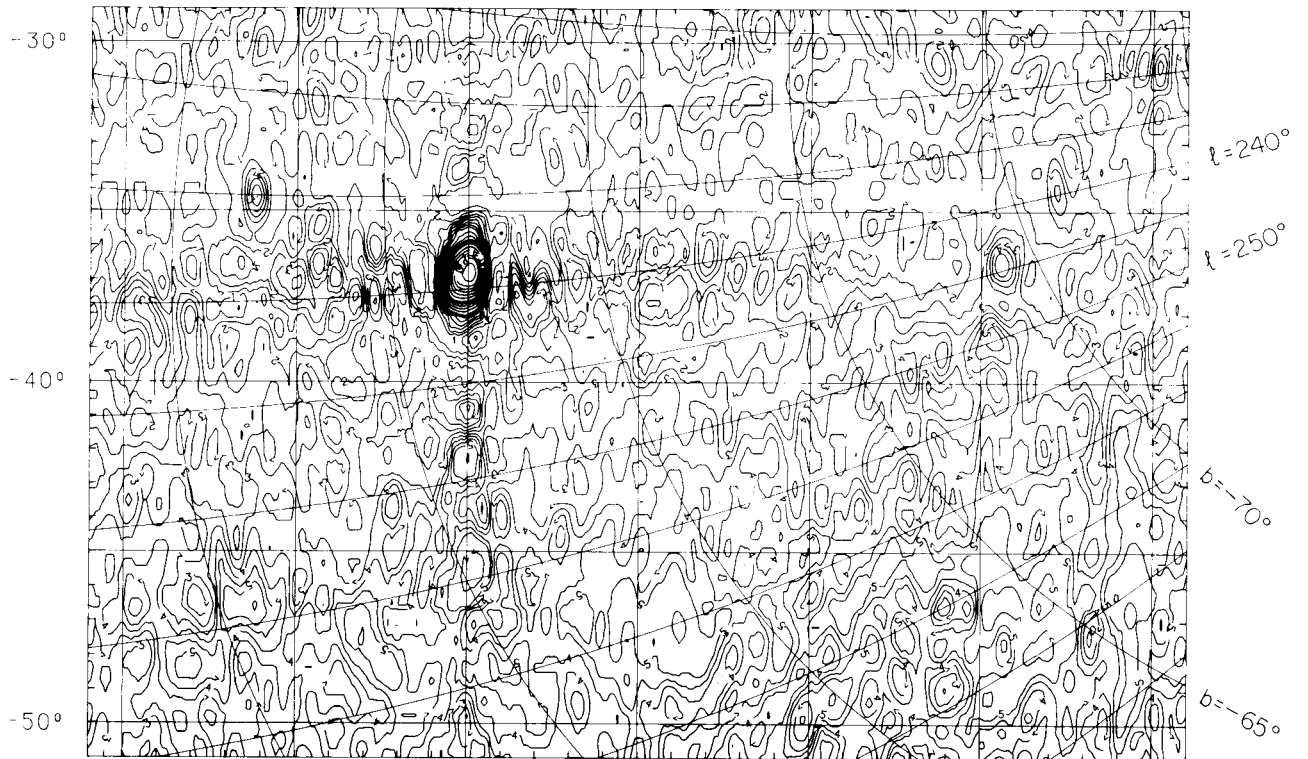
Due to the problems mentioned in Chapter 3, **CLEANing** the region around Cas A posed problems and could not be cleaned down to the level one would have liked (5σ). Consequently, the

dynamic range around Cas A is not as good as around Cyg A. The kind of dynamic range obtained around Cyg A is present here only beyond 20 degrees from the source in declination and beyond ≈ 30 minutes in RA.

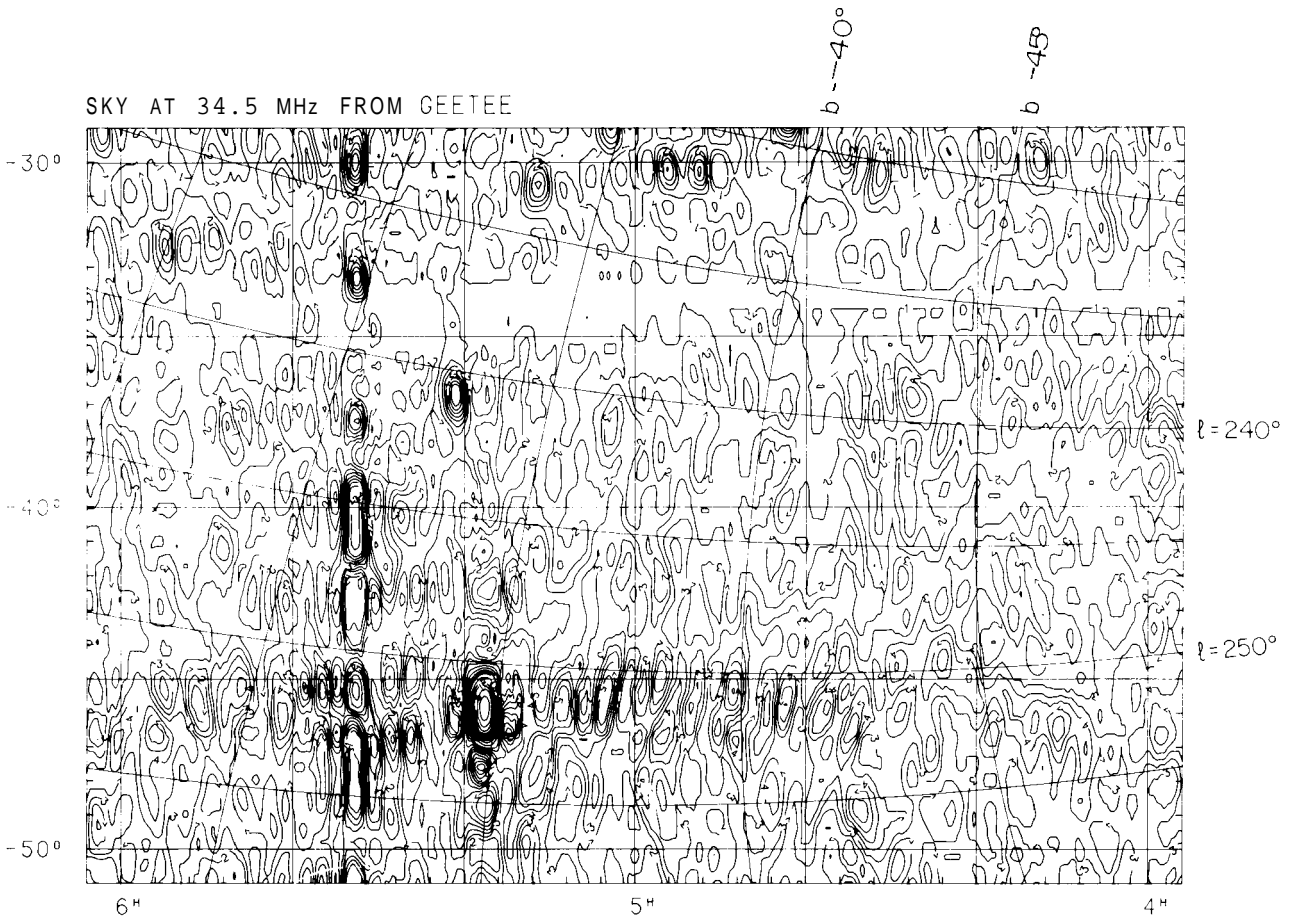
SKY AT 34.5 MHz FROM GEETEE



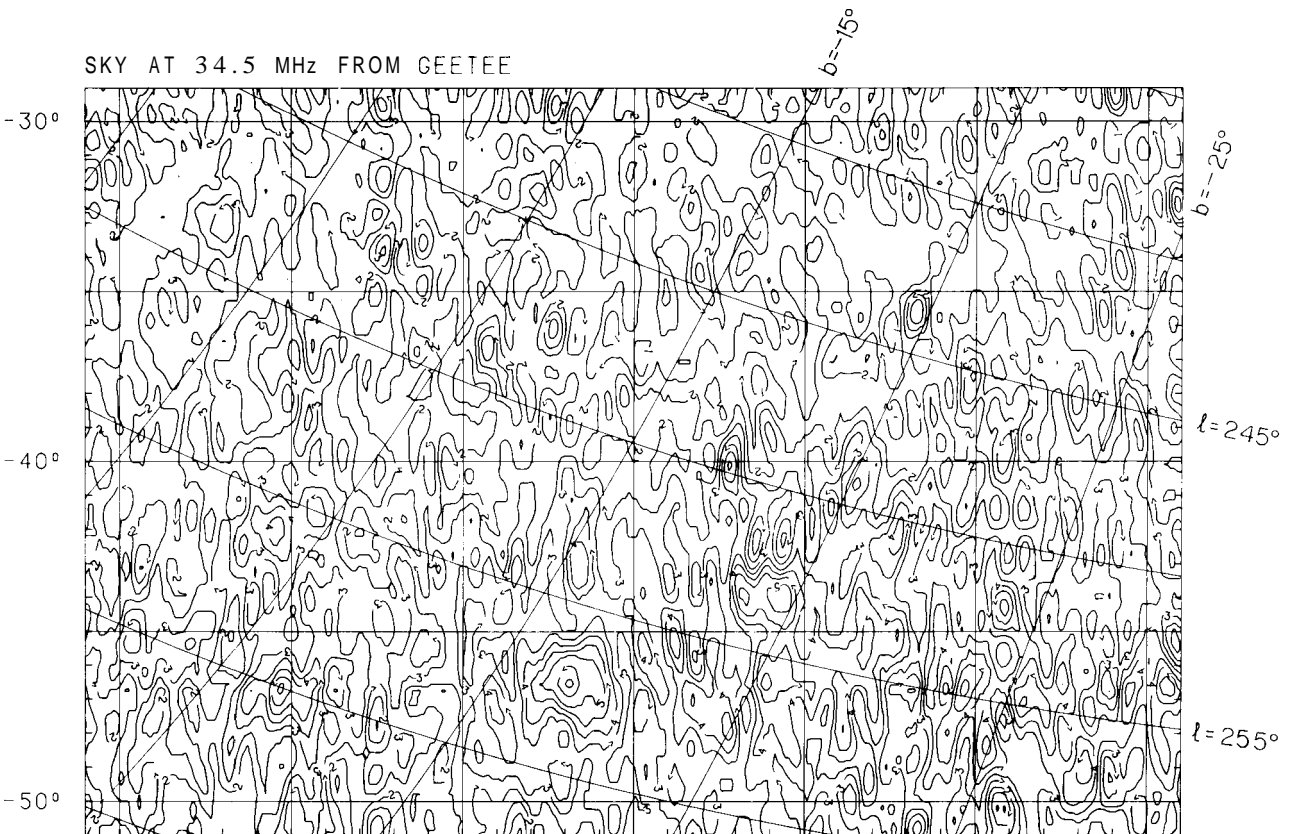
SKY AT 34.5 MHz FROM GEETEE



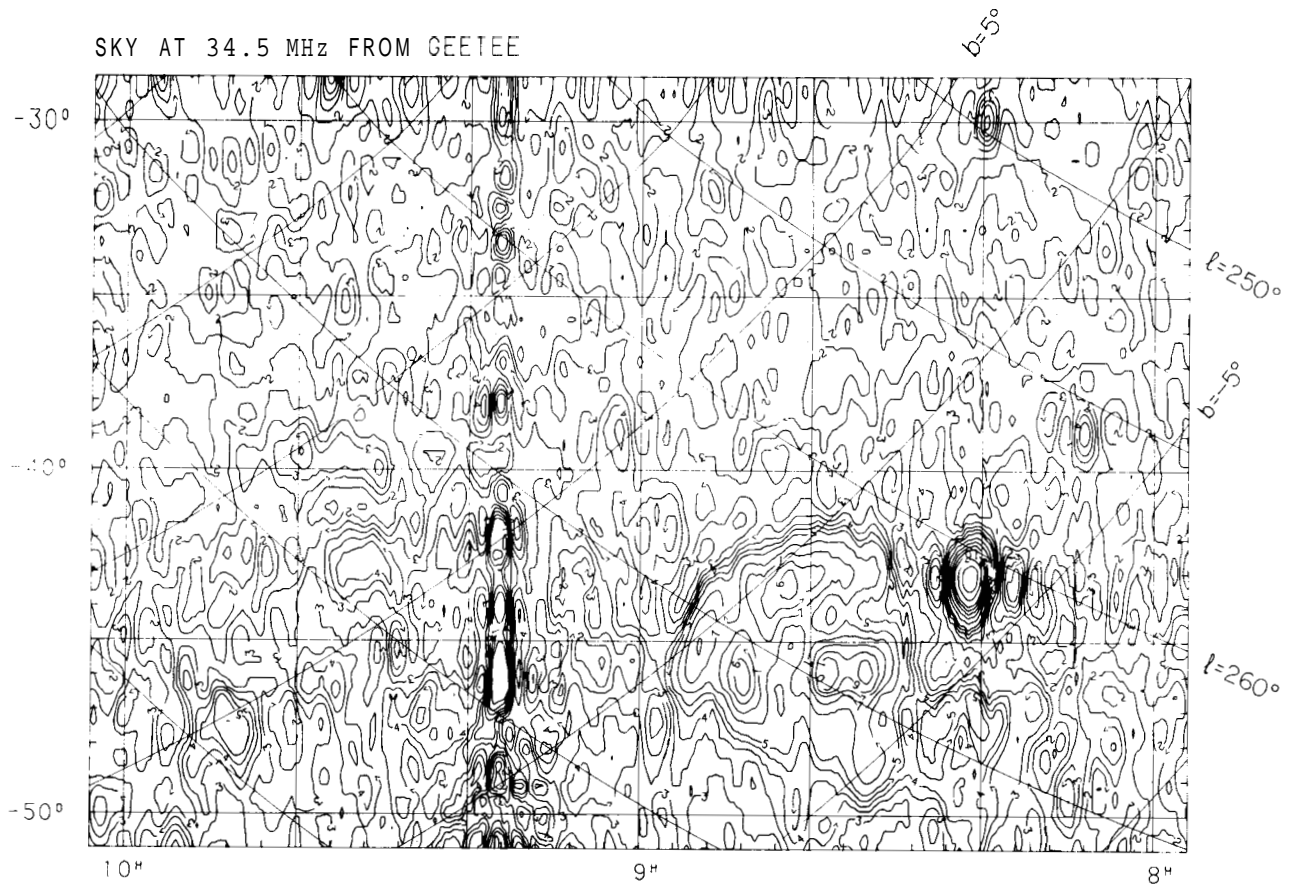
SKY AT 34.5 MHz FROM GEETEE



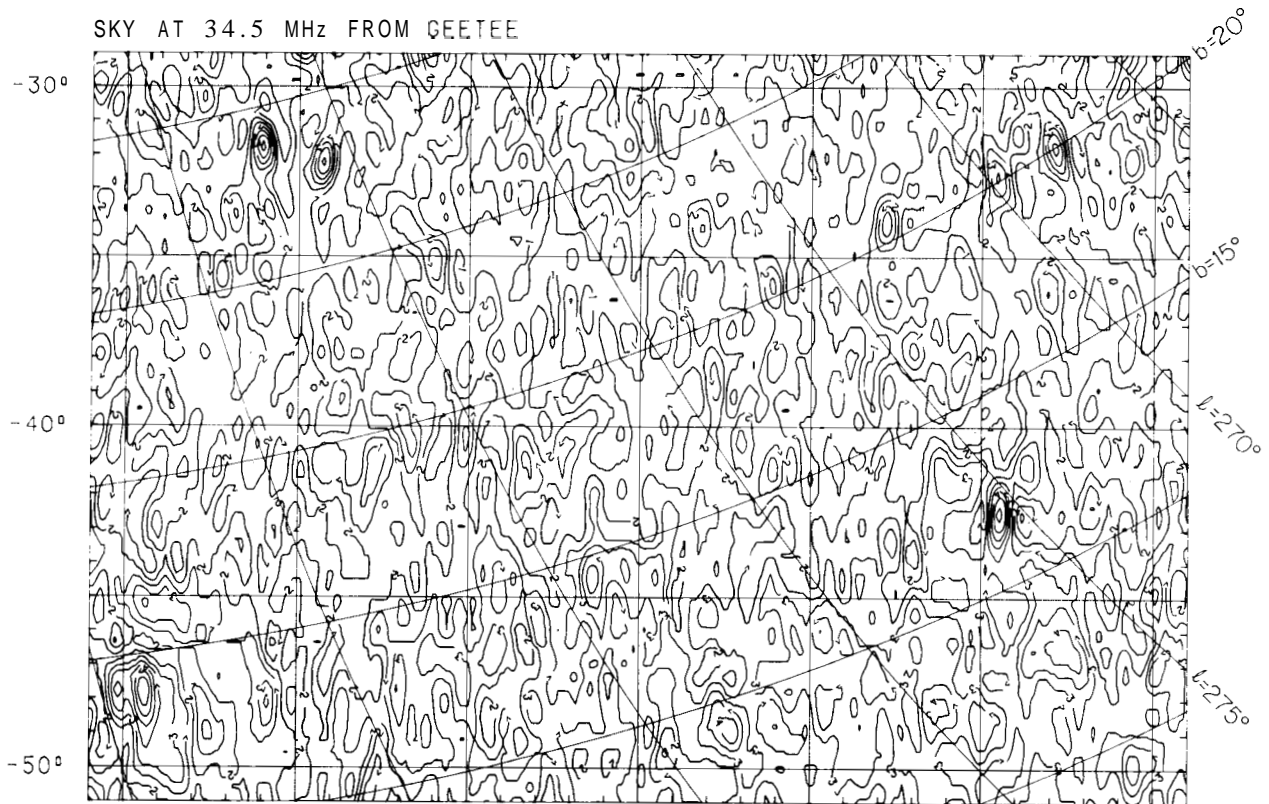
SKY AT 34.5 MHz FROM GEETEE



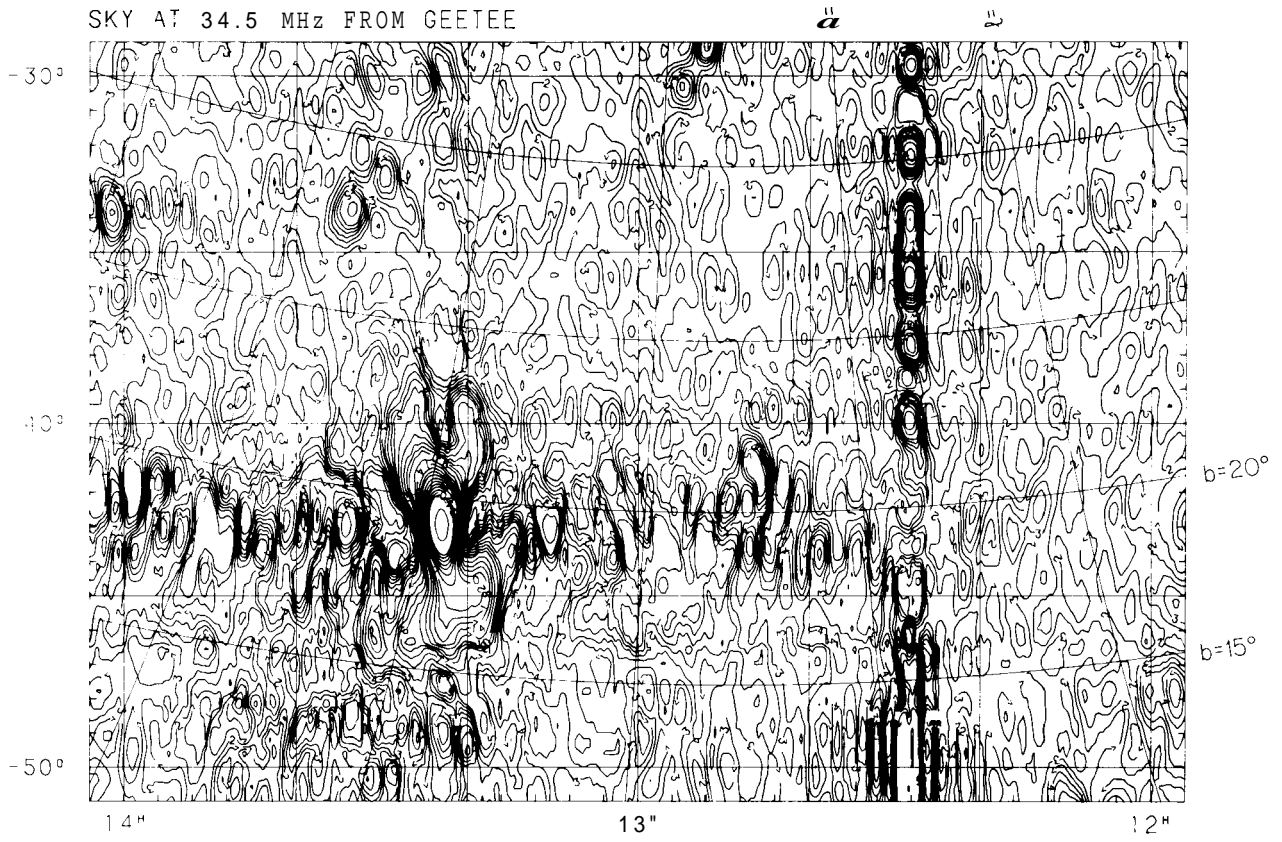
SKY AT 34.5 MHz FROM GEETEE



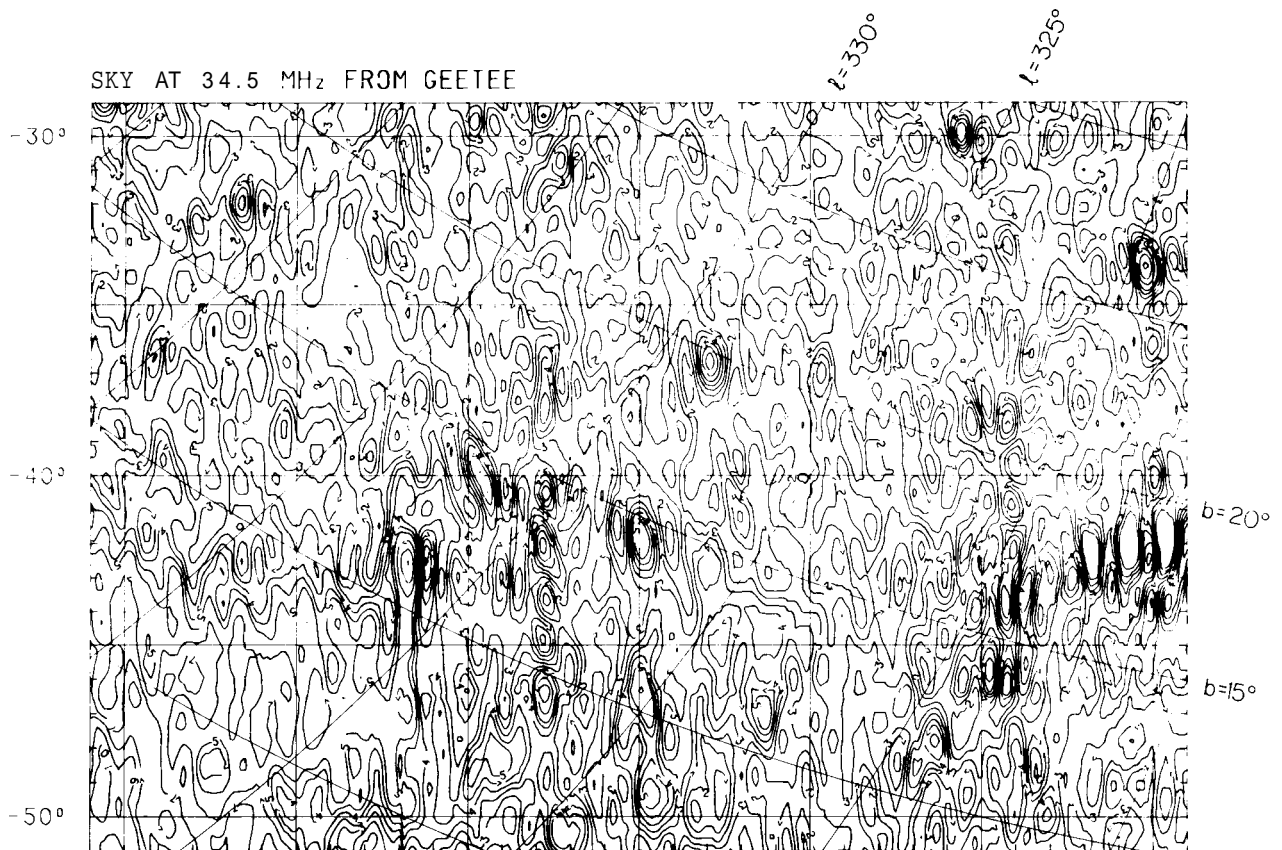
SKY AT 34.5 MHz FROM GEETEE



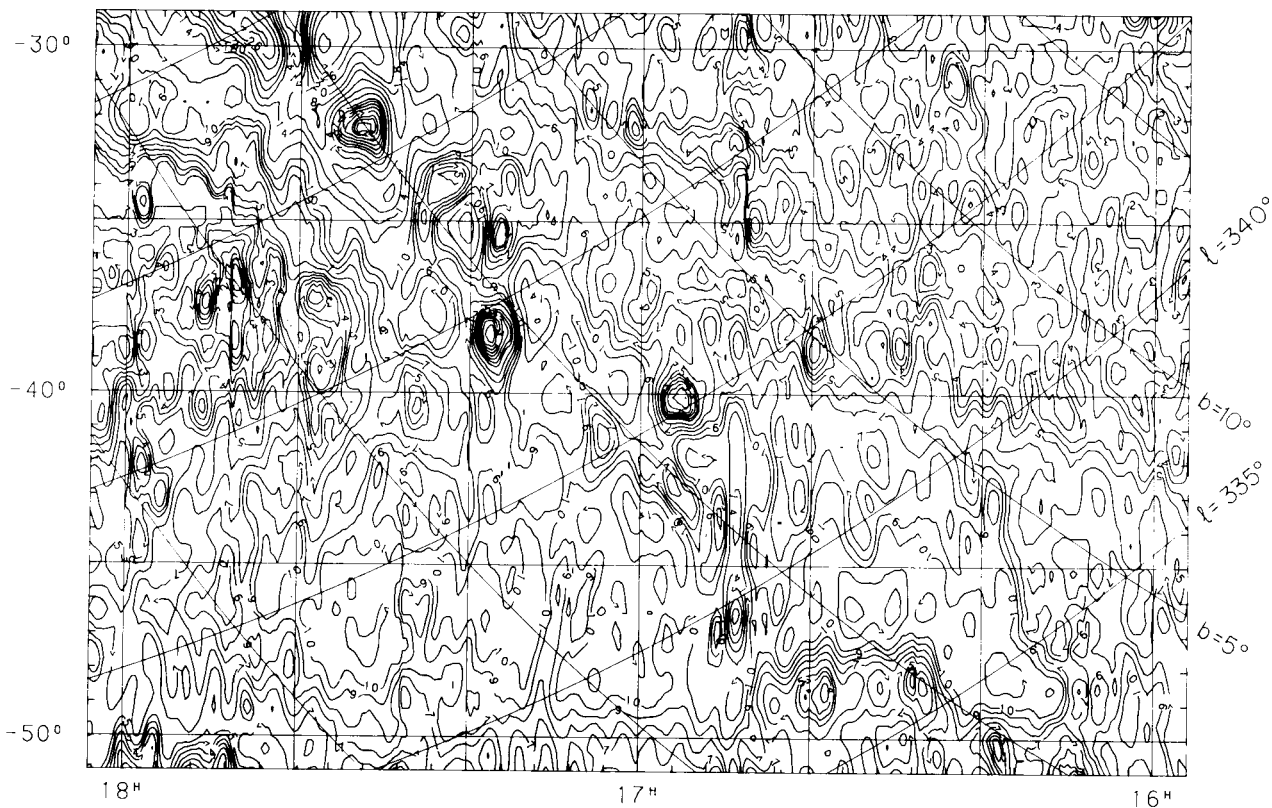
SKY AT 34.5 MHz FROM GEETEE



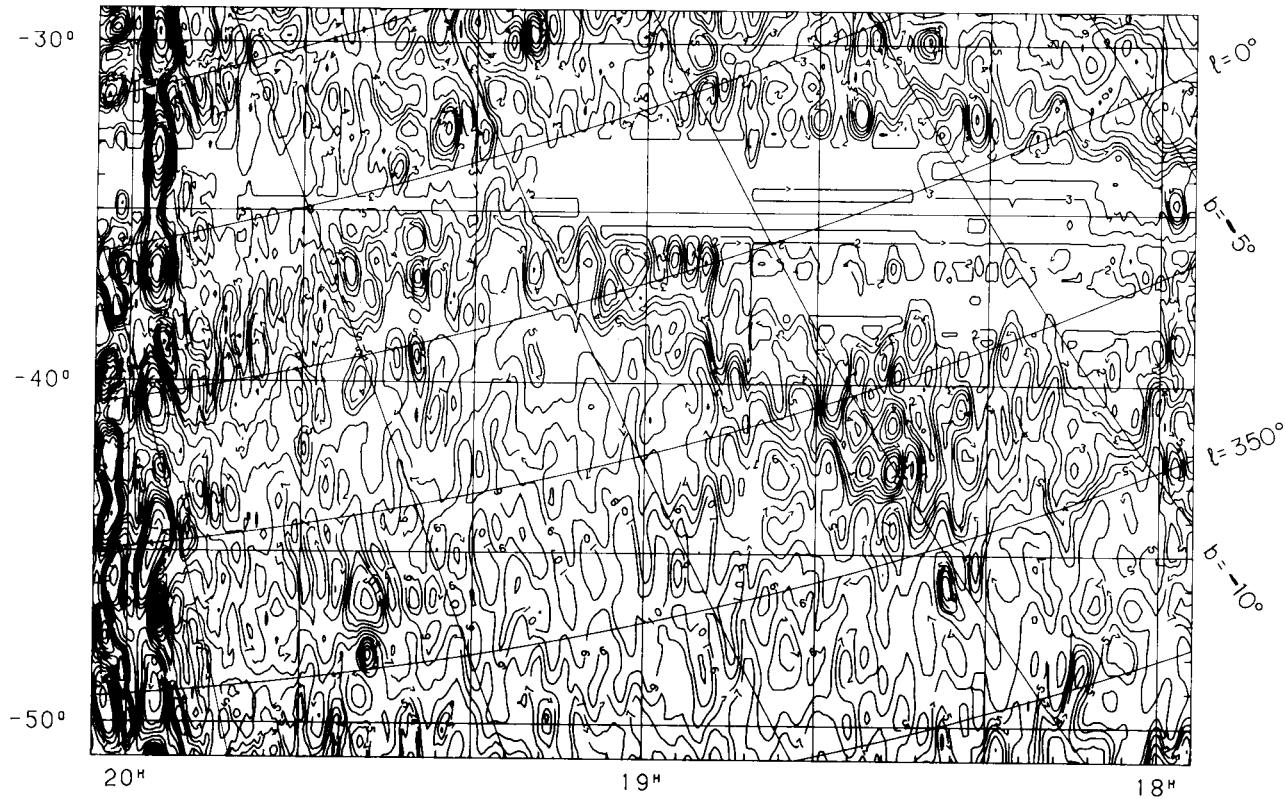
SKY AT 34.5 MHz FROM GEETEE



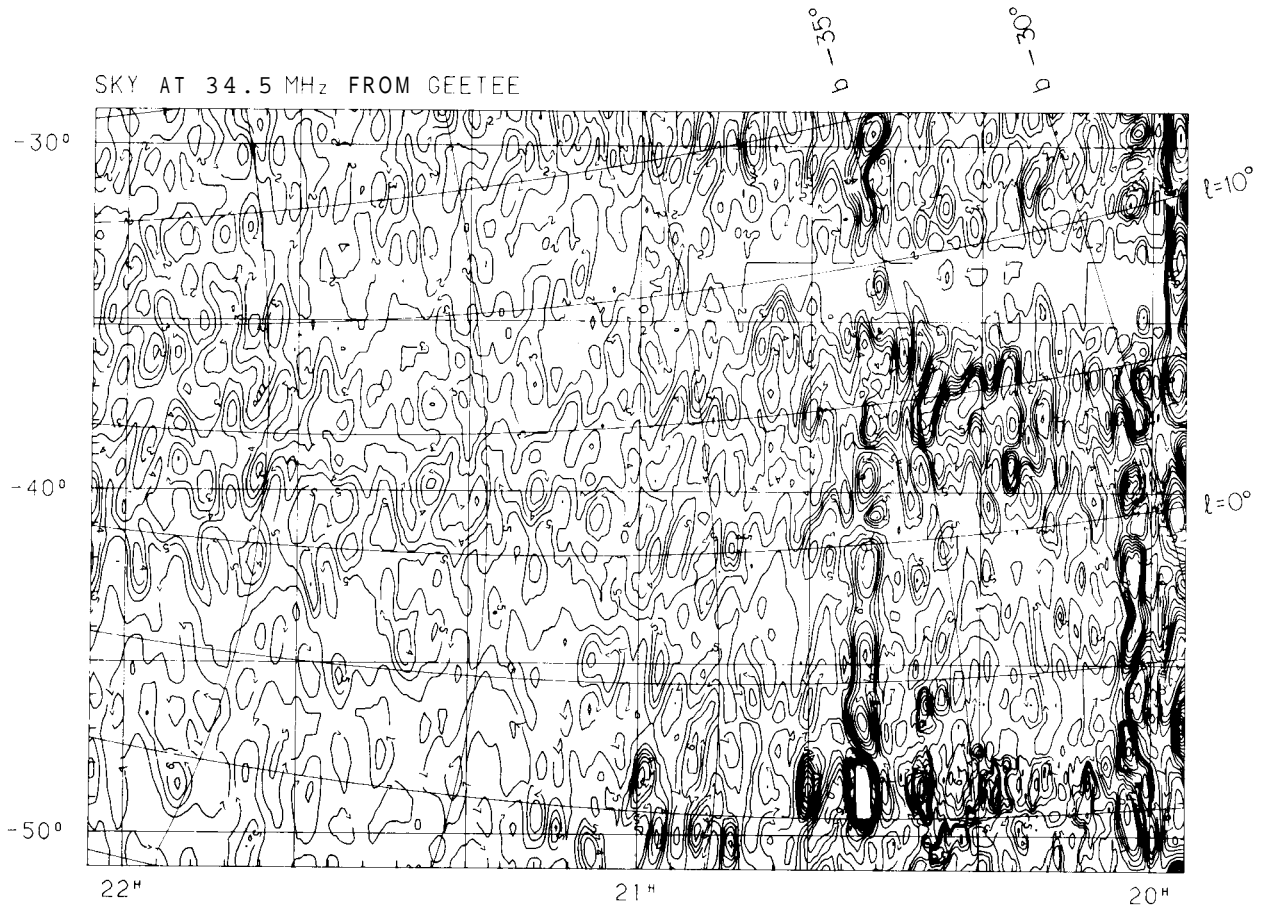
SKY AT 34.5 MHz FROM GEETEE



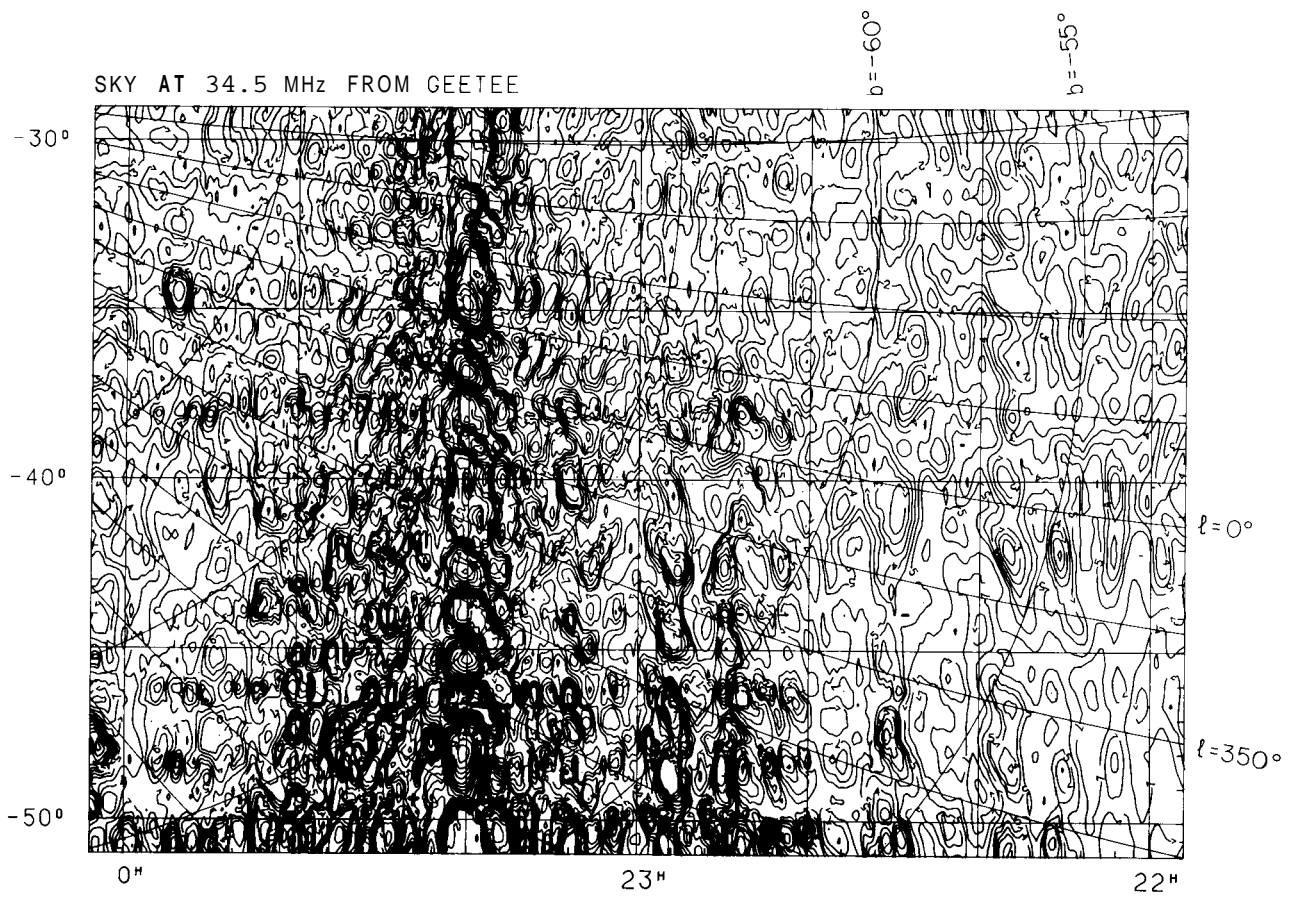
SKY AT 34.5 MHz FROM GEETEE



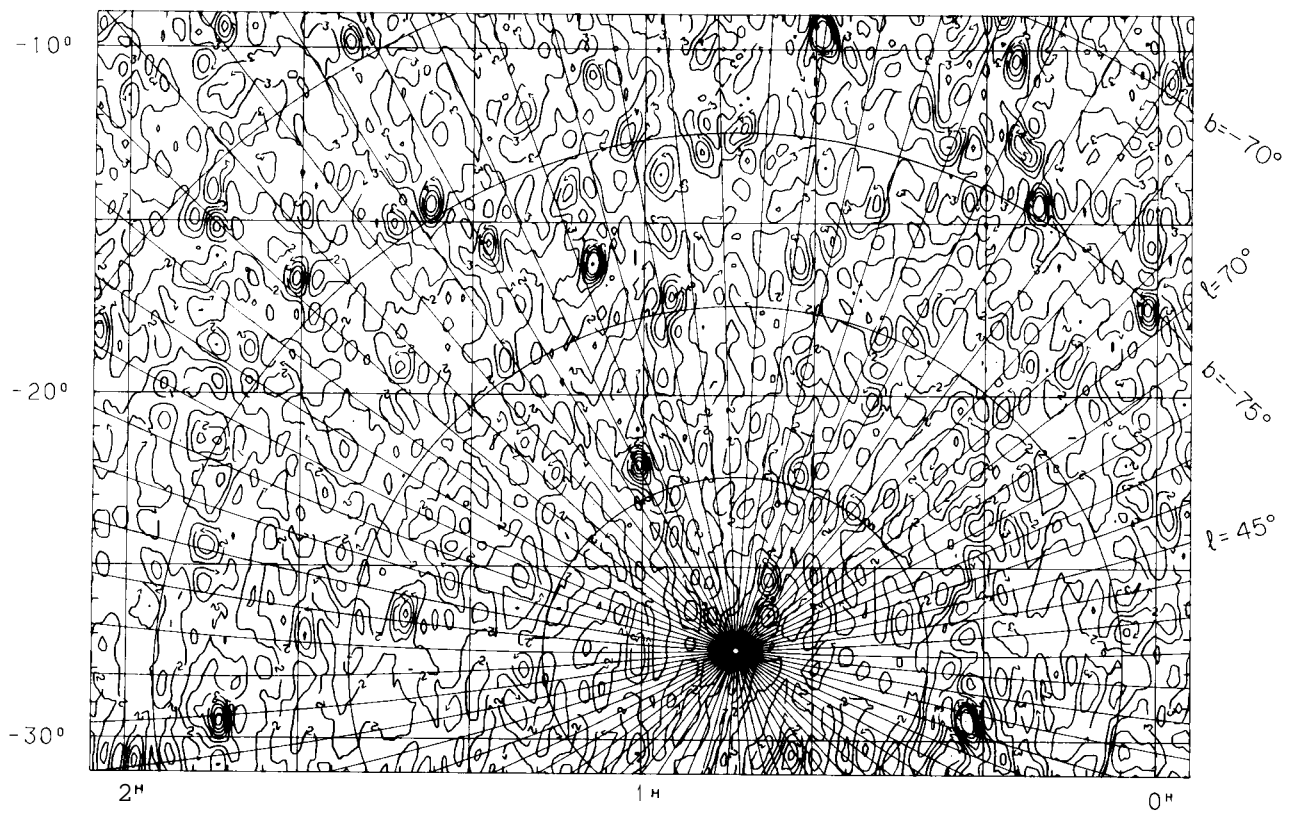
SKY AT 34.5 MHz FROM GEETEE



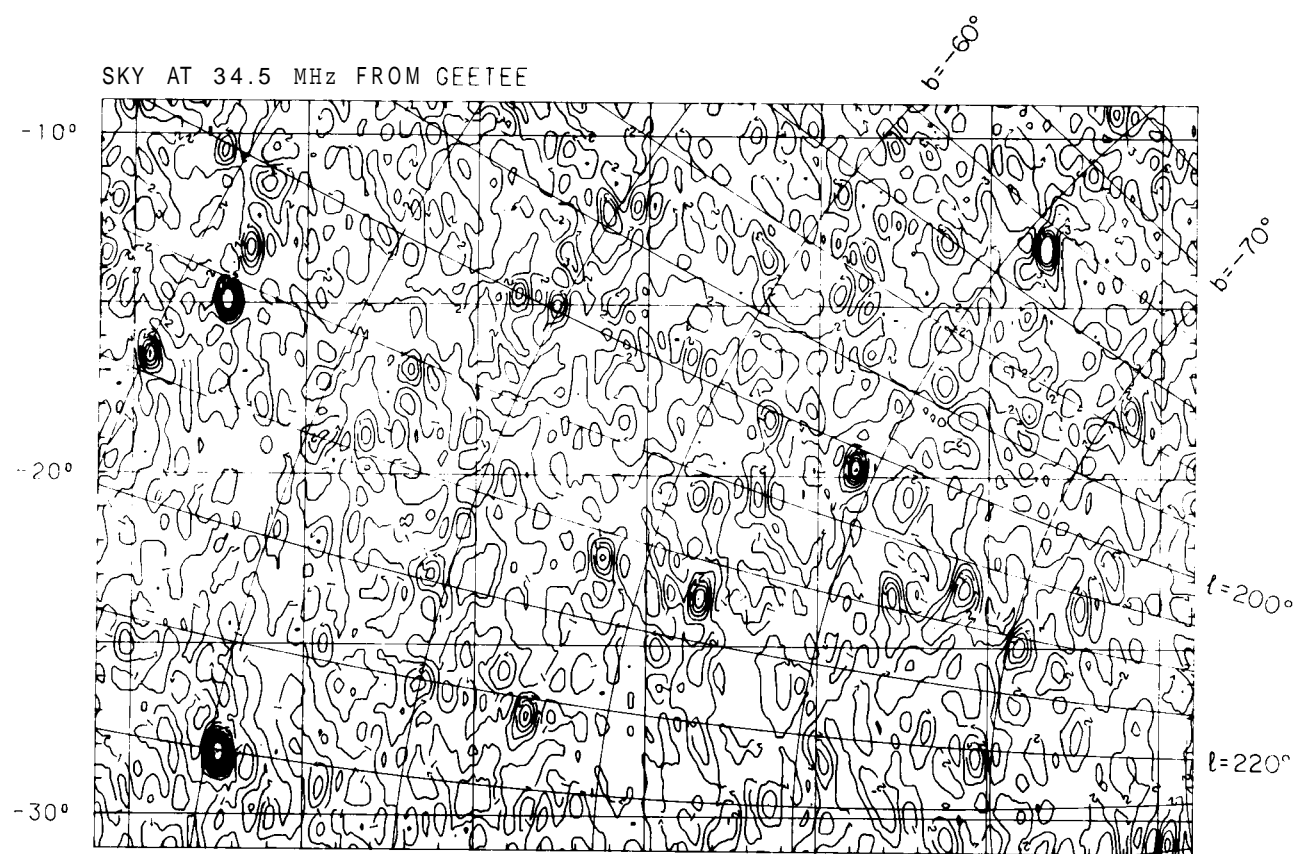
SKY AT 34.5 MHz FROM GEETEE



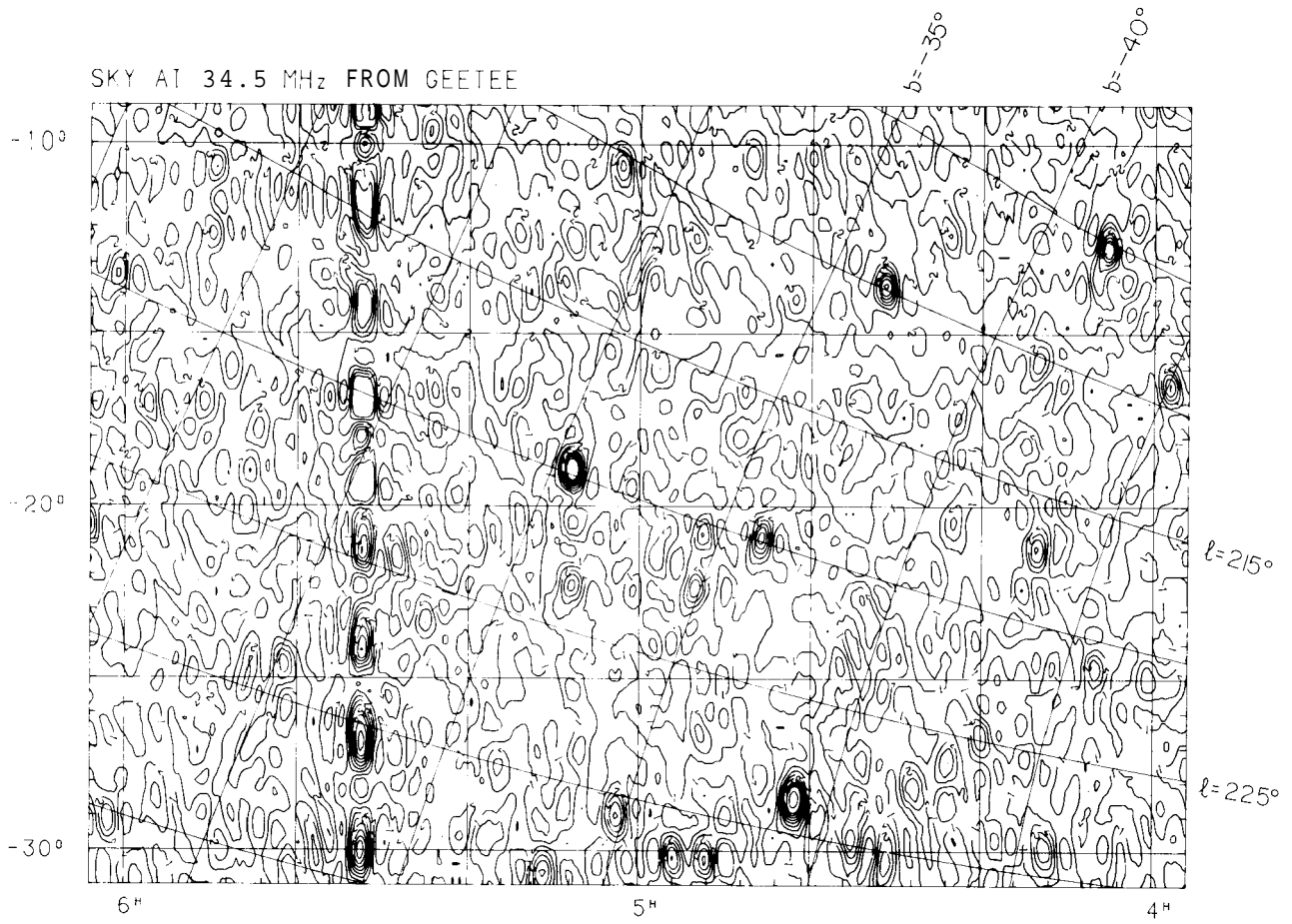
SKY AT 34.5 MHz FROM GEETEE



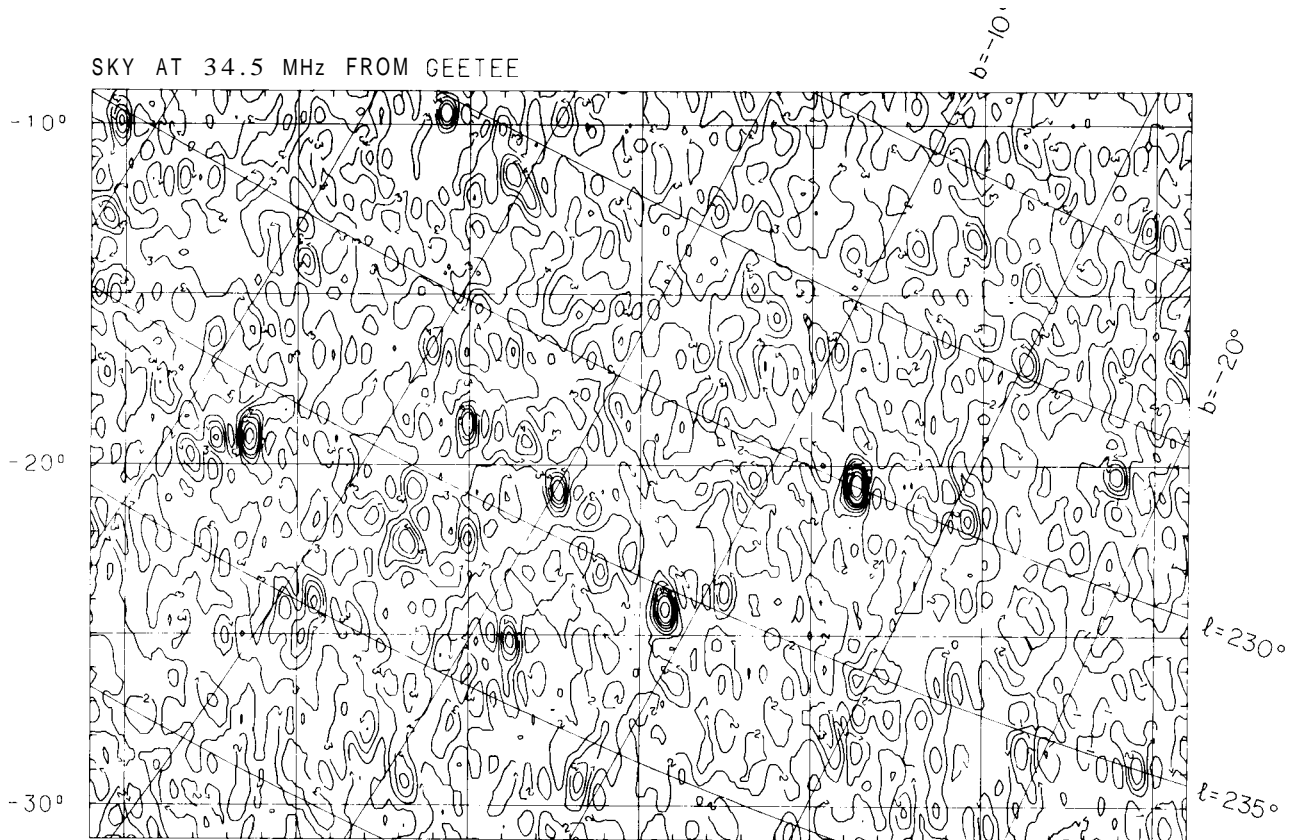
SKY AT 34.5 MHz FROM GEETEE



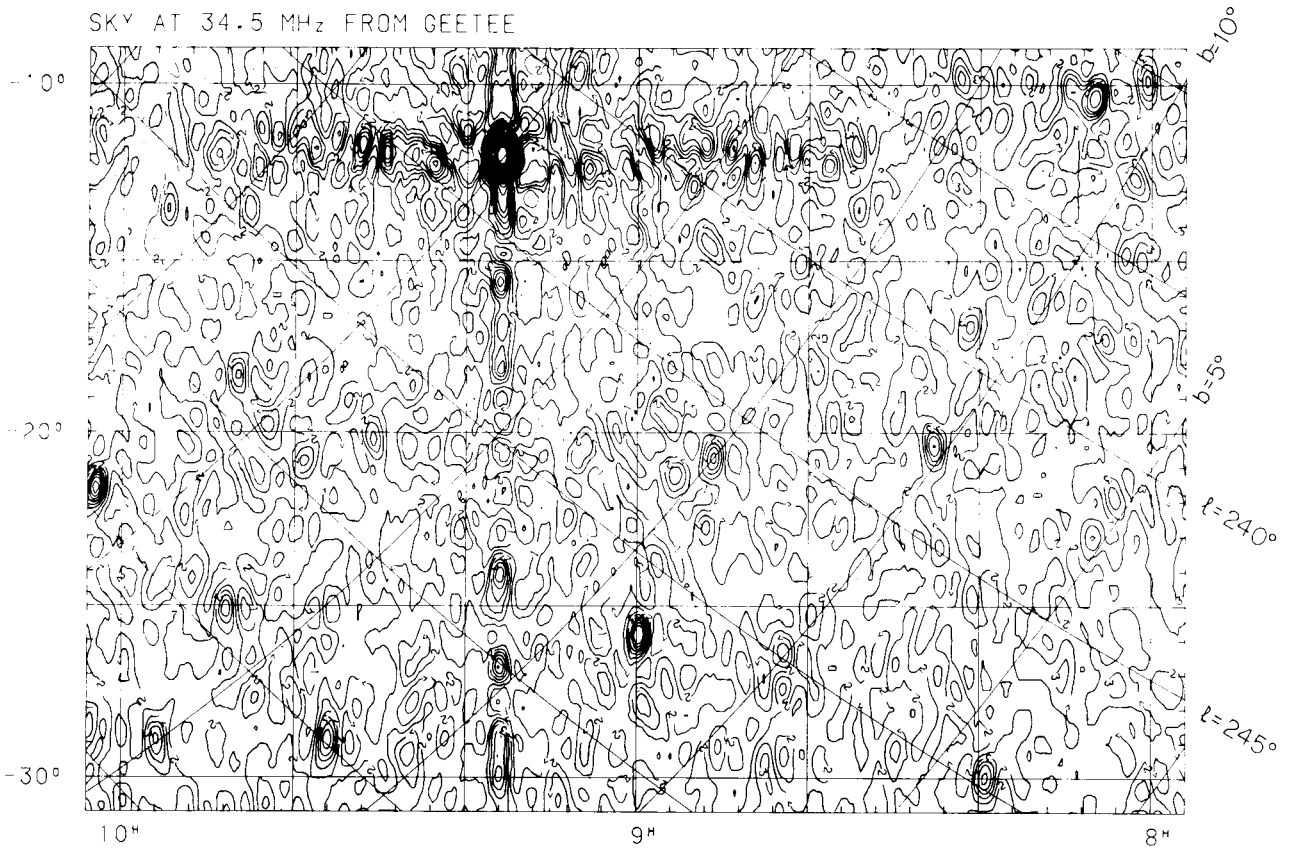
SKY AT 34.5 MHz FROM GEETEE



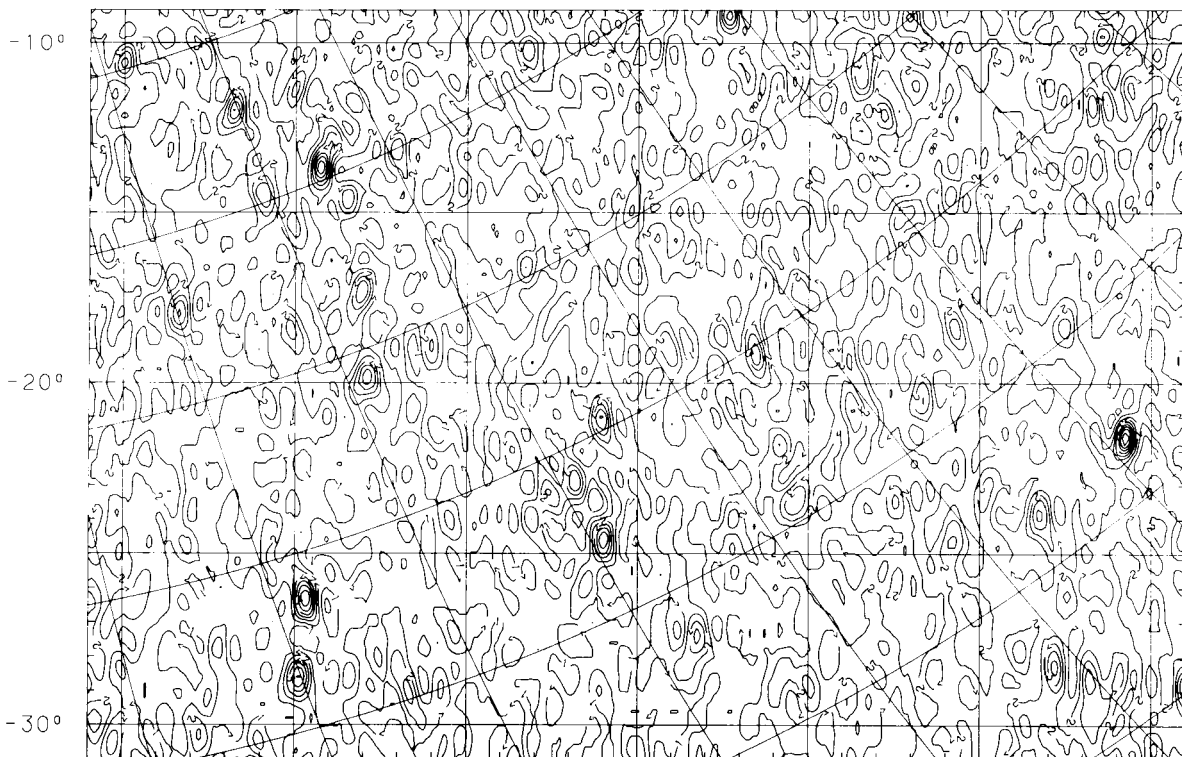
SKY AT 34.5 MHz FROM GEETEE



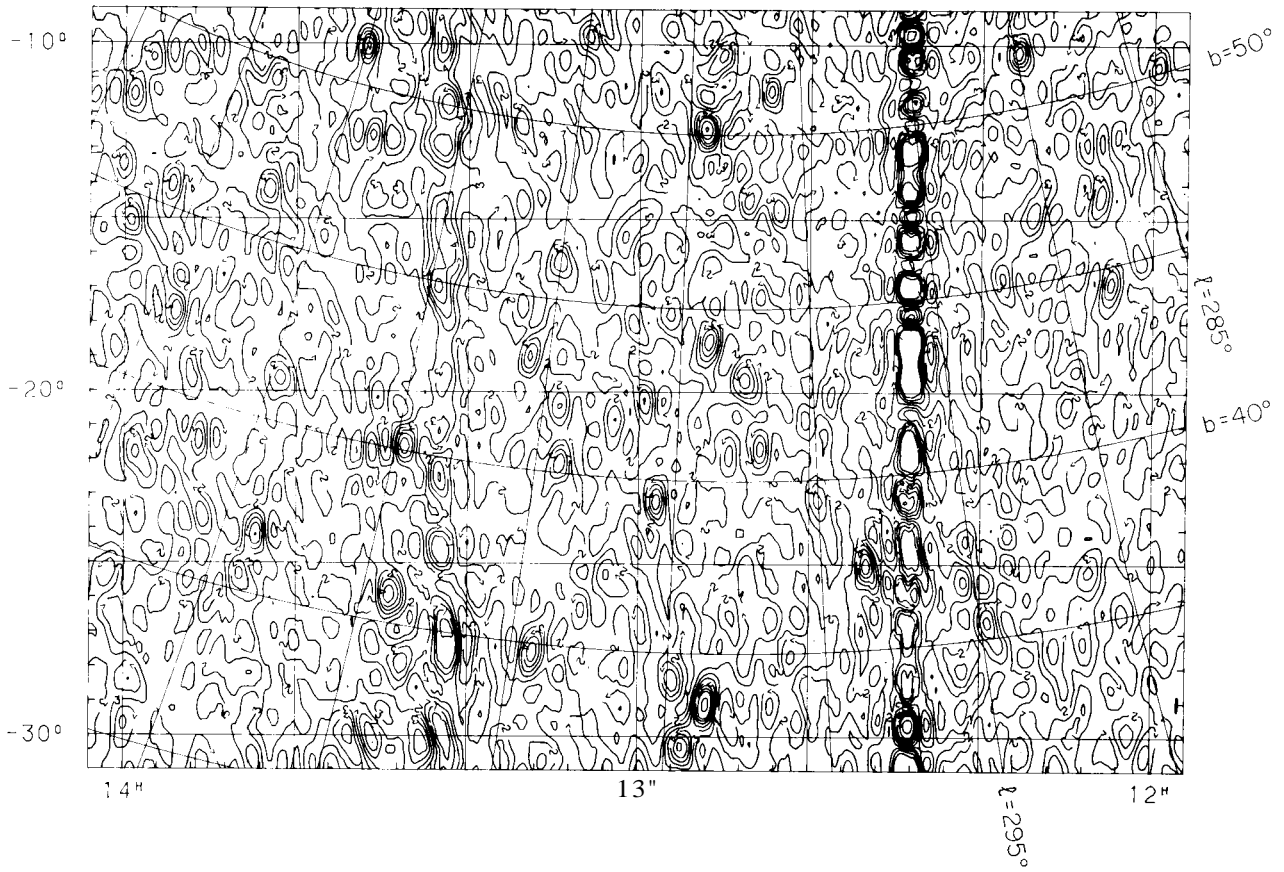
SKY AT 34.5 MHz FROM GEETEE



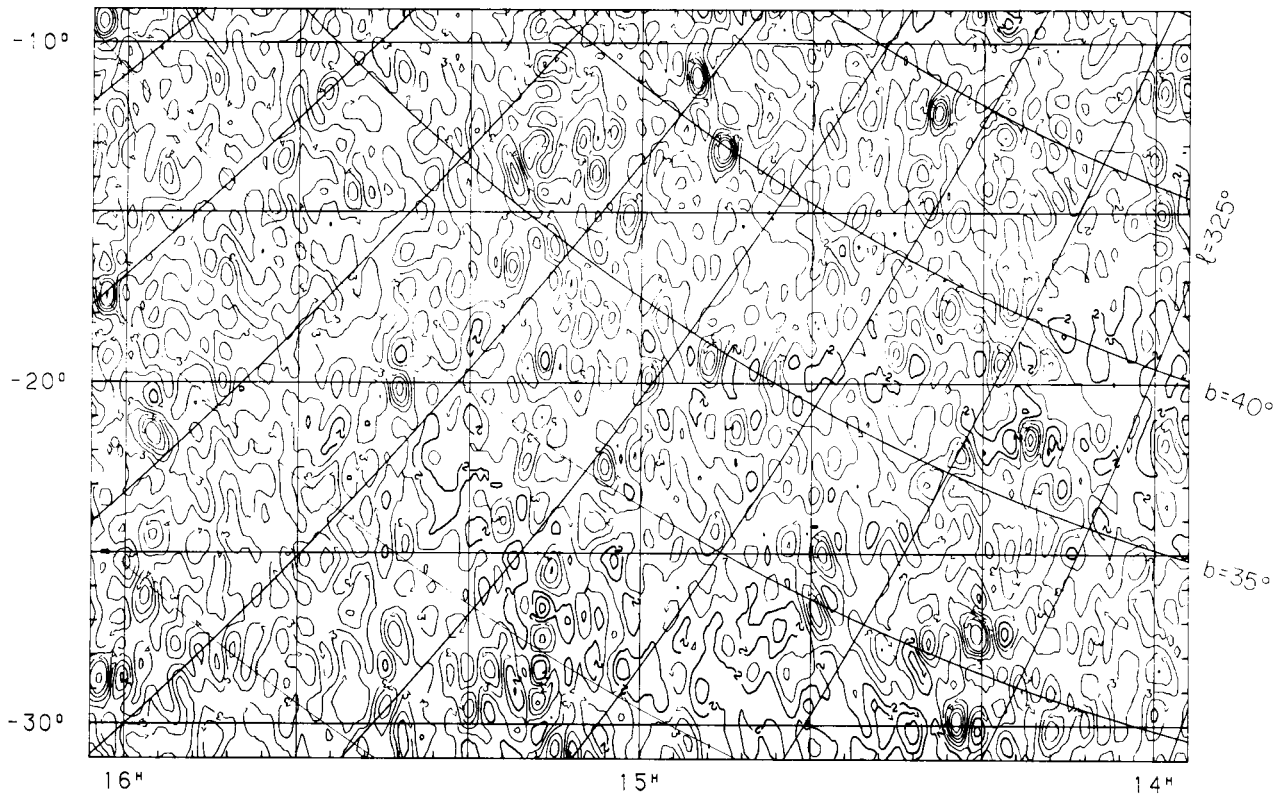
SKY AT 34.5 MHz FROM GEETEE



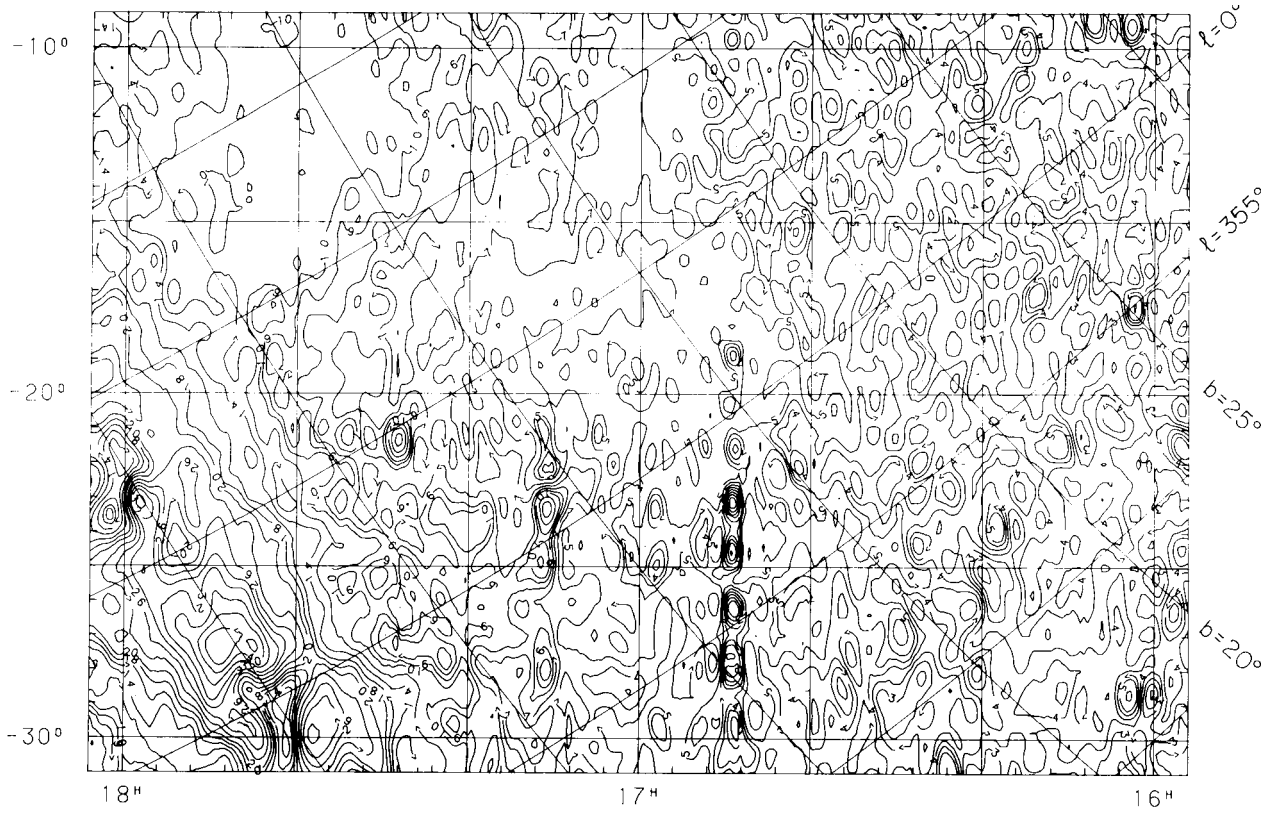
SKY AT 34.5 MHz FROM GEETEE



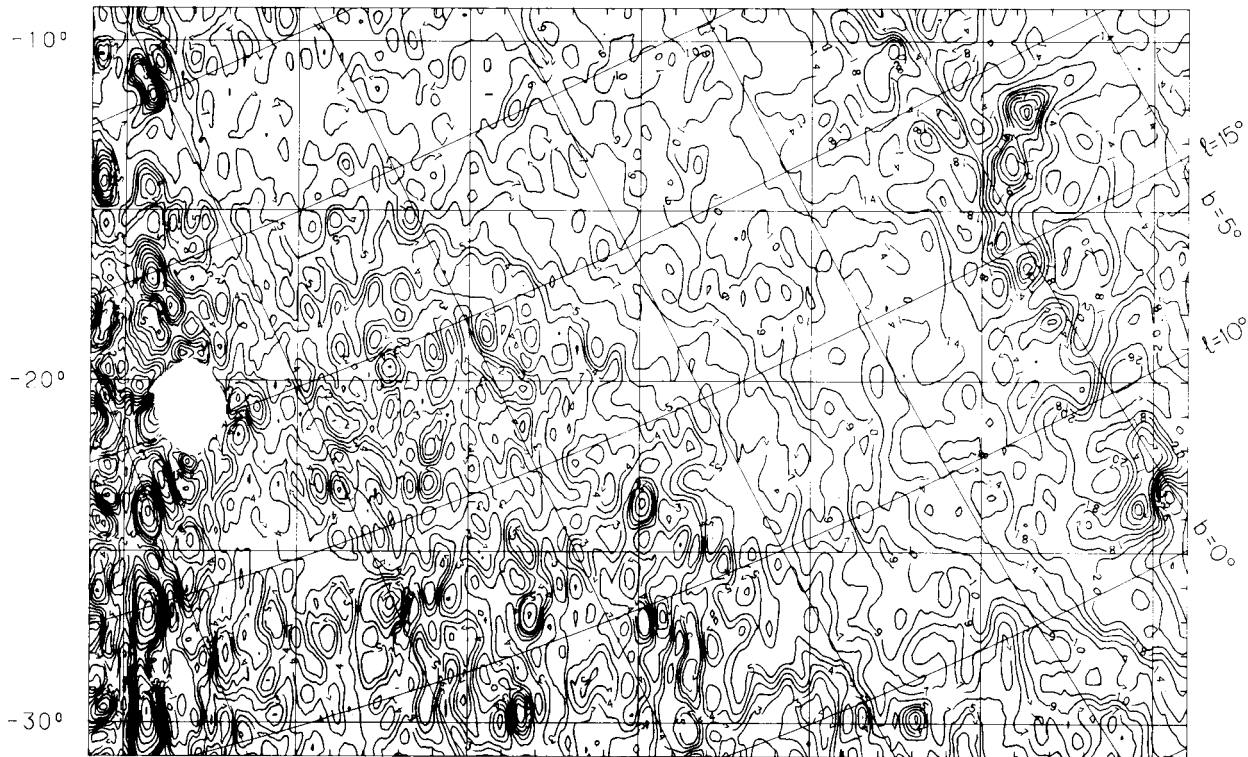
SKY AT 34.5 MHz FROM GEETEE



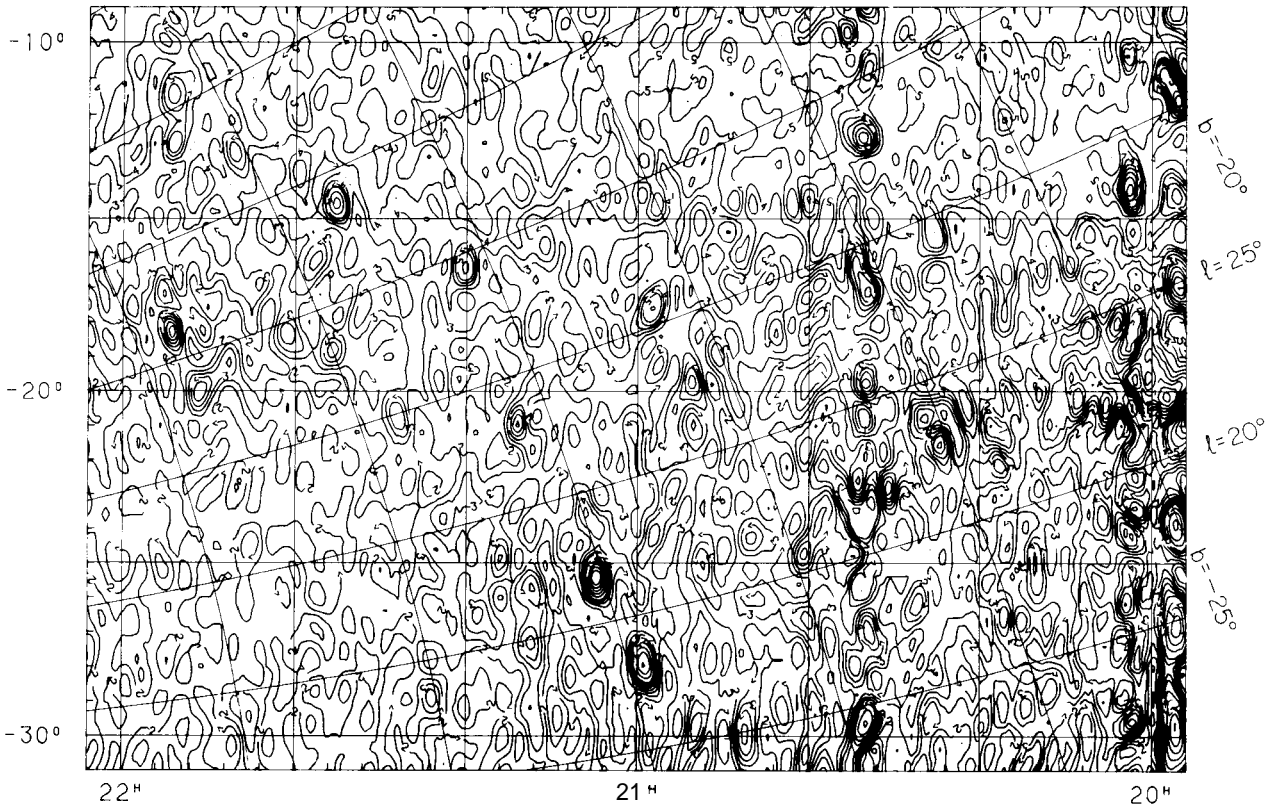
SKY AT 34.5 MHz FROM GEETEE



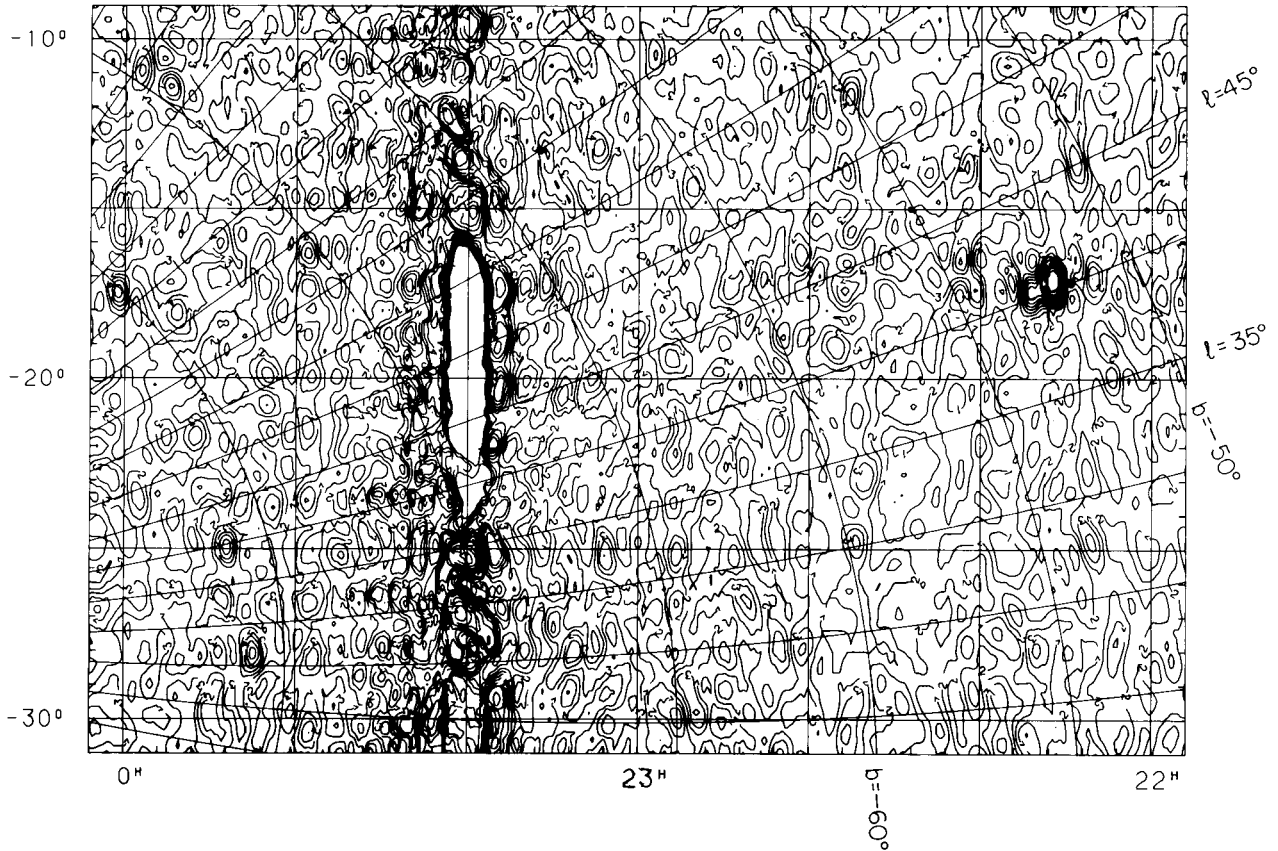
SKY AT 34.5 MHz FROM GEETEE



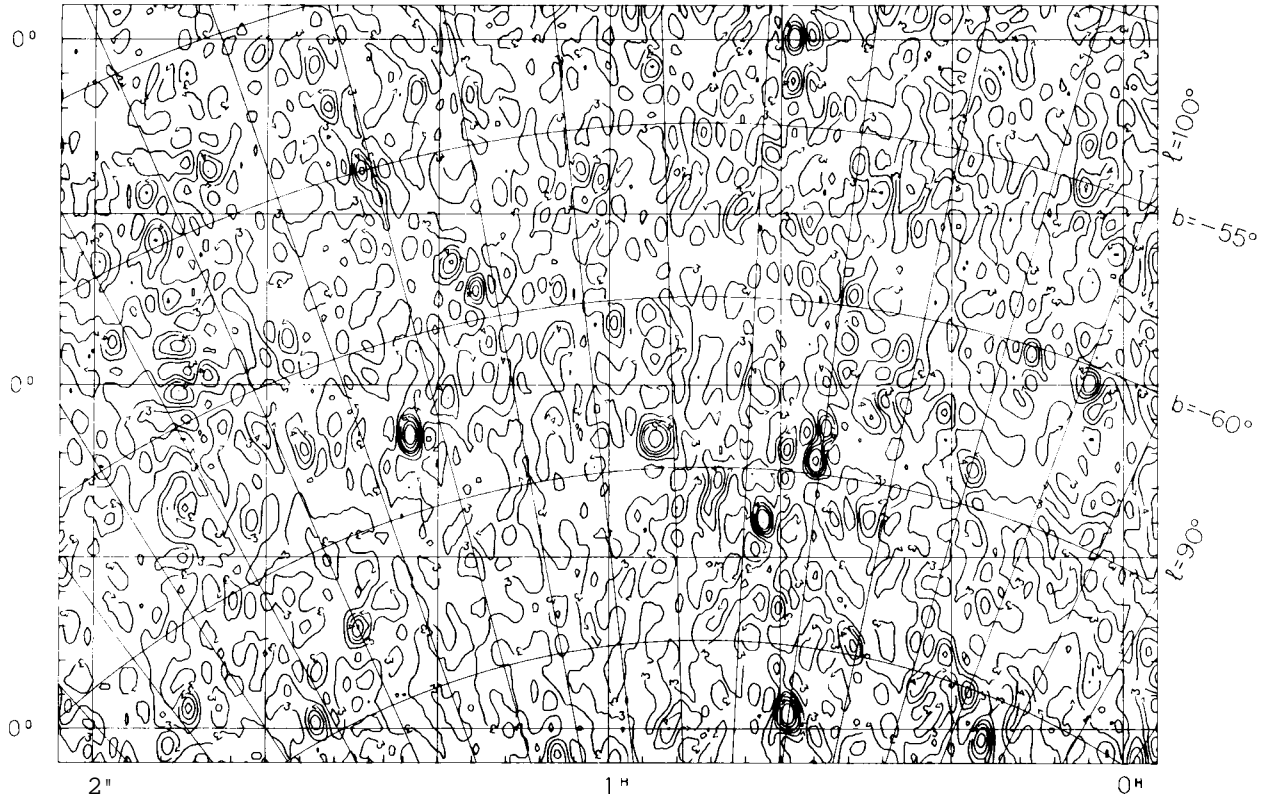
SKY AT 34.5 MHz FROM GEETEE



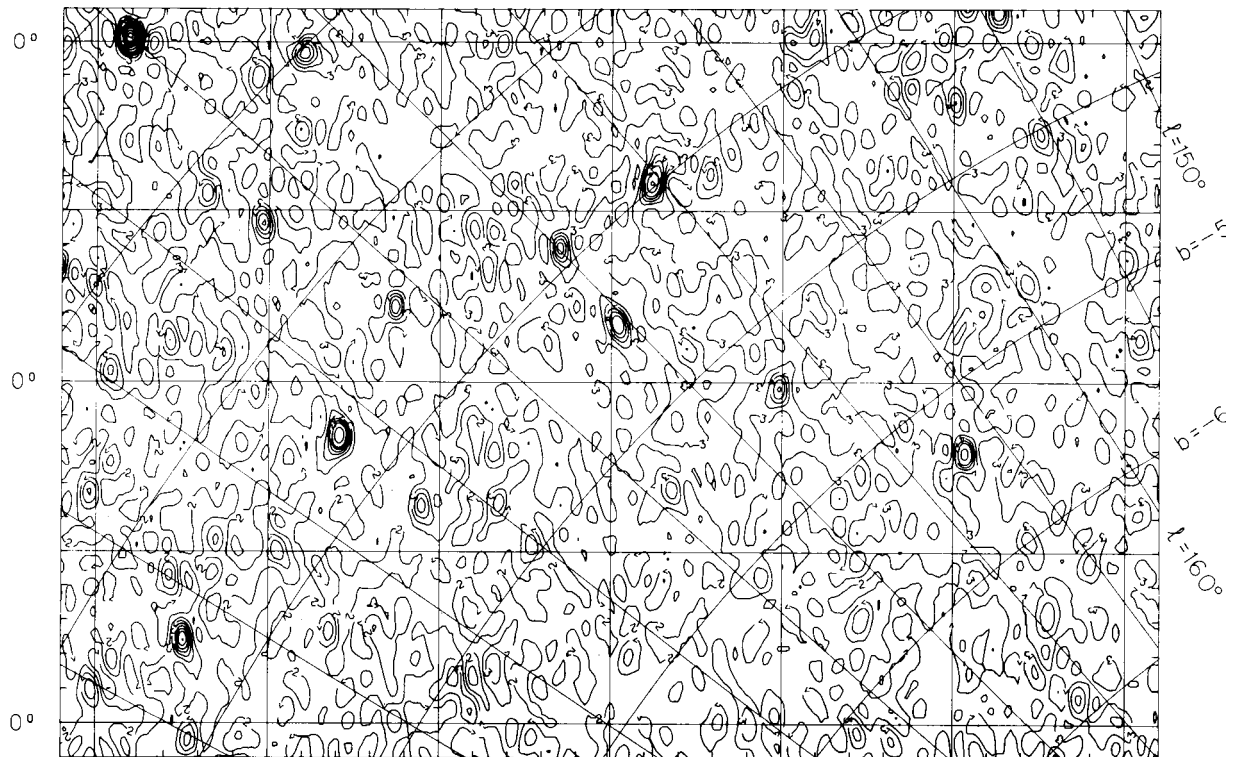
SKY AT 34.5 MHz FROM GEETEE



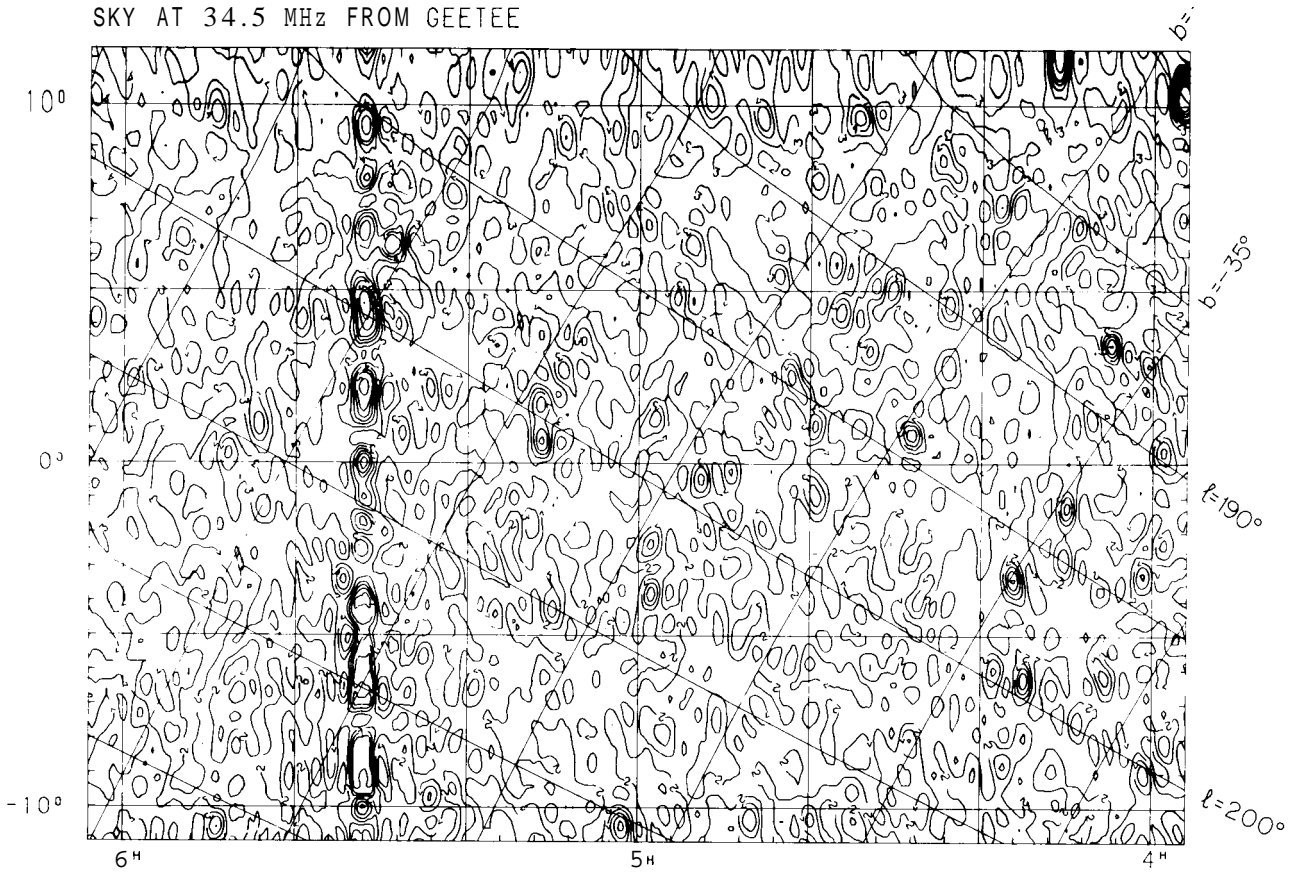
SKY AT 34.5 MHz FROM GEETEE



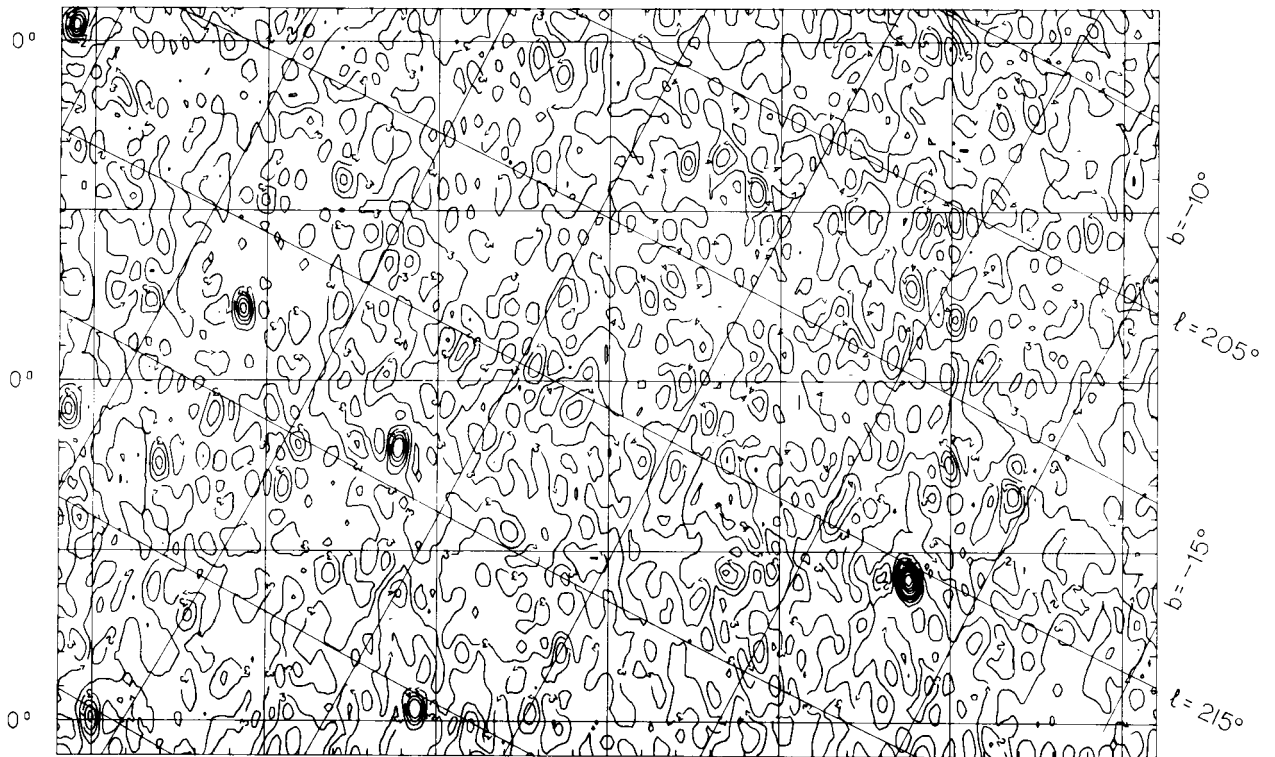
SKY AT 34.5 MHz FROM GEETEE



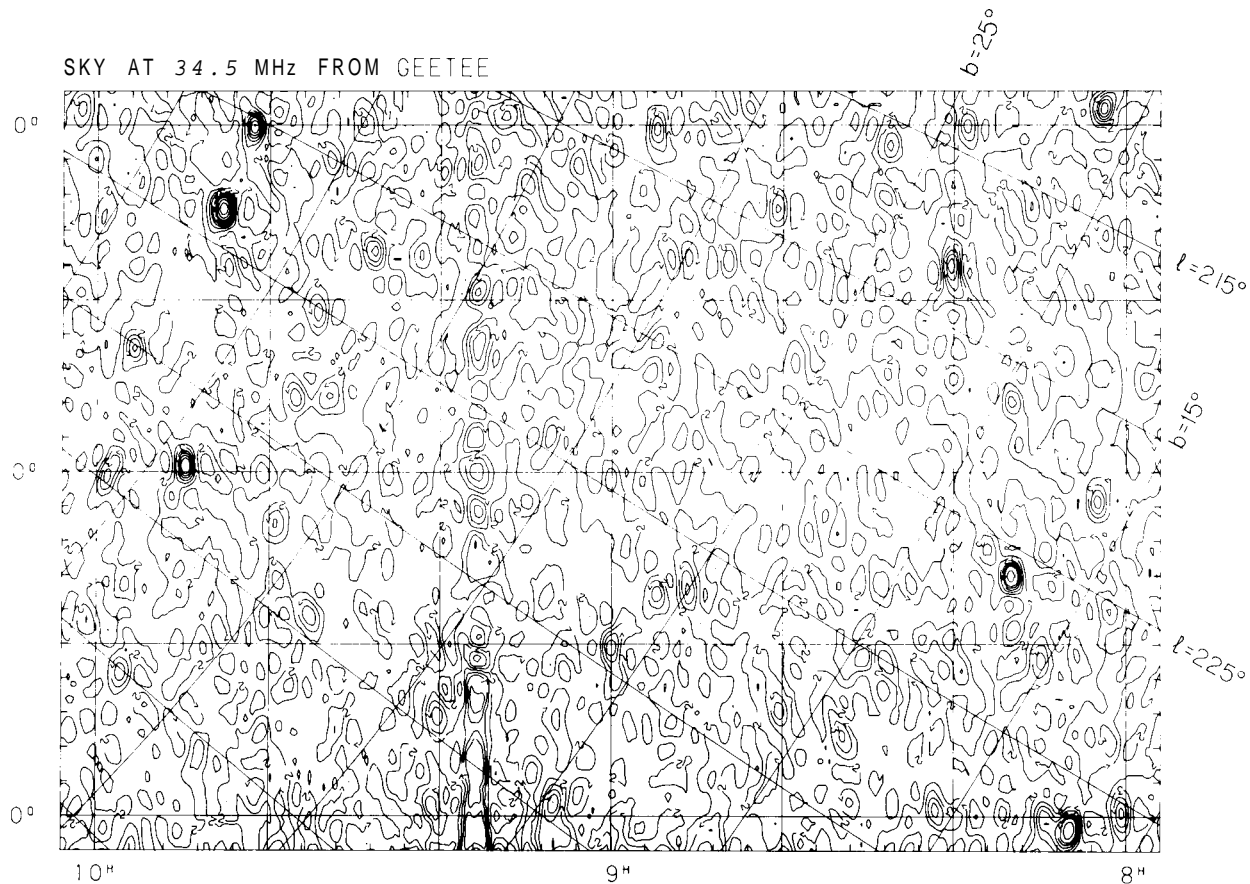
SKY AT 34.5 MHz FROM GEETEE



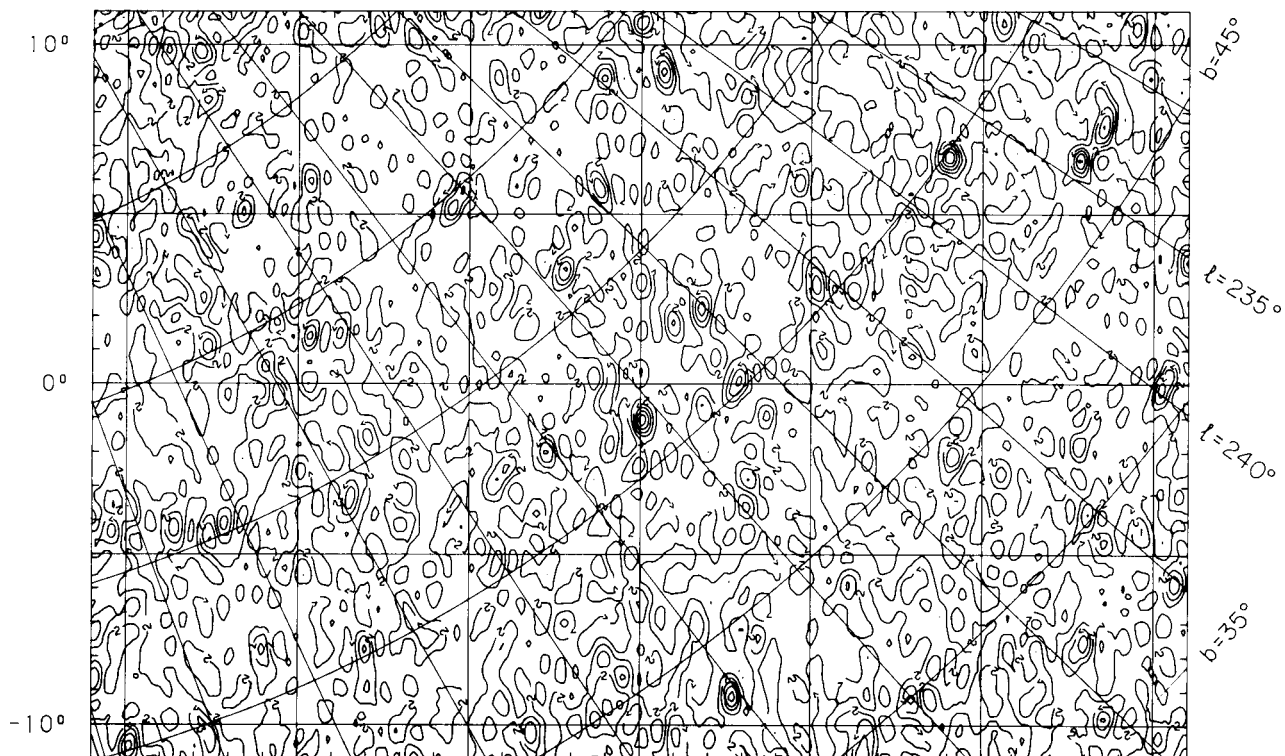
SKY AT 34.5 MHz FROM GEETEE



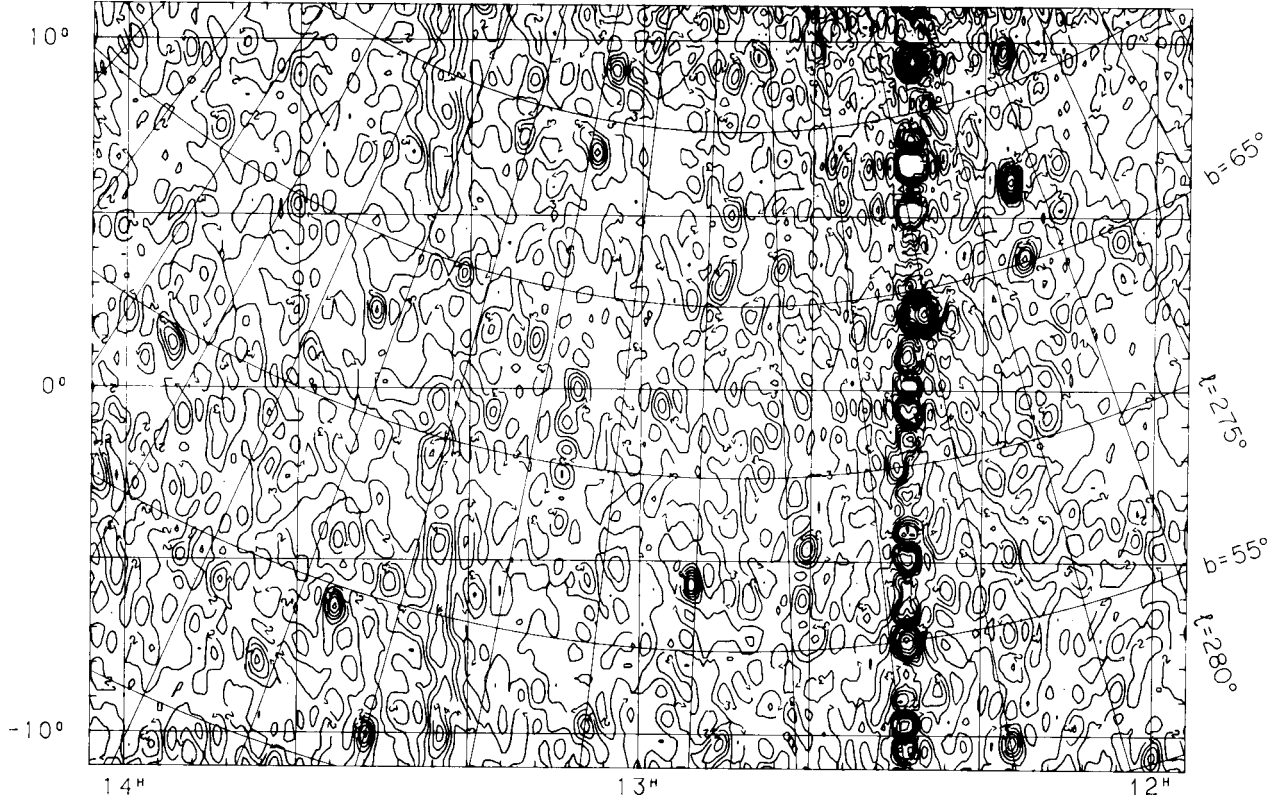
SKY AT 34.5 MHz FROM GEETEE



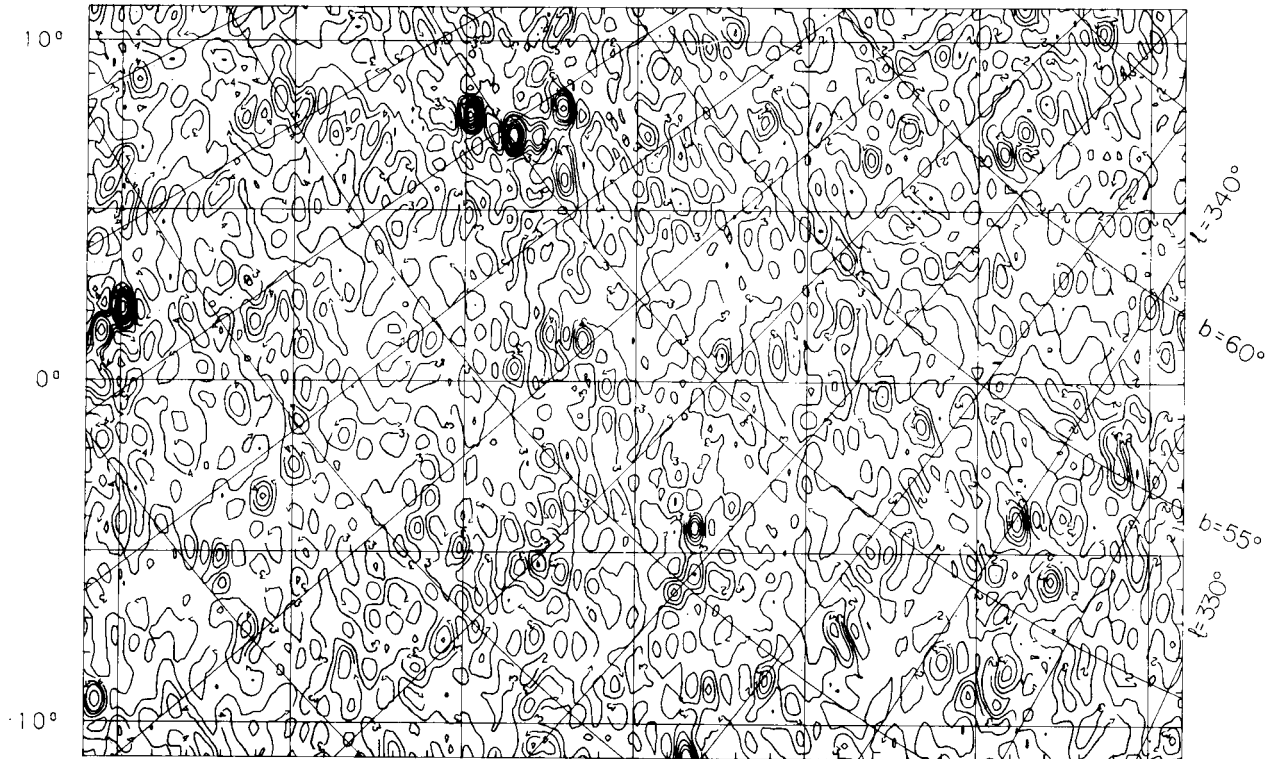
SKY AT 34.5 MHz FROM GEETEE



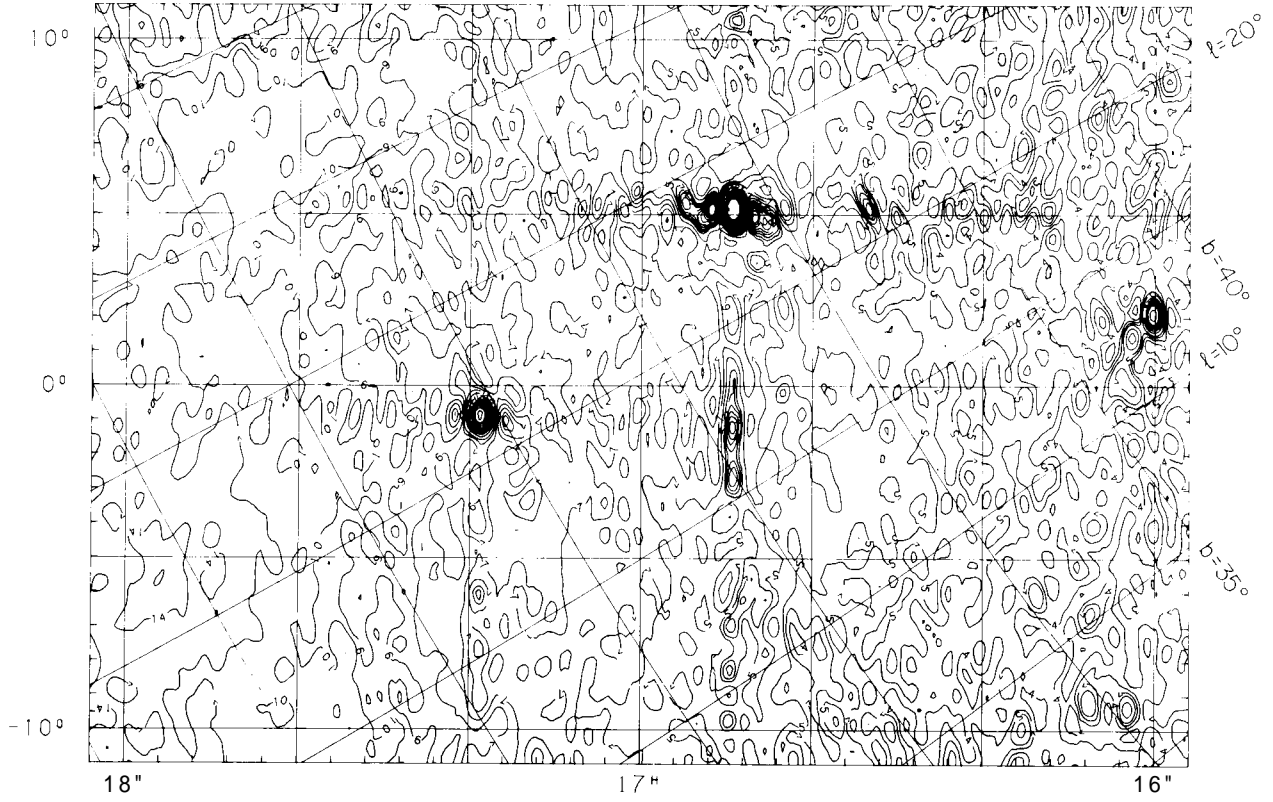
SKY AT 34.5 MHz FROM GEETEE



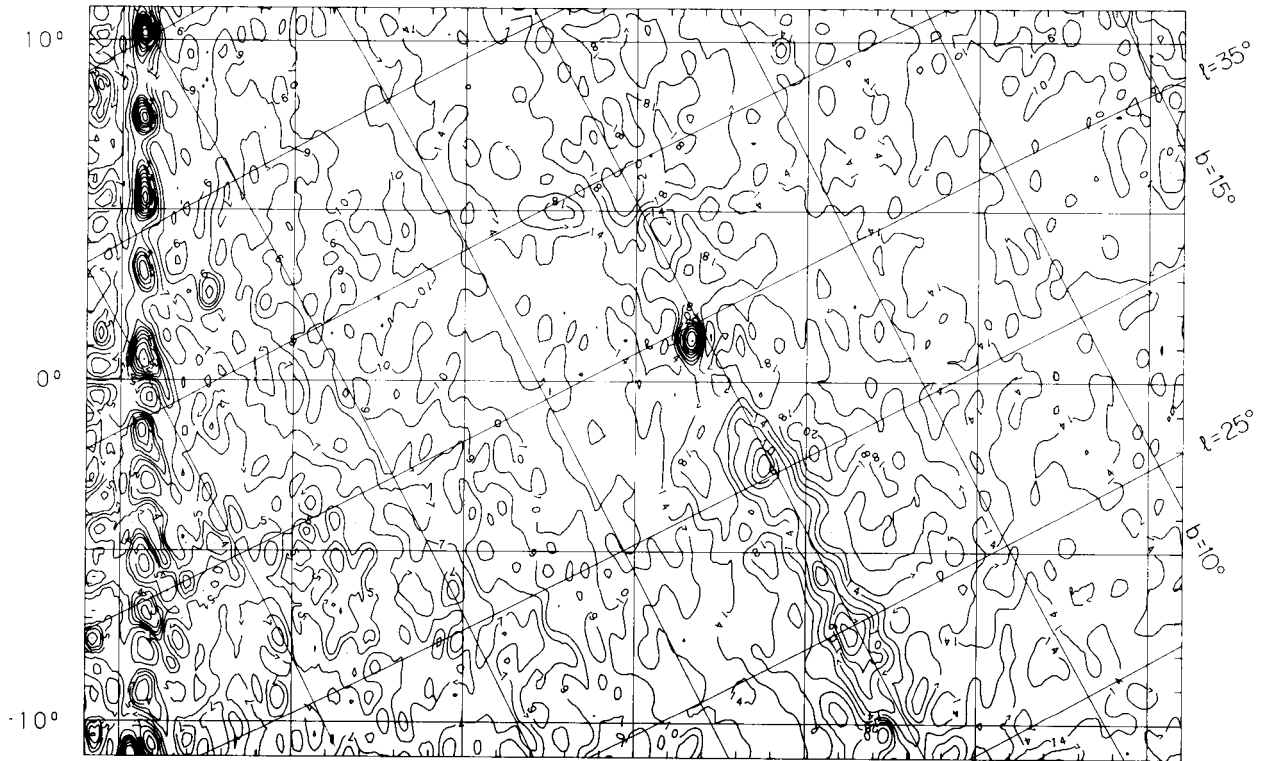
SKY AT 34.5 MHz FROM GEETEE



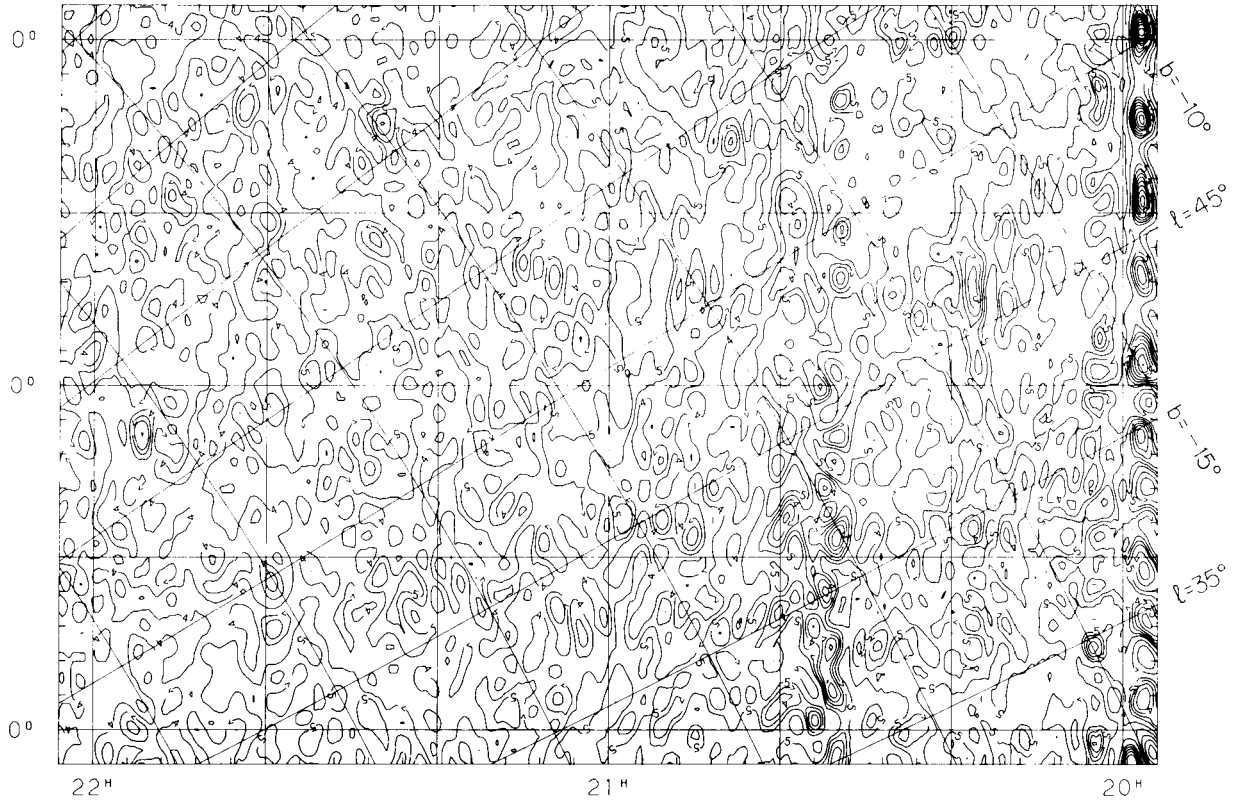
SKY AT 34.5 MHz FROM GFETEE



SKY AT 34.5 MHz FROM GEETEE



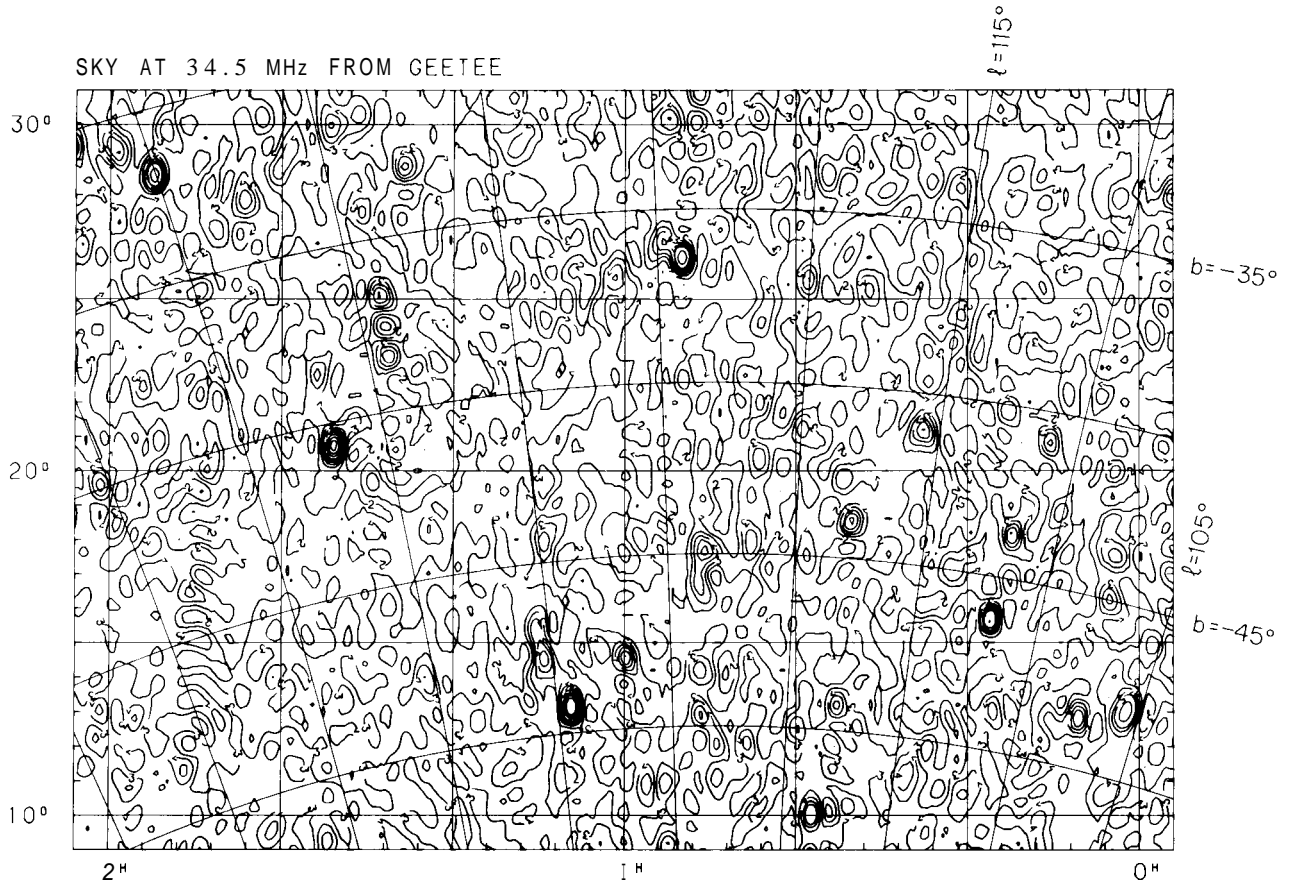
SKY AT 34.5 MHz FROM GEETEE



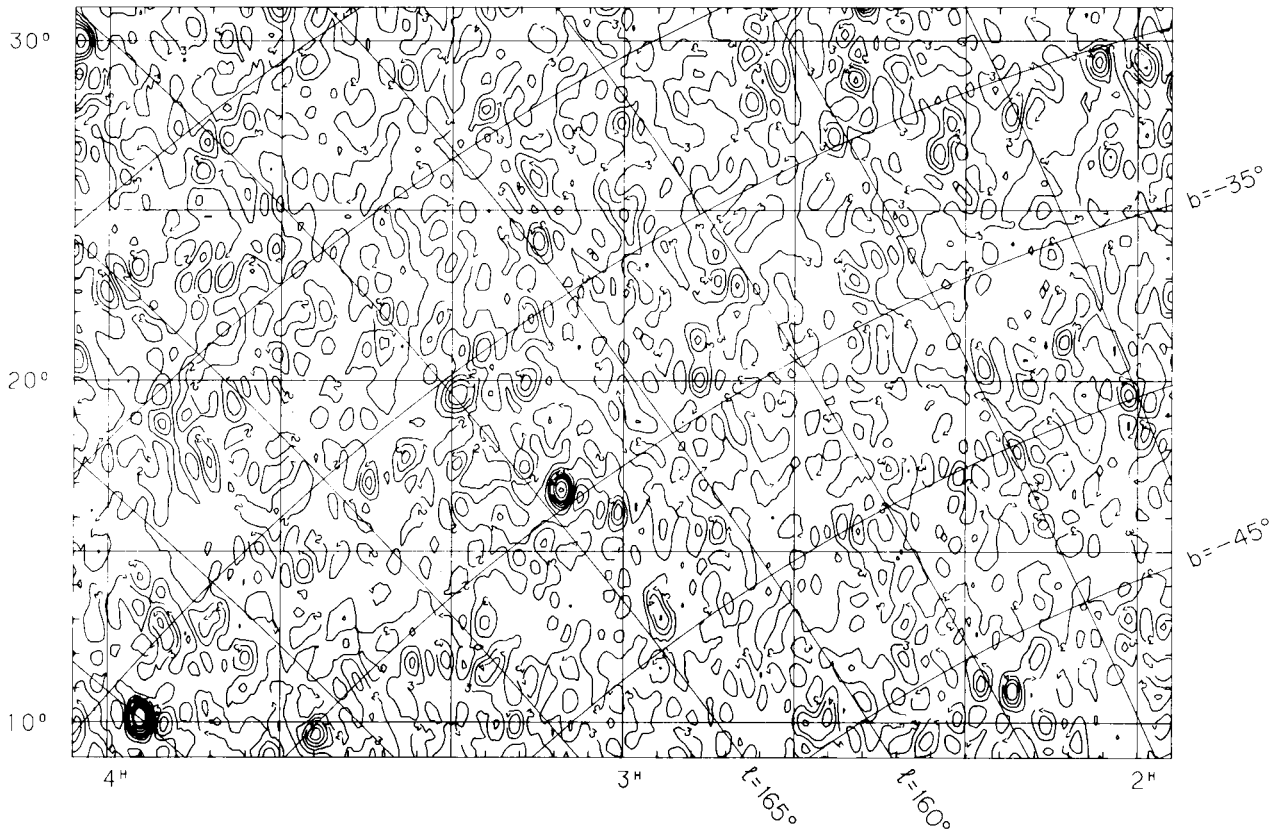
SKY AT 34.5 MHz FROM GEETEE



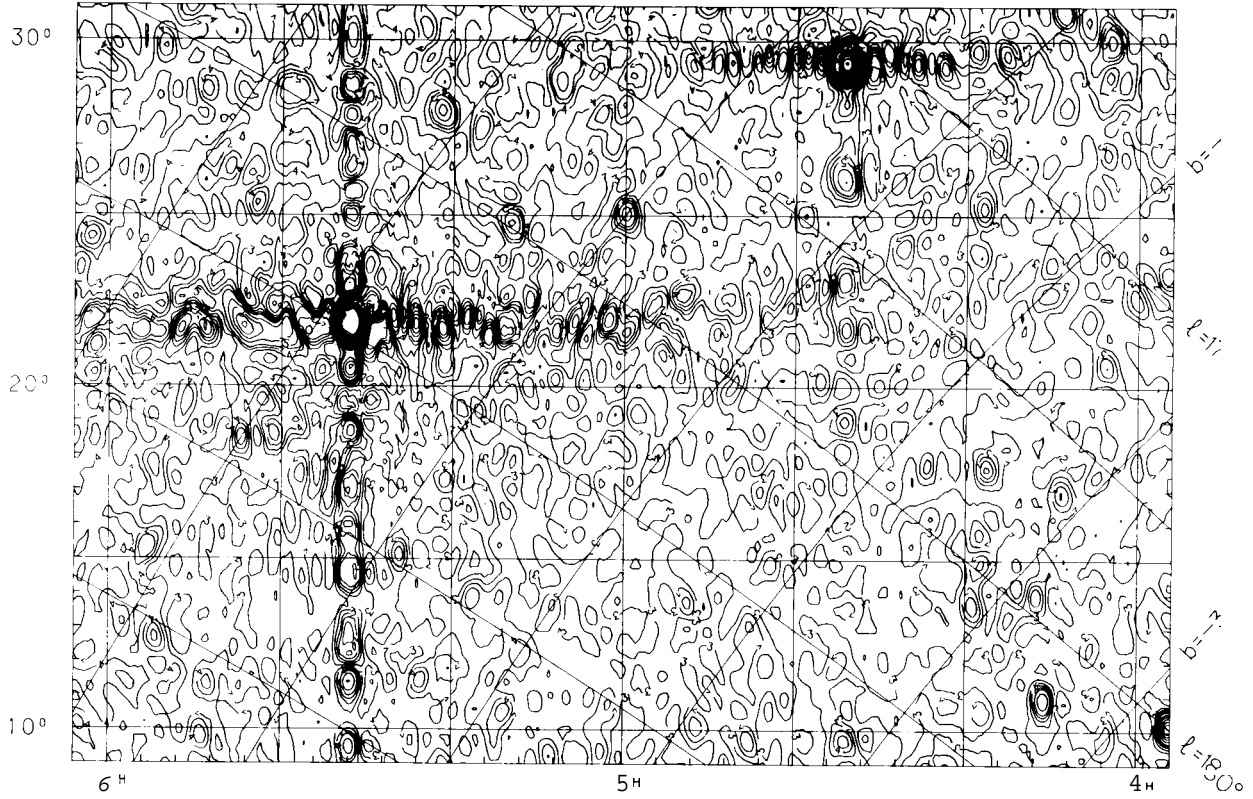
SKY AT 34.5 MHz FROM GEETEE



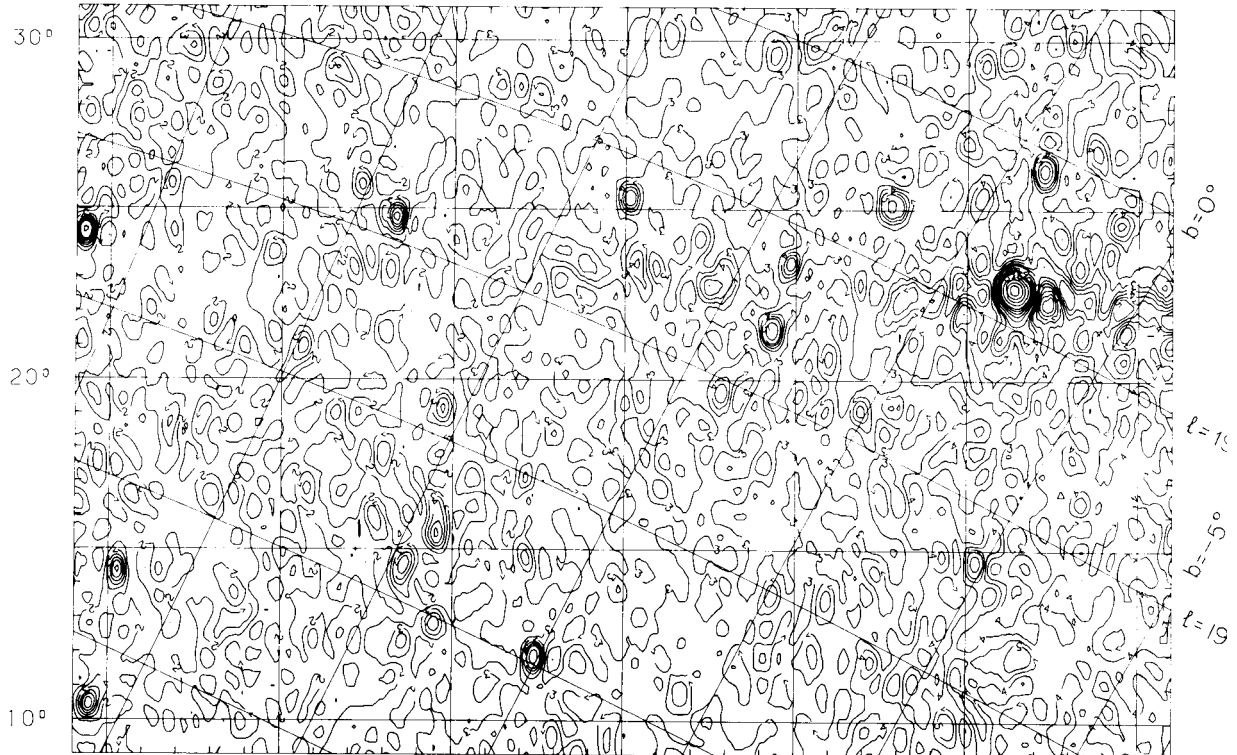
SKY AT 34.5 MHz FROM GEETEE



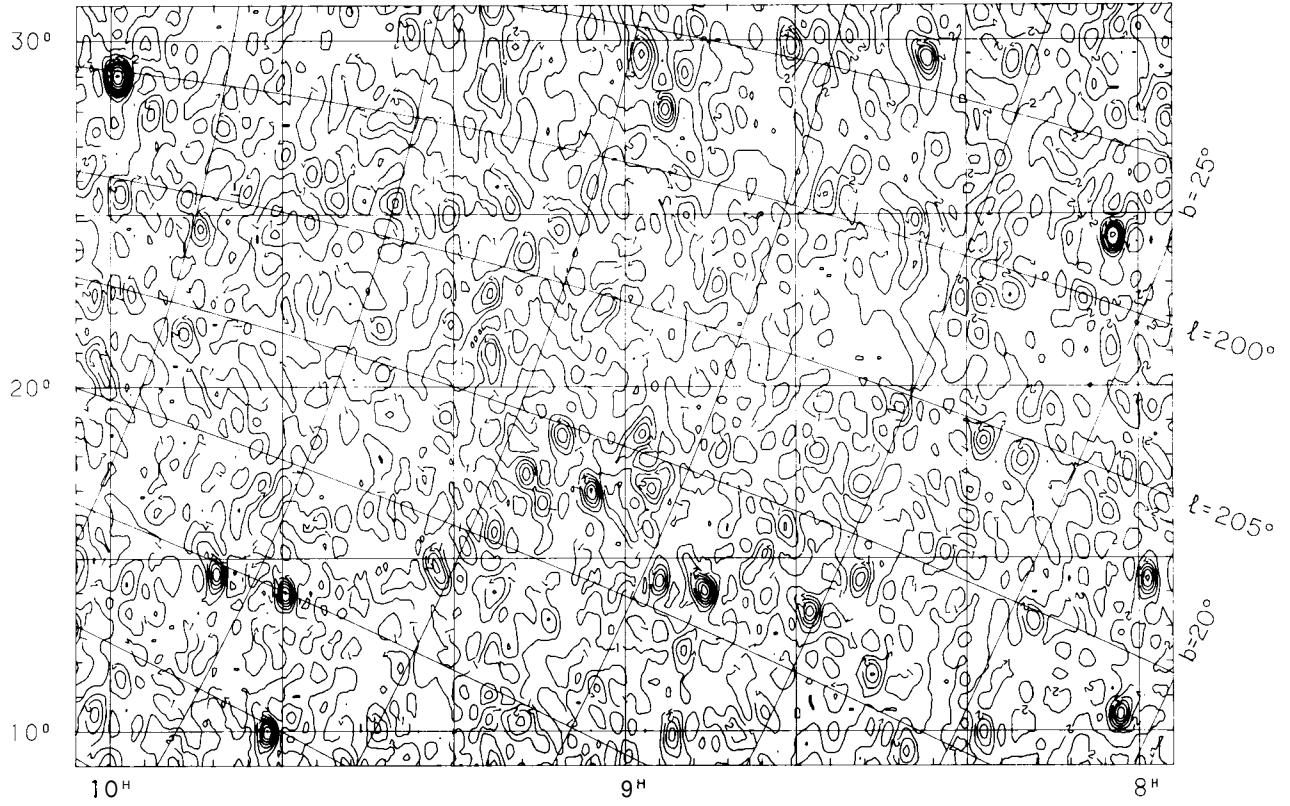
SKY AT 34.5 MHz FROM GEETEE



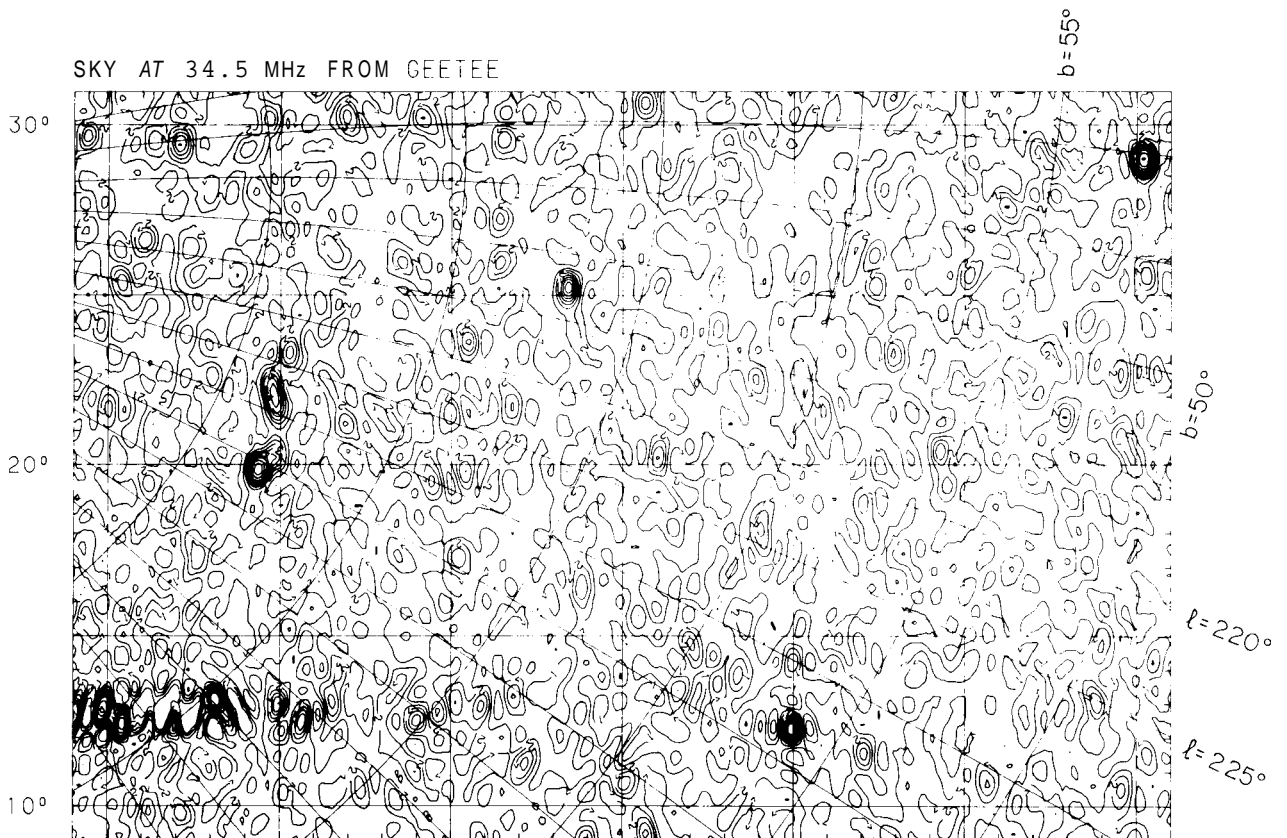
SKY AT 34.5 MHz FROM GEETEE



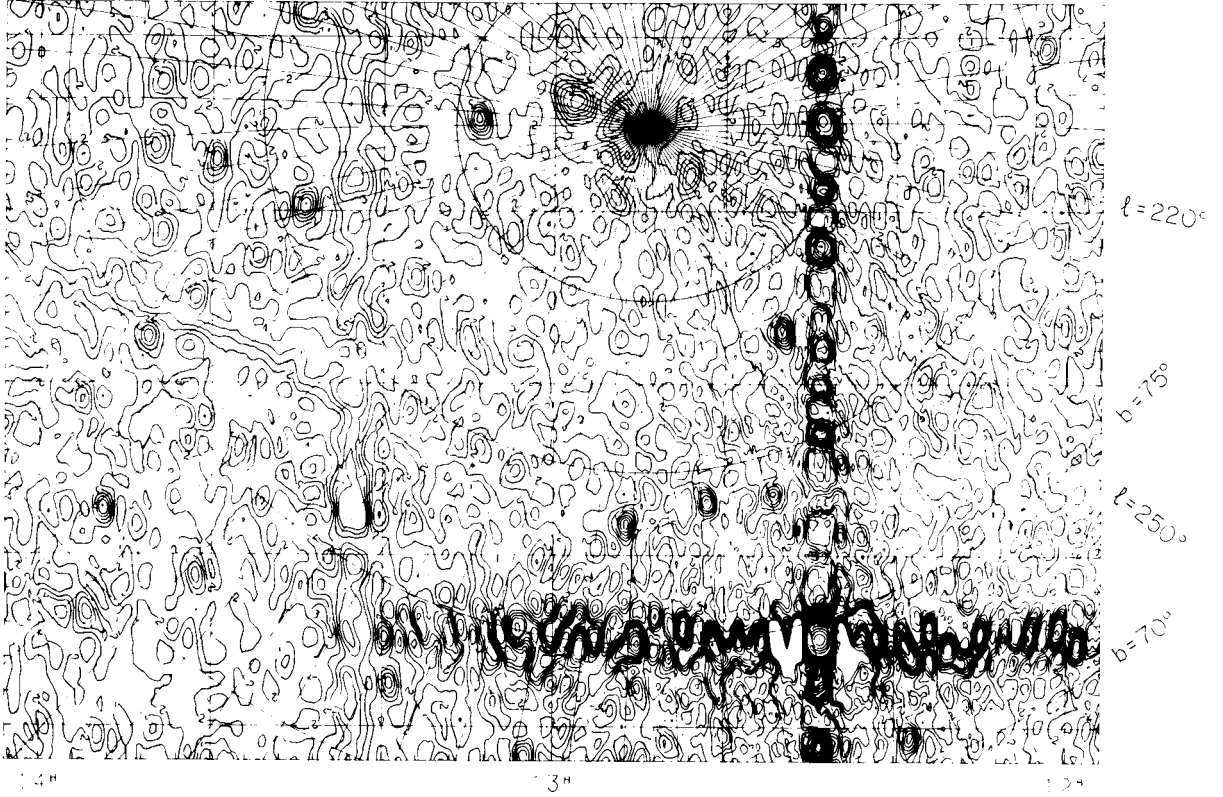
SKY AT 34.5 MHz FROM GEETEE



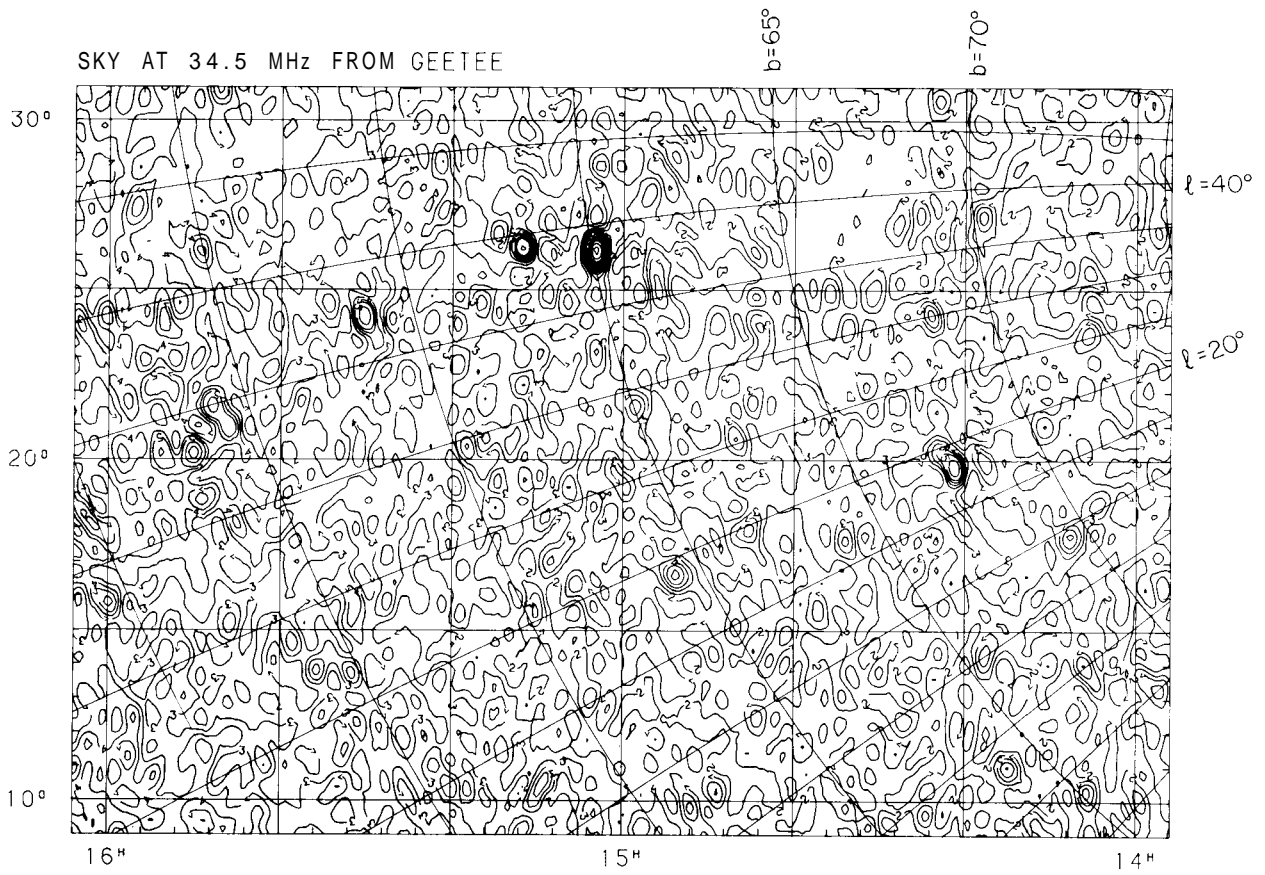
SKY AT 34.5 MHz FROM GEETEE



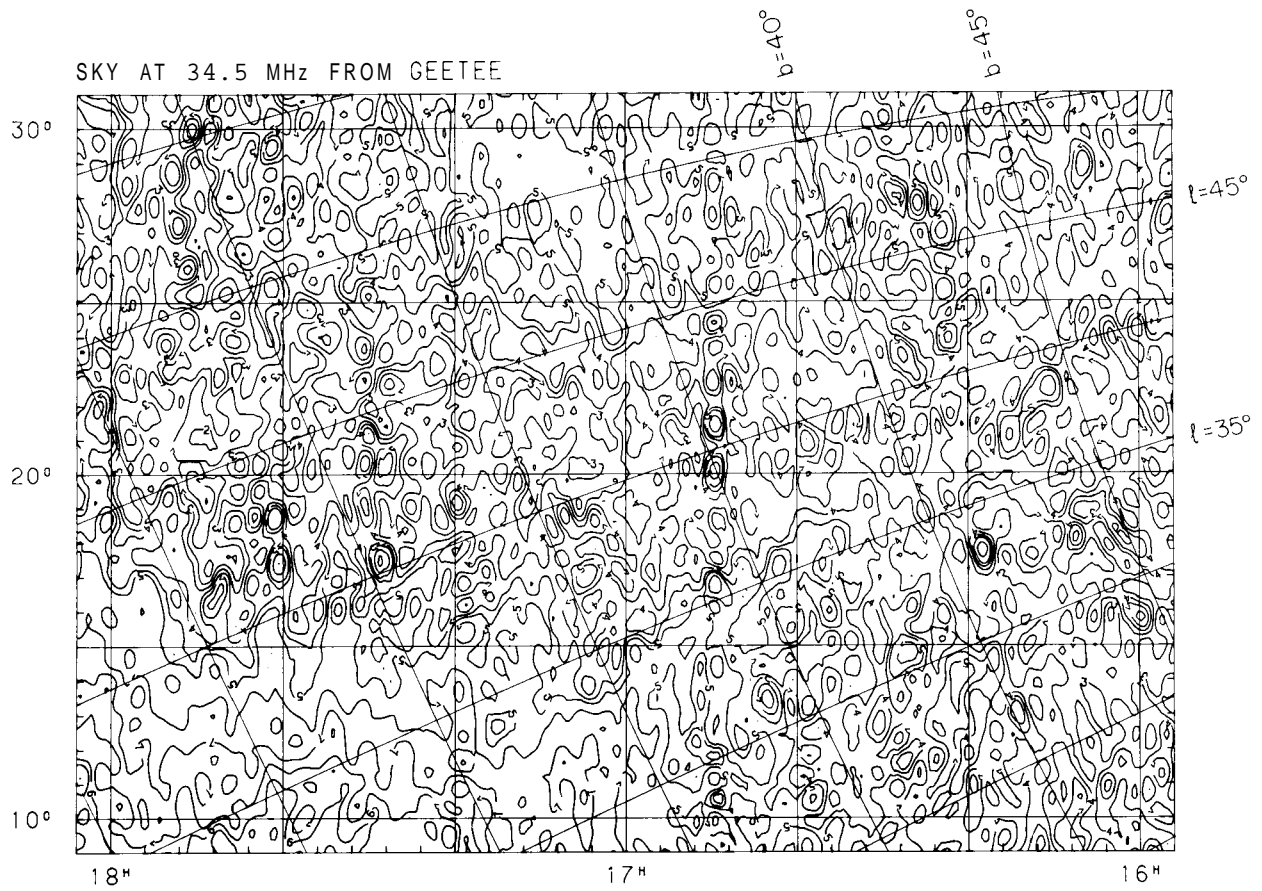
SKY AT 34.5 MHz FROM GEETEE



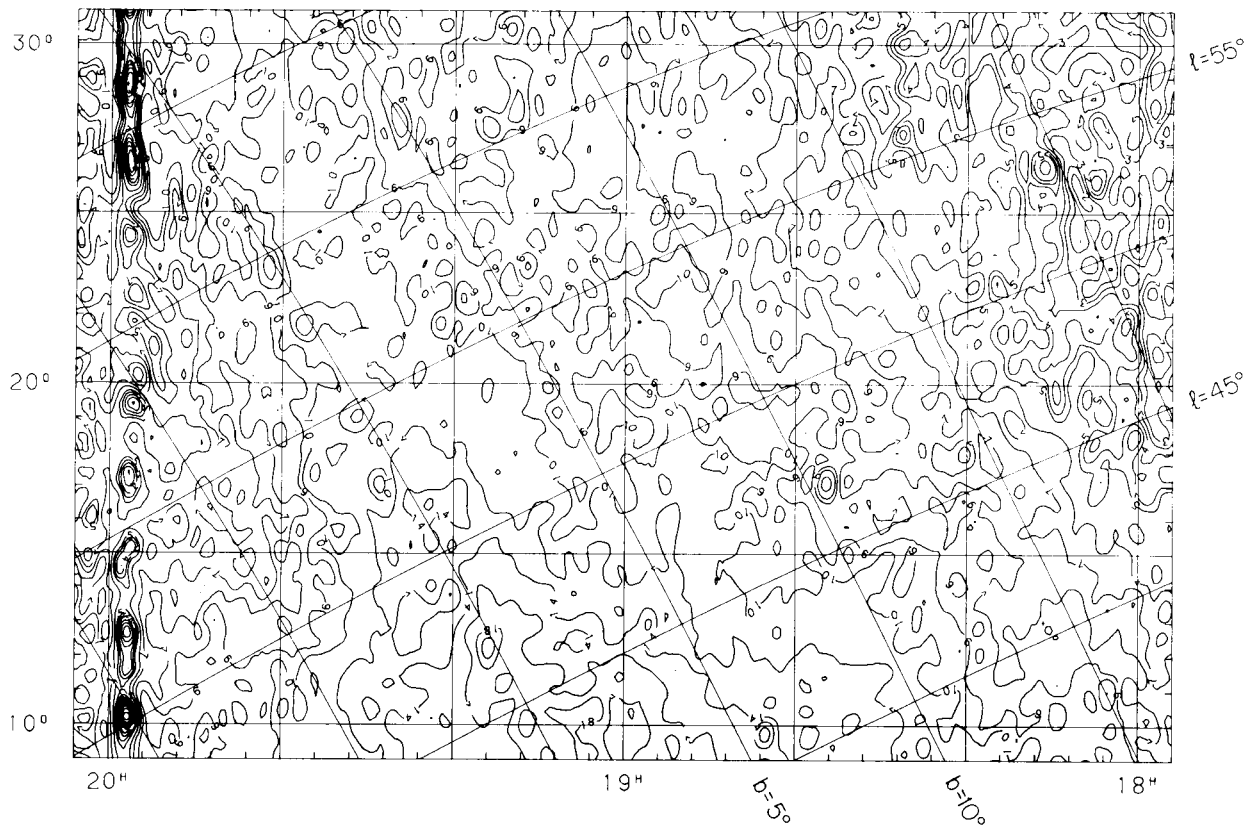
SKY AT 34.5 MHz FROM GEETEE



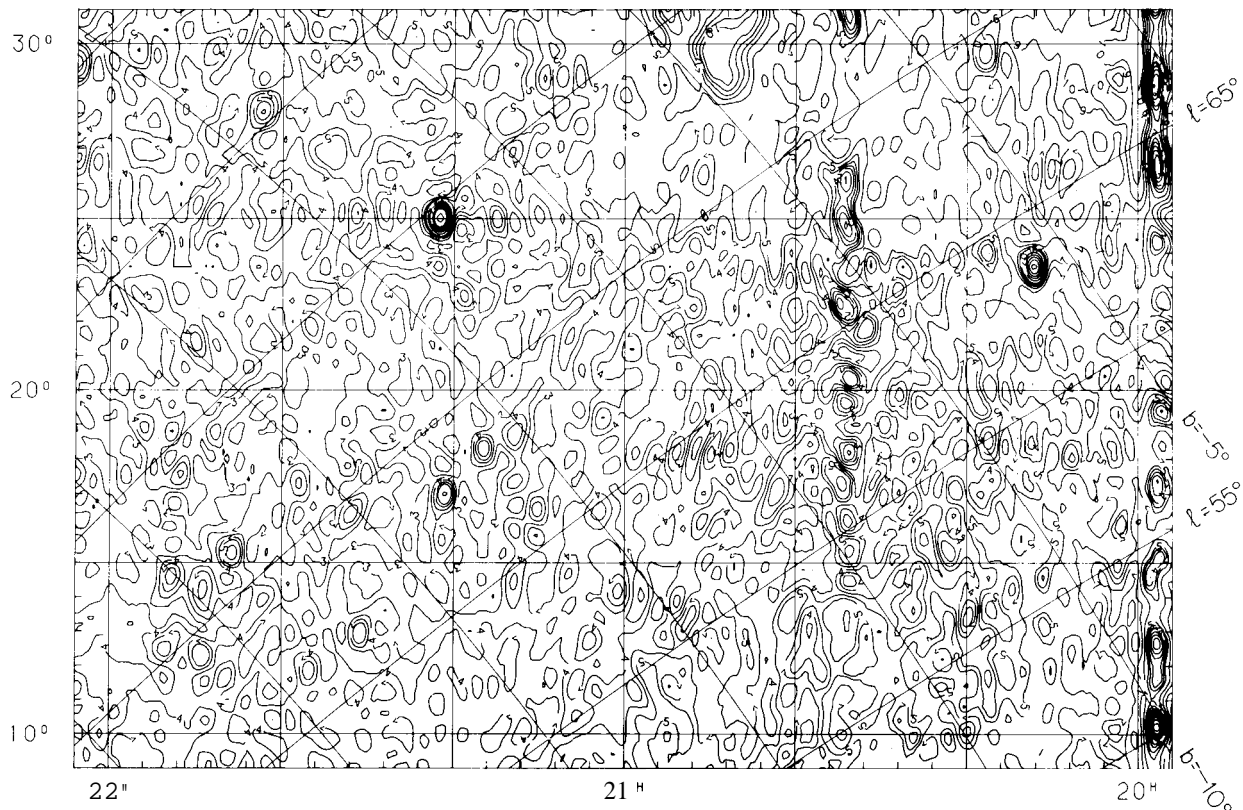
SKY AT 34.5 MHz FROM GEETEE



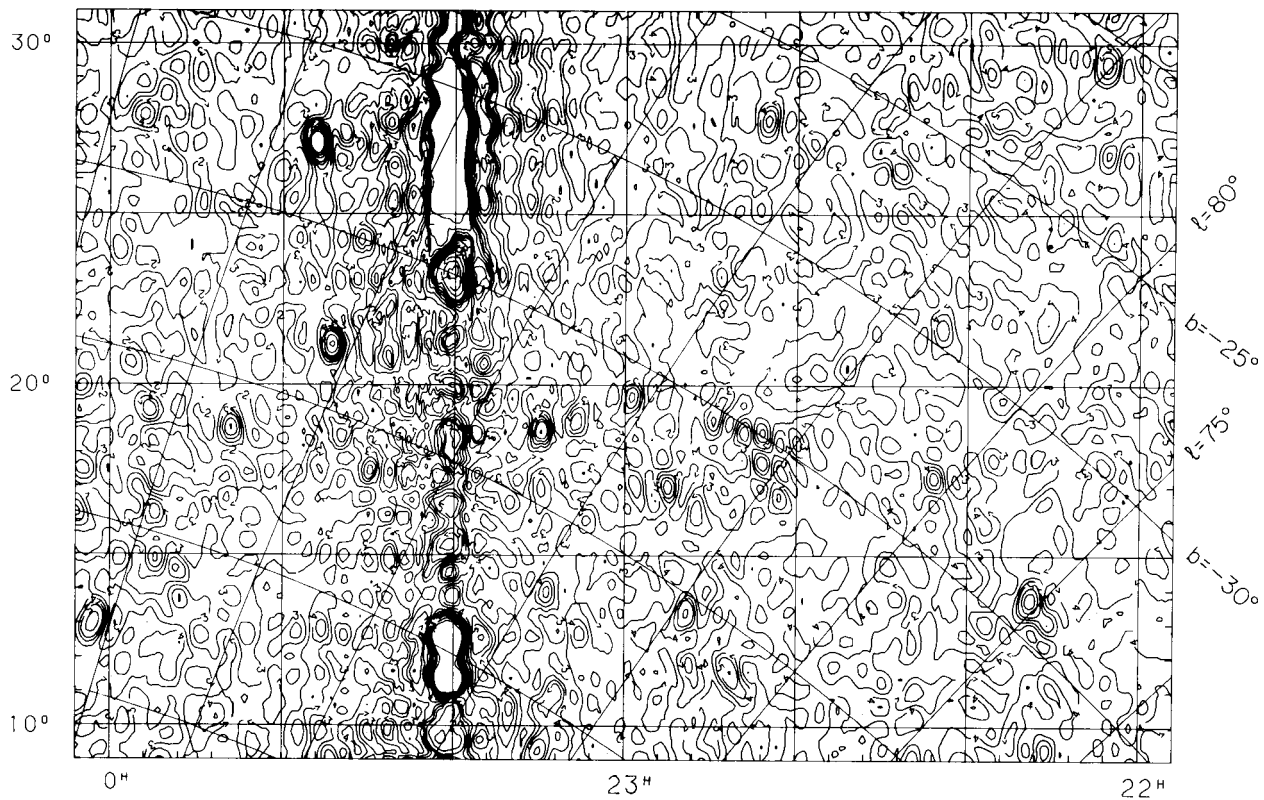
SKY AT 34.5 MHz FROM GEETEE



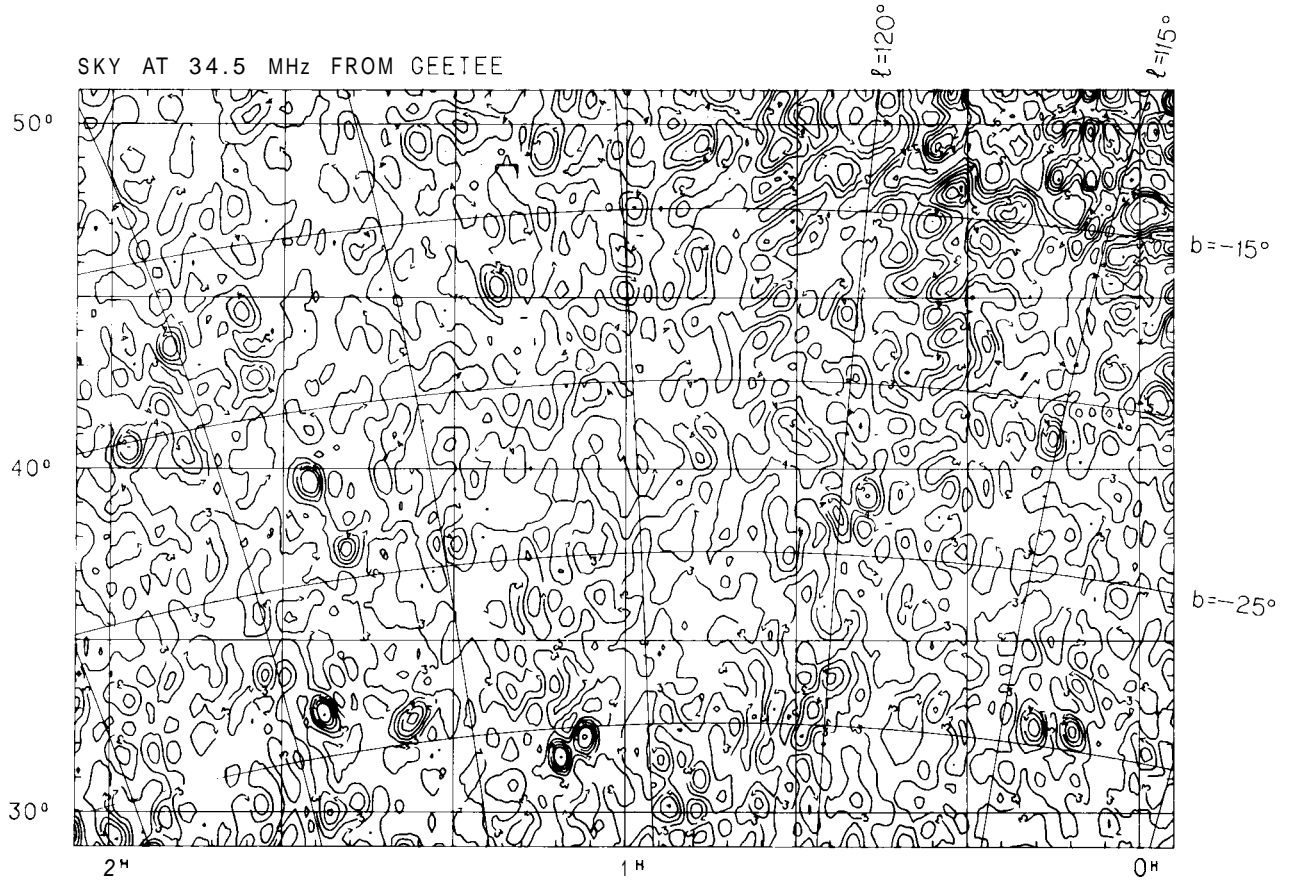
SKY AT 34.5 MHz FROM GEETEE



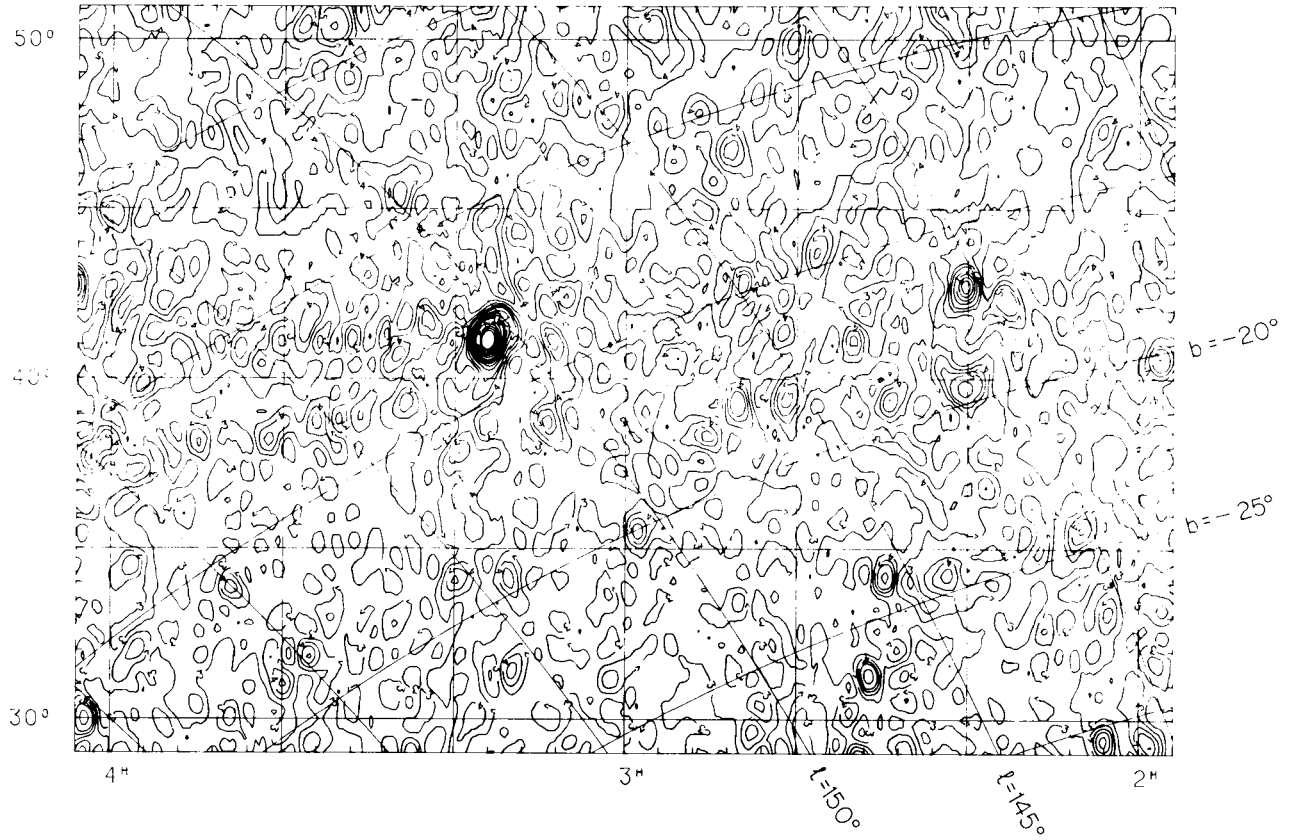
SKY AT 34.5 MHz FROM GEETEE



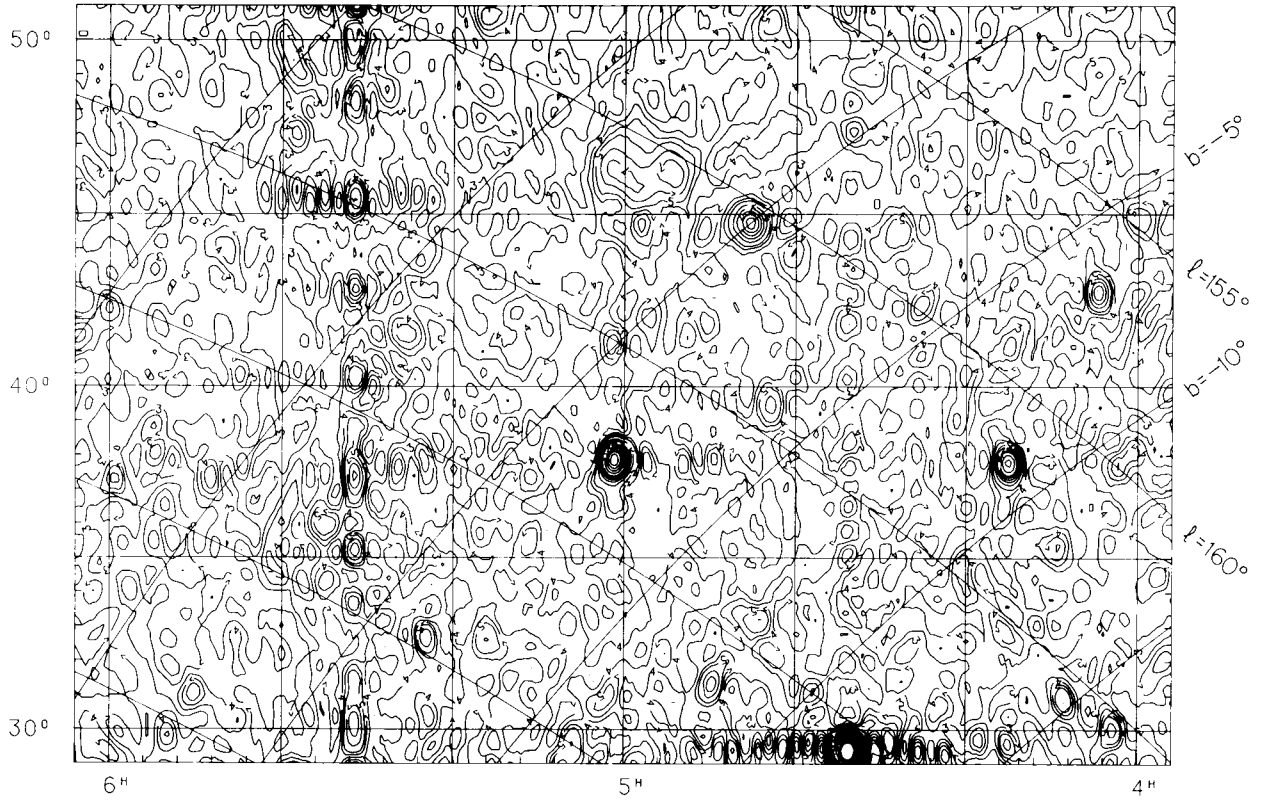
SKY AT 34.5 MHz FROM GEETEE



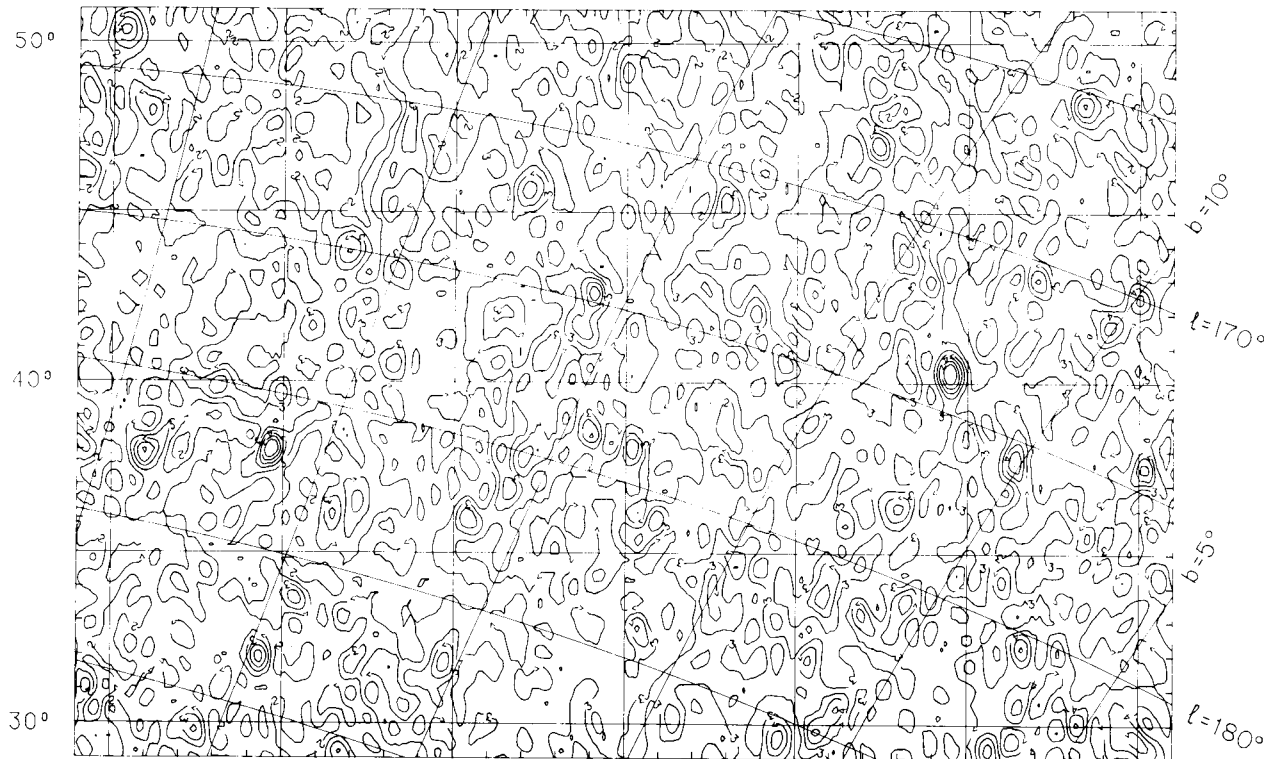
SKY AT 34.5 MHz FROM GEETEE



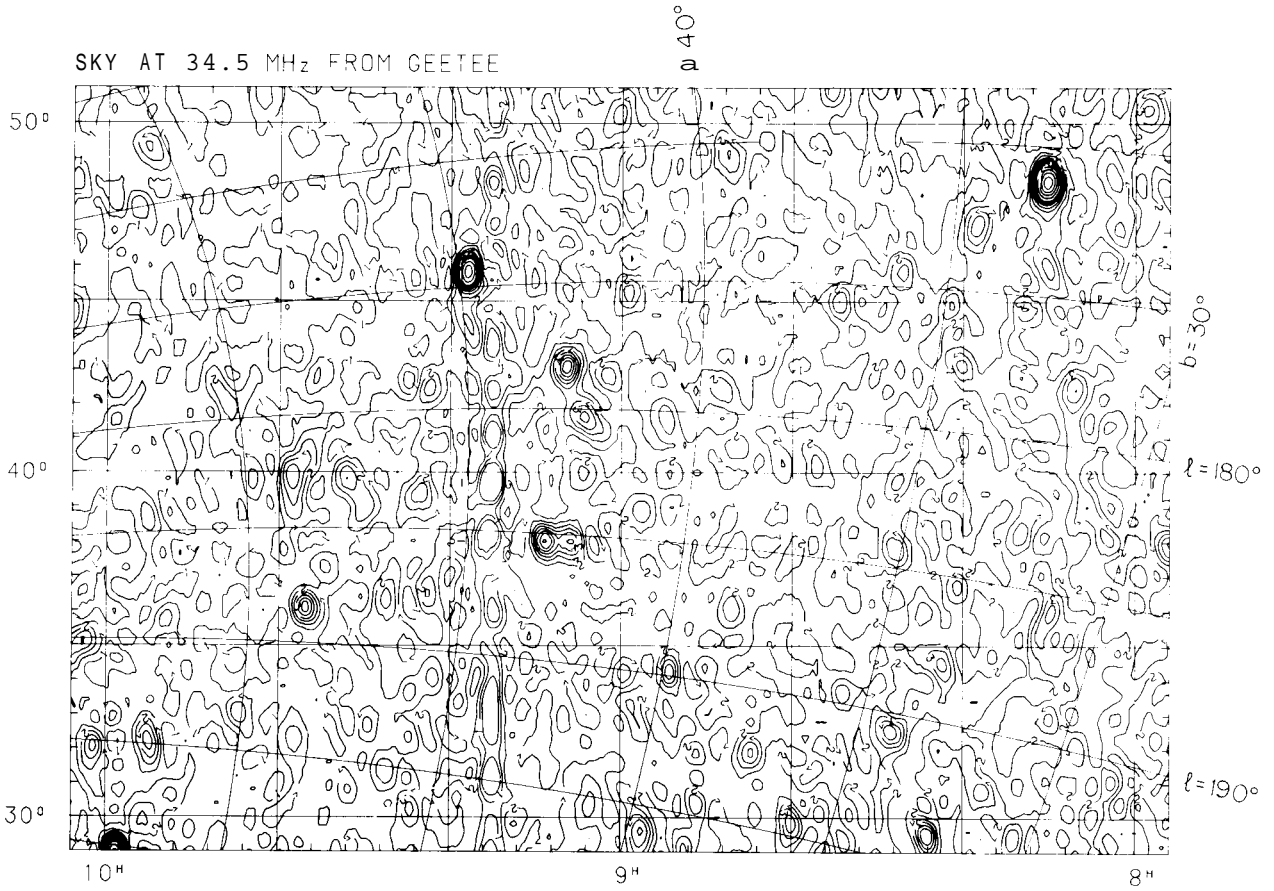
SKY AT 34.5 MHz FROM GEETEE



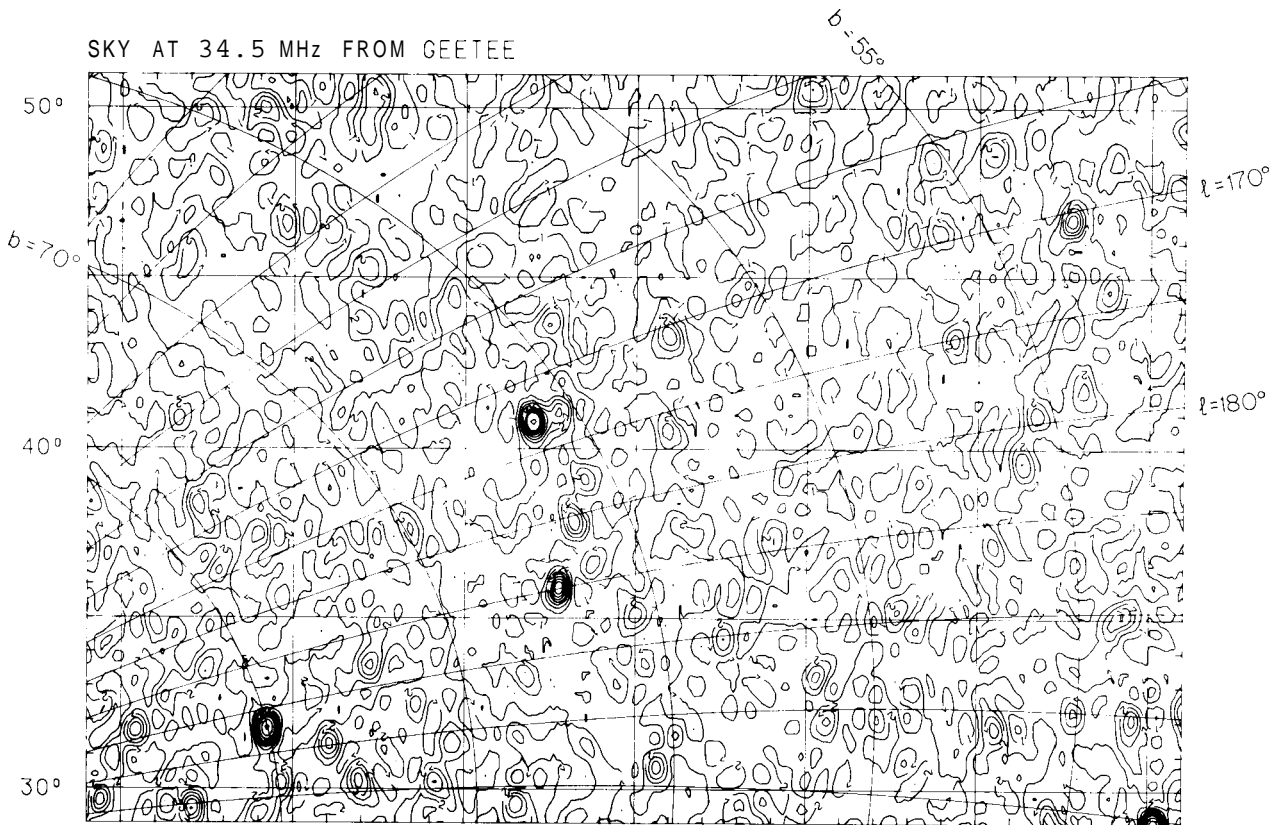
SKY AT 34.5 MHz FROM GEETEE



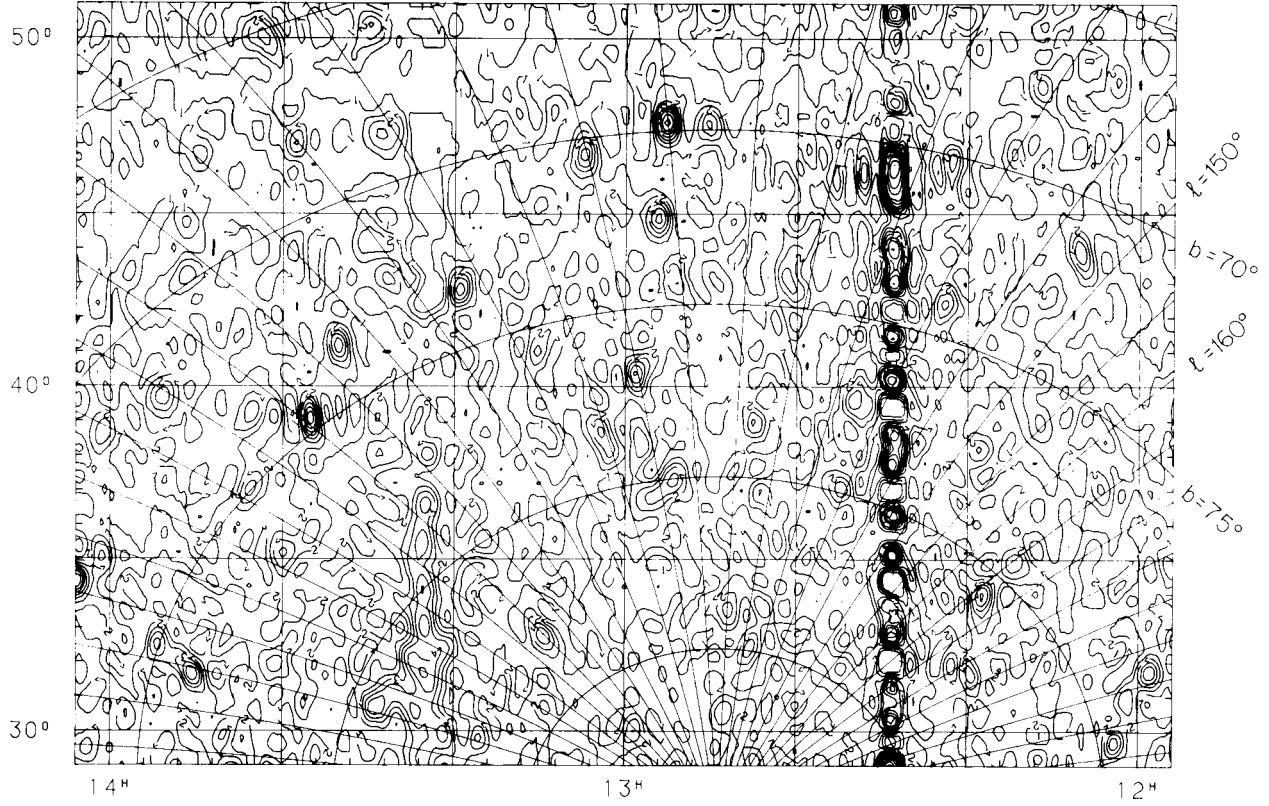
SKY AT 34.5 MHz FROM GEETEE



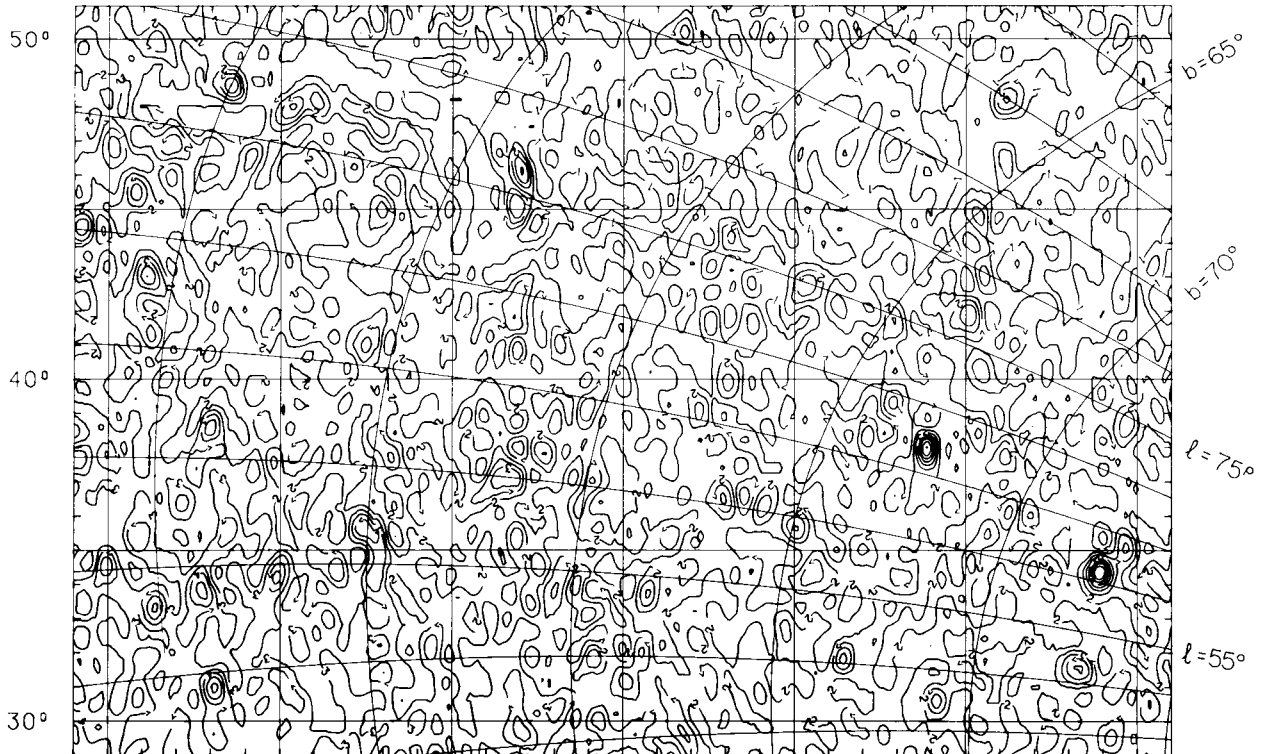
SKY AT 34.5 MHz FROM GEETEE



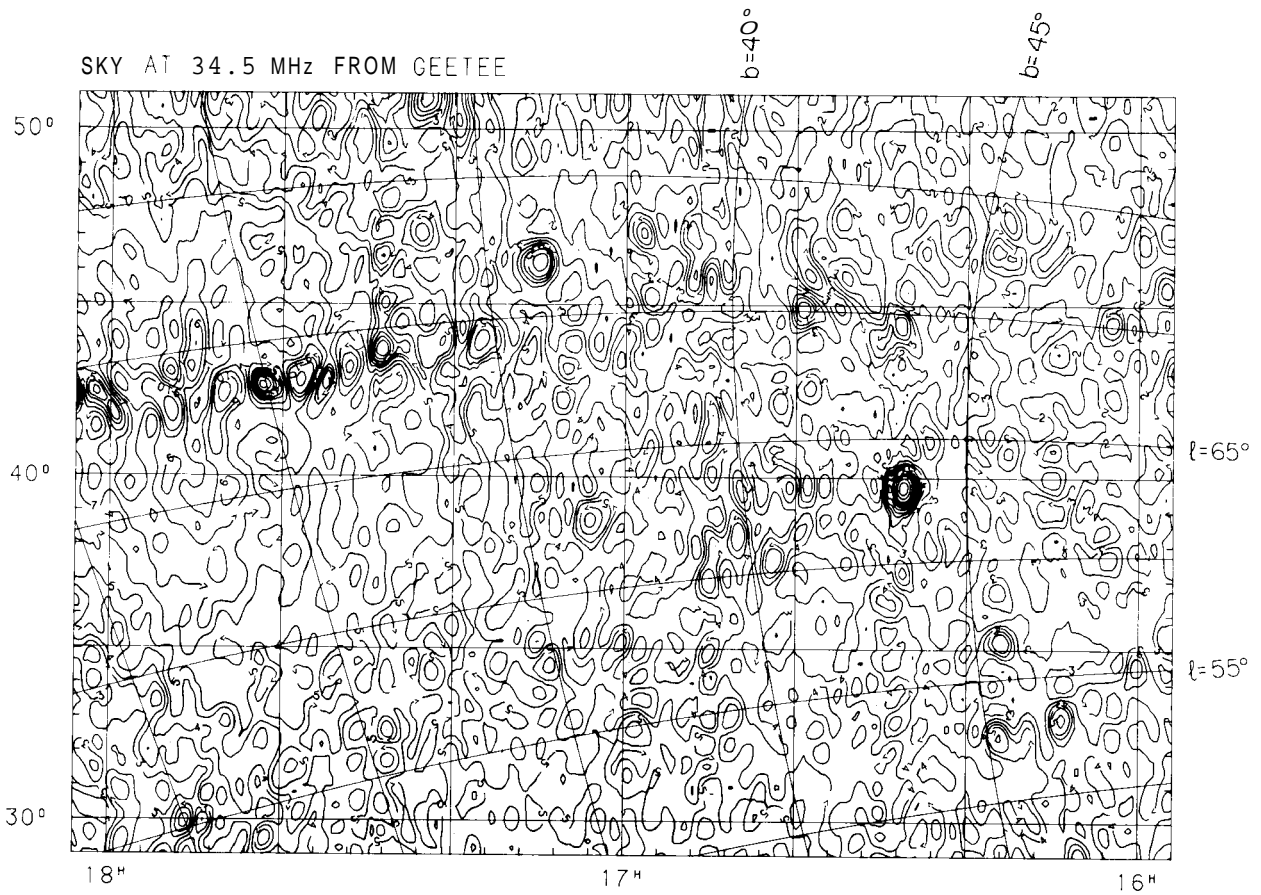
SKY AT 34.5 MHz FROM GEETEE



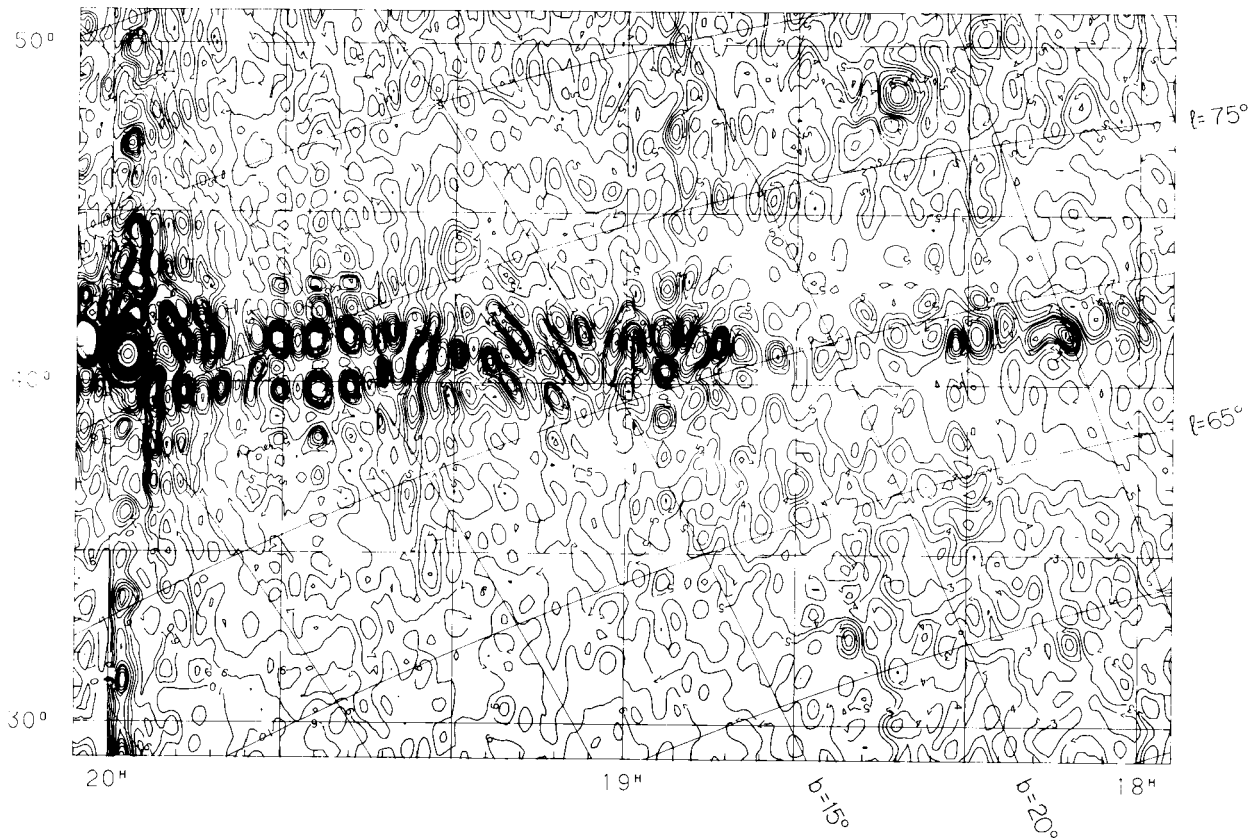
SKY AT 34.5 MHz FROM GEETEE



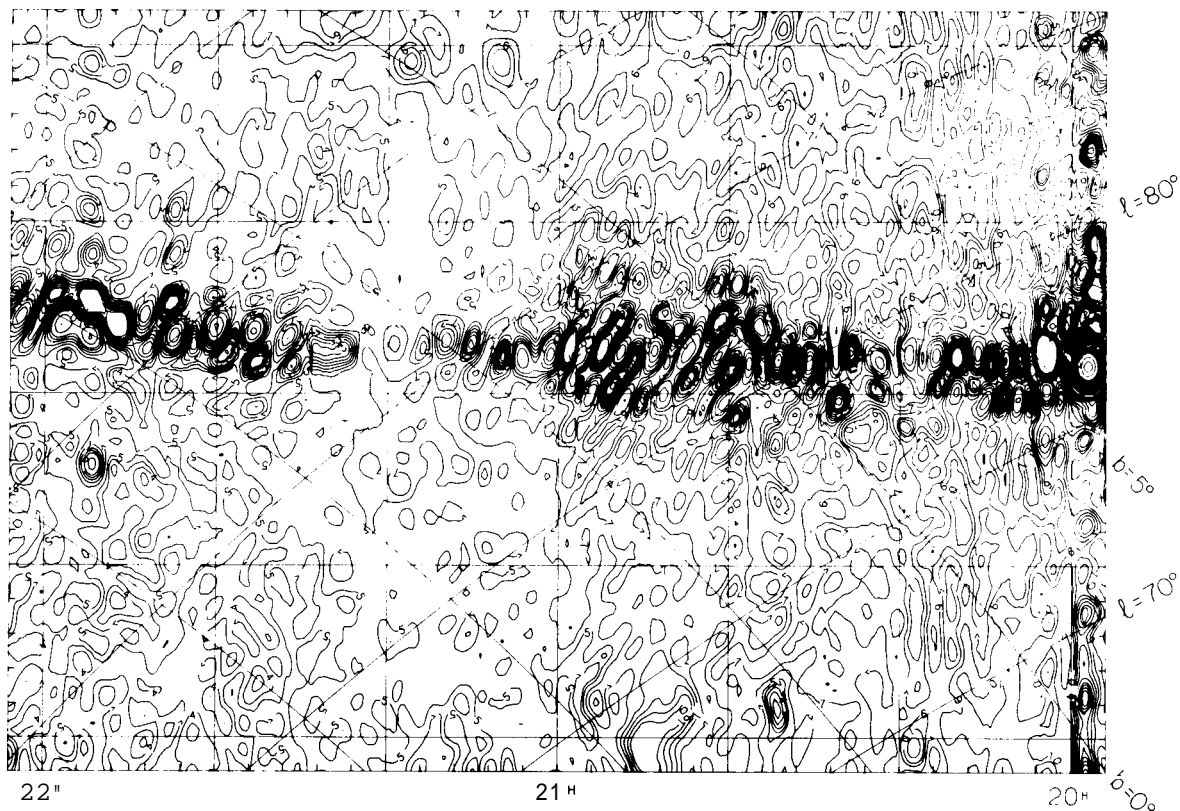
SKY AT 34.5 MHz FROM GEETEE



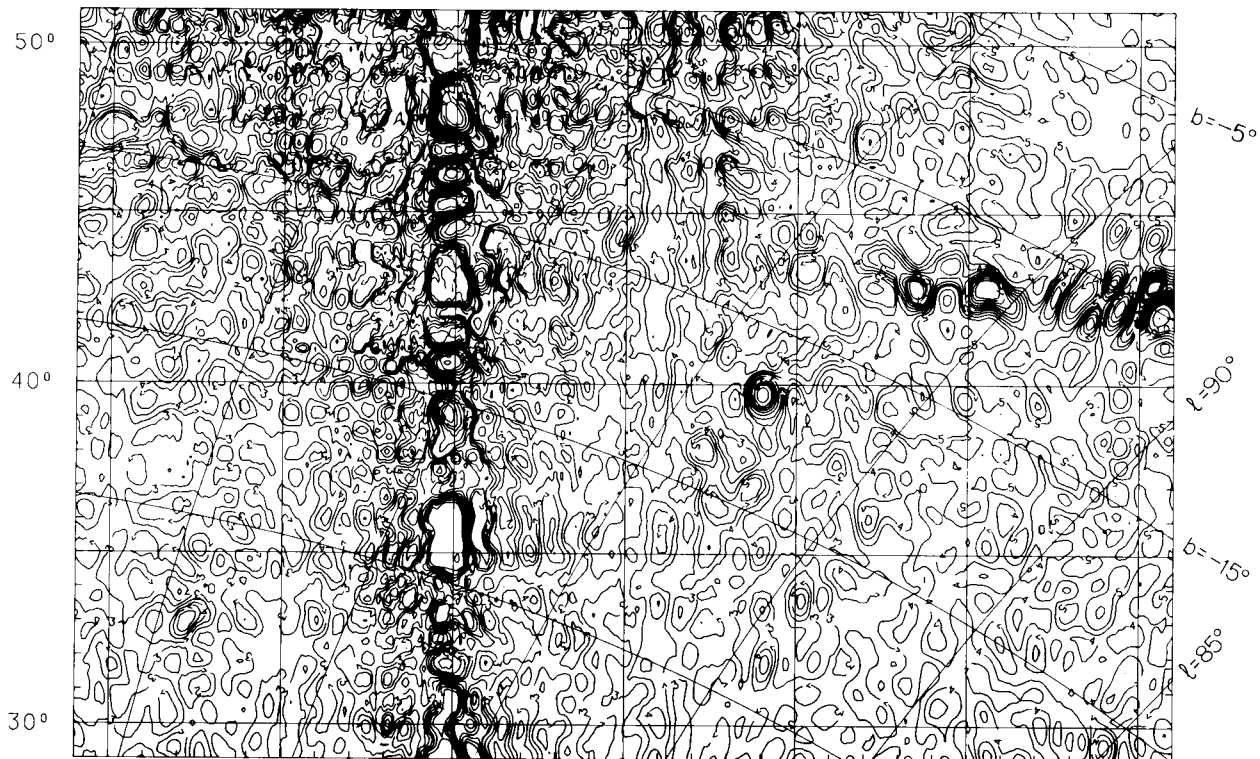
SKY AT 34.5 MHz FROM GEETEE



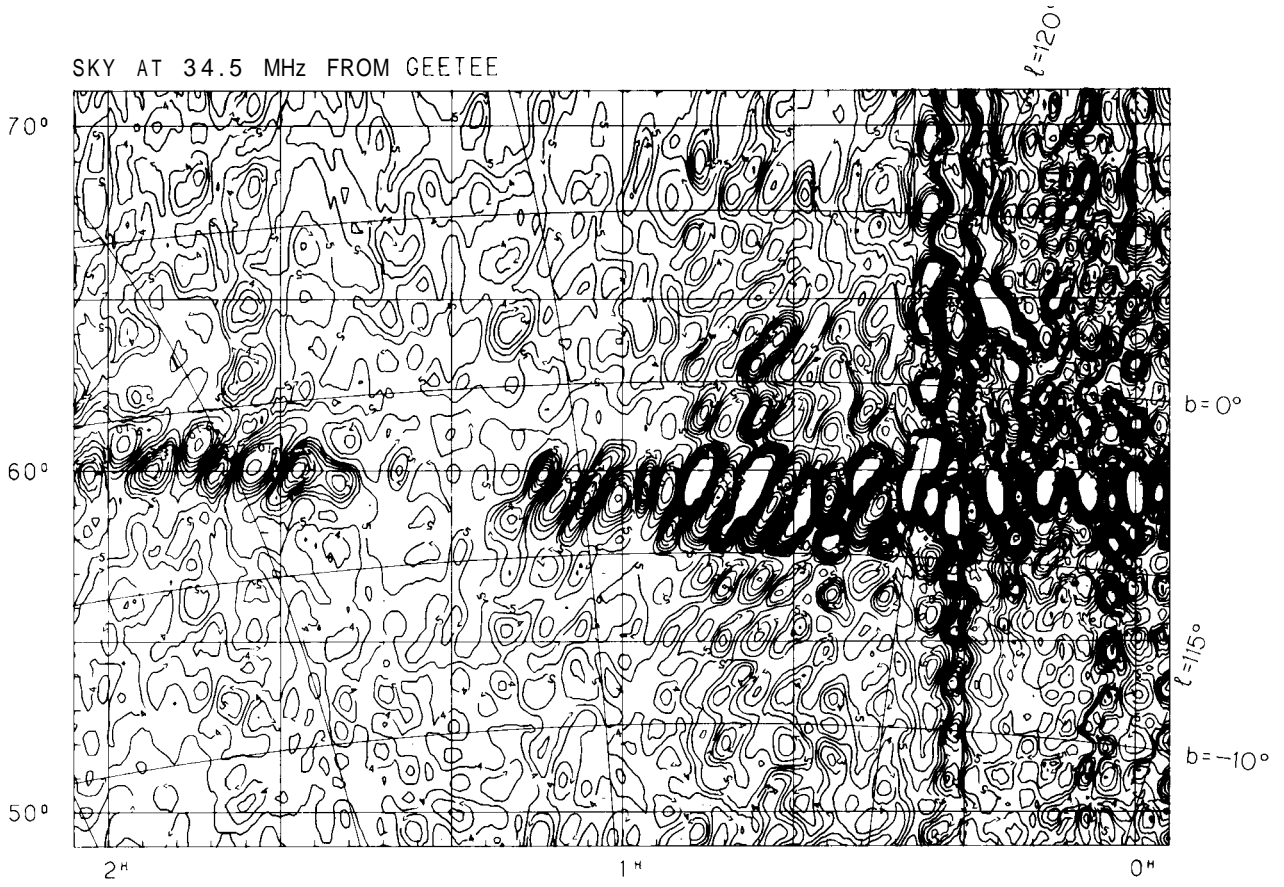
SKY AT 33.5 MHz FROM GEETEF



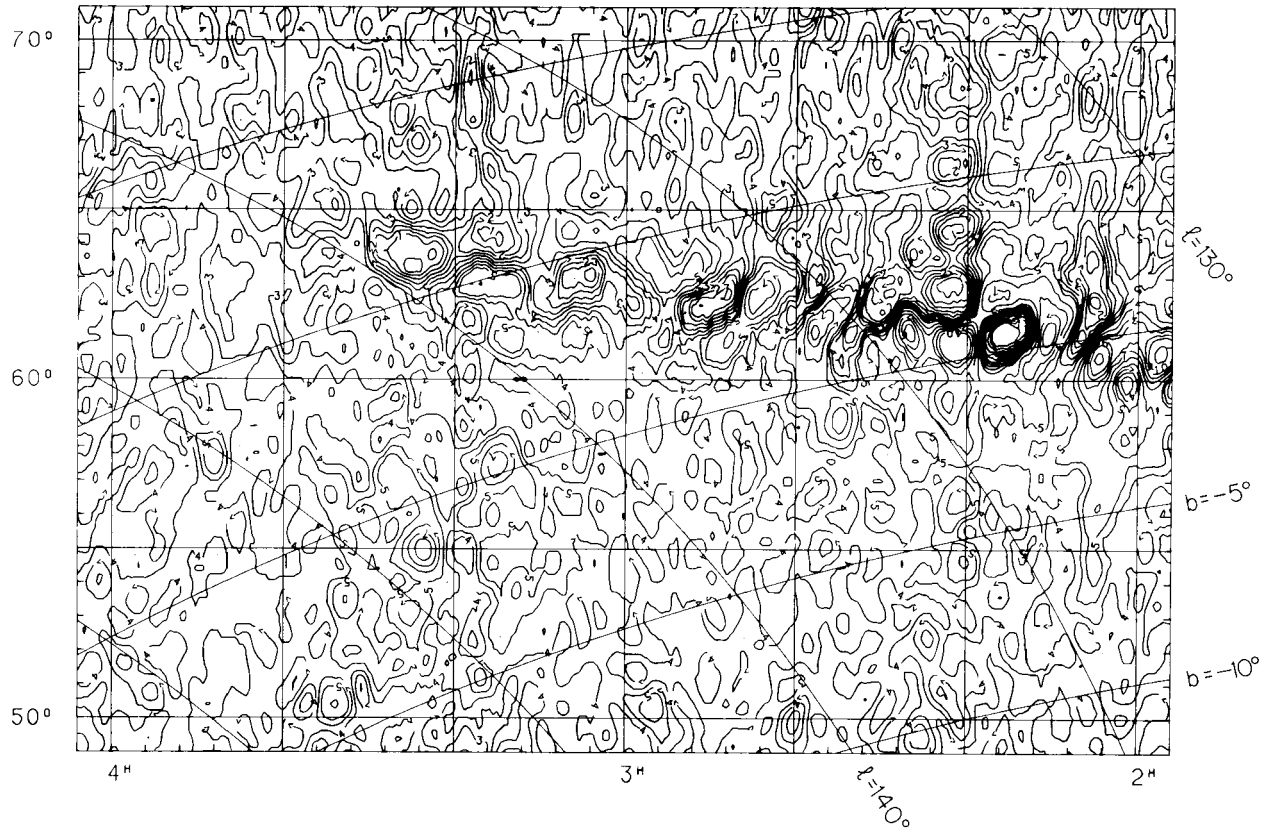
SKY AT 34.5 MHz FROM GEETEE



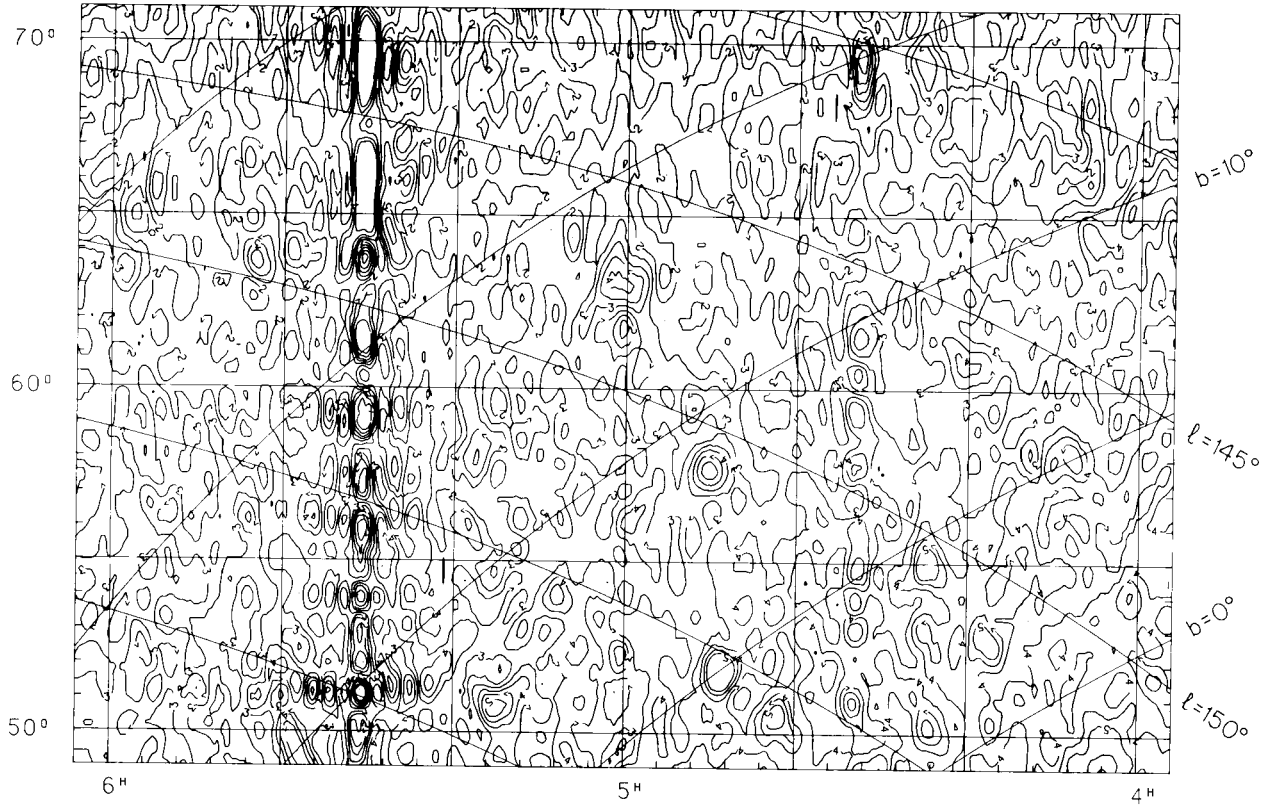
SKY AT 34.5 MHz FROM GEETEE



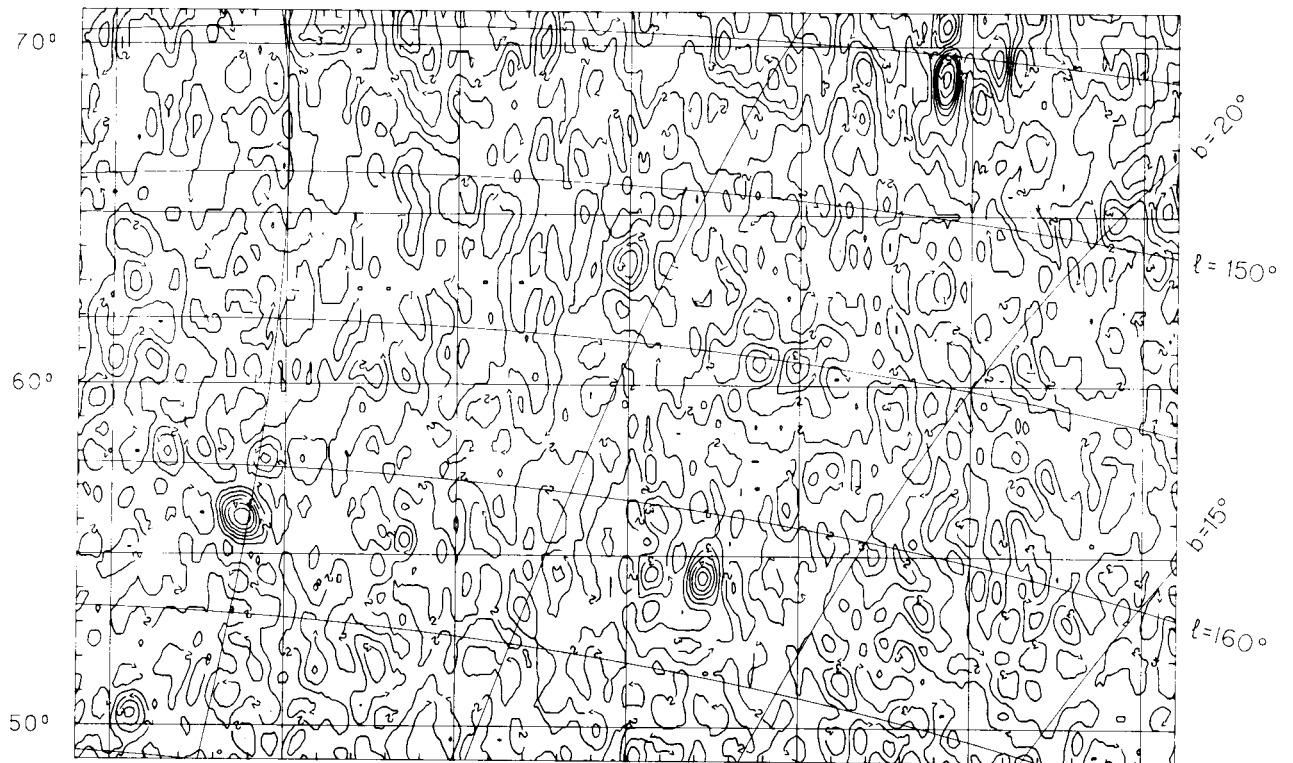
SKY AT 34.5 MHz FROM GEETEE



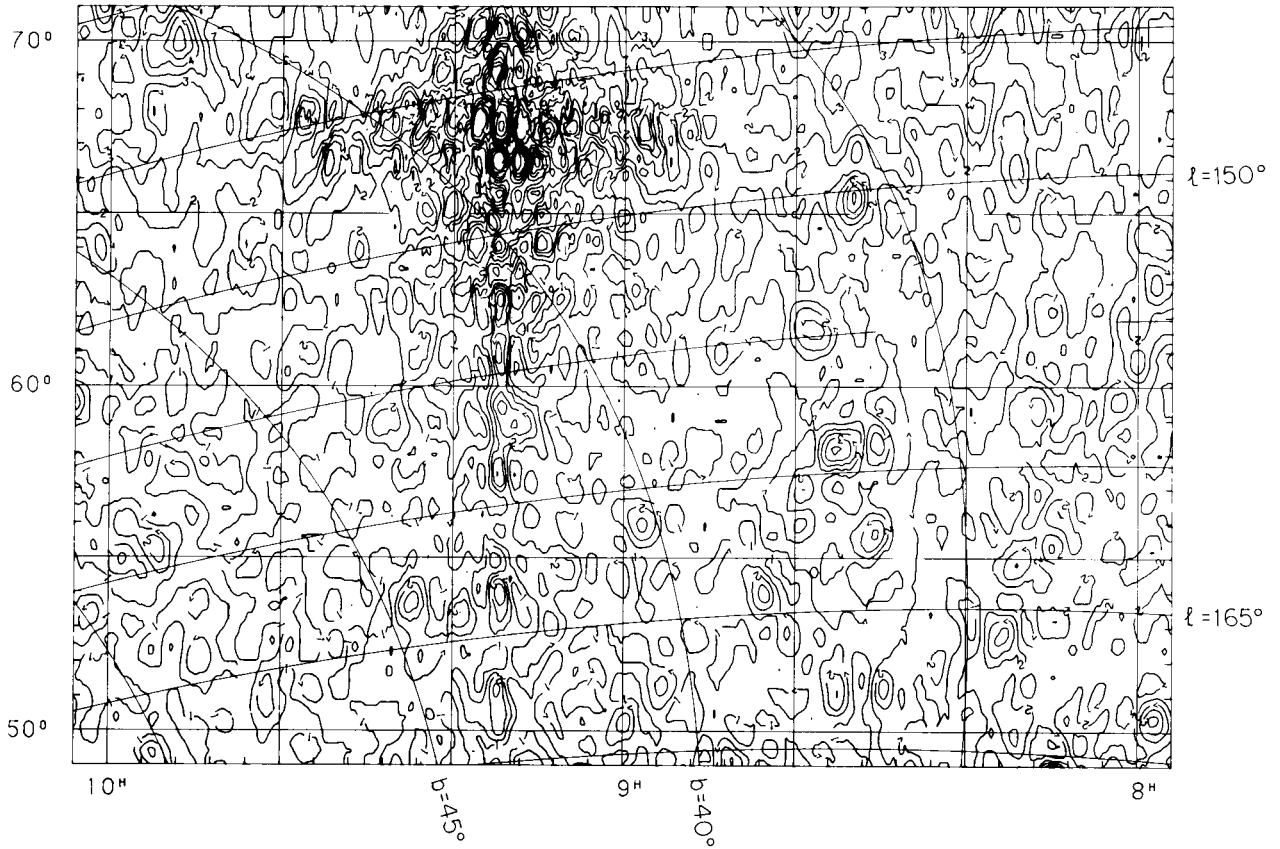
SKY AT 34.5 MHz FROM GEETEE



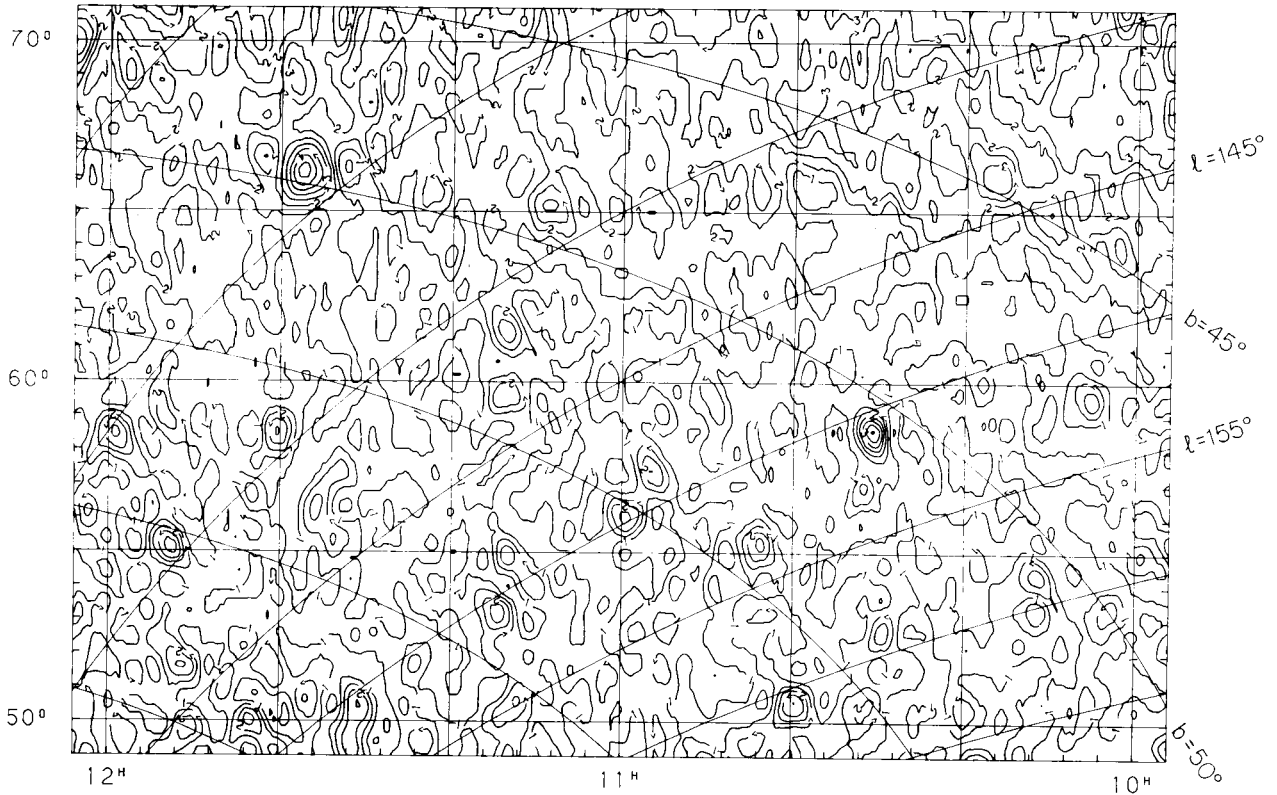
SKY AT 34.5 MHz FROM GEETEE



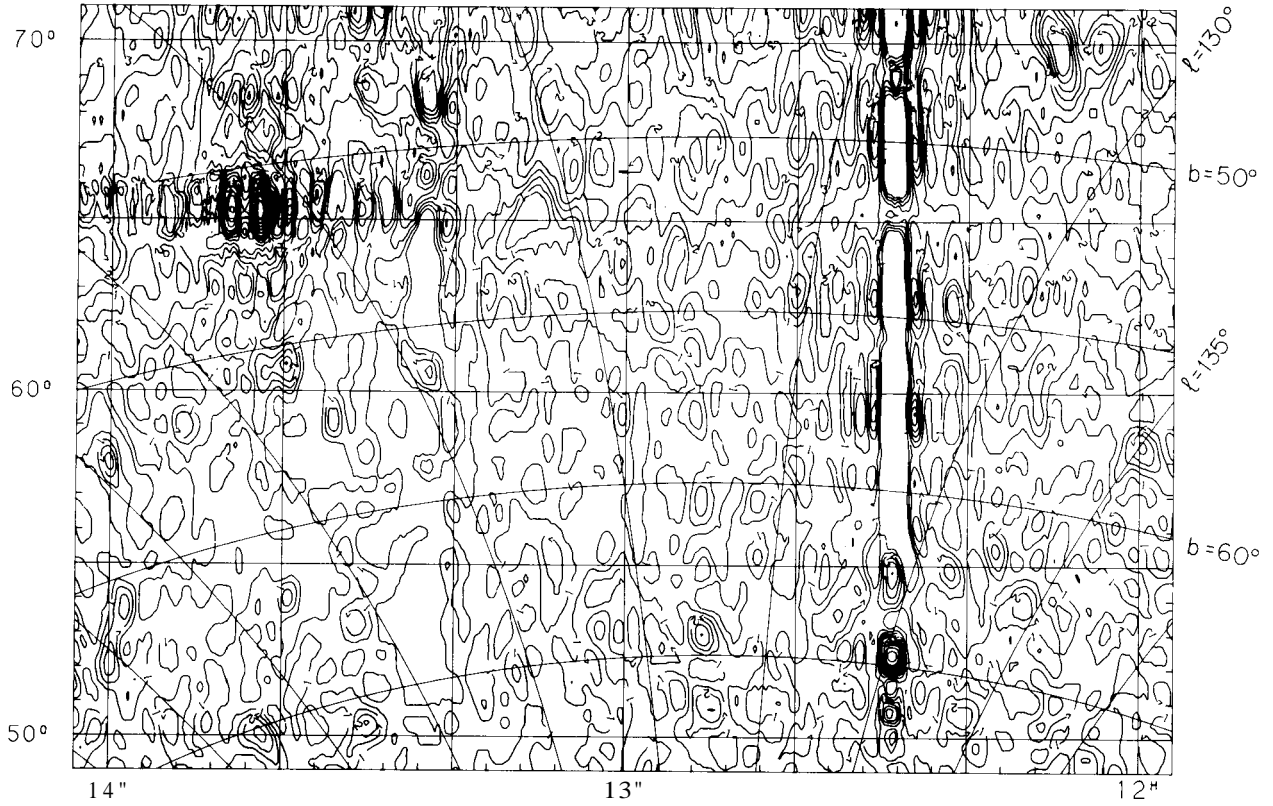
SKY AT 34.5 MHz FROM GEETEE



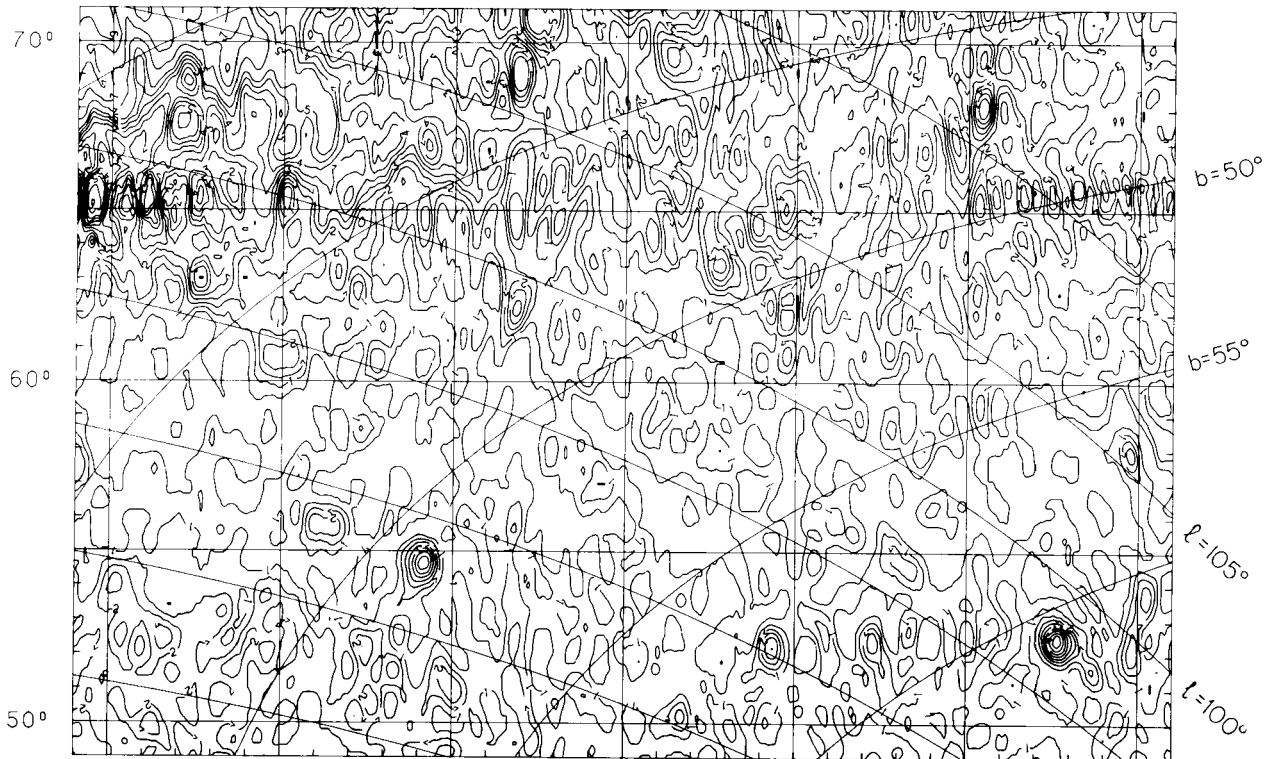
SKY AT 34.5 MHz FROM GEETEE



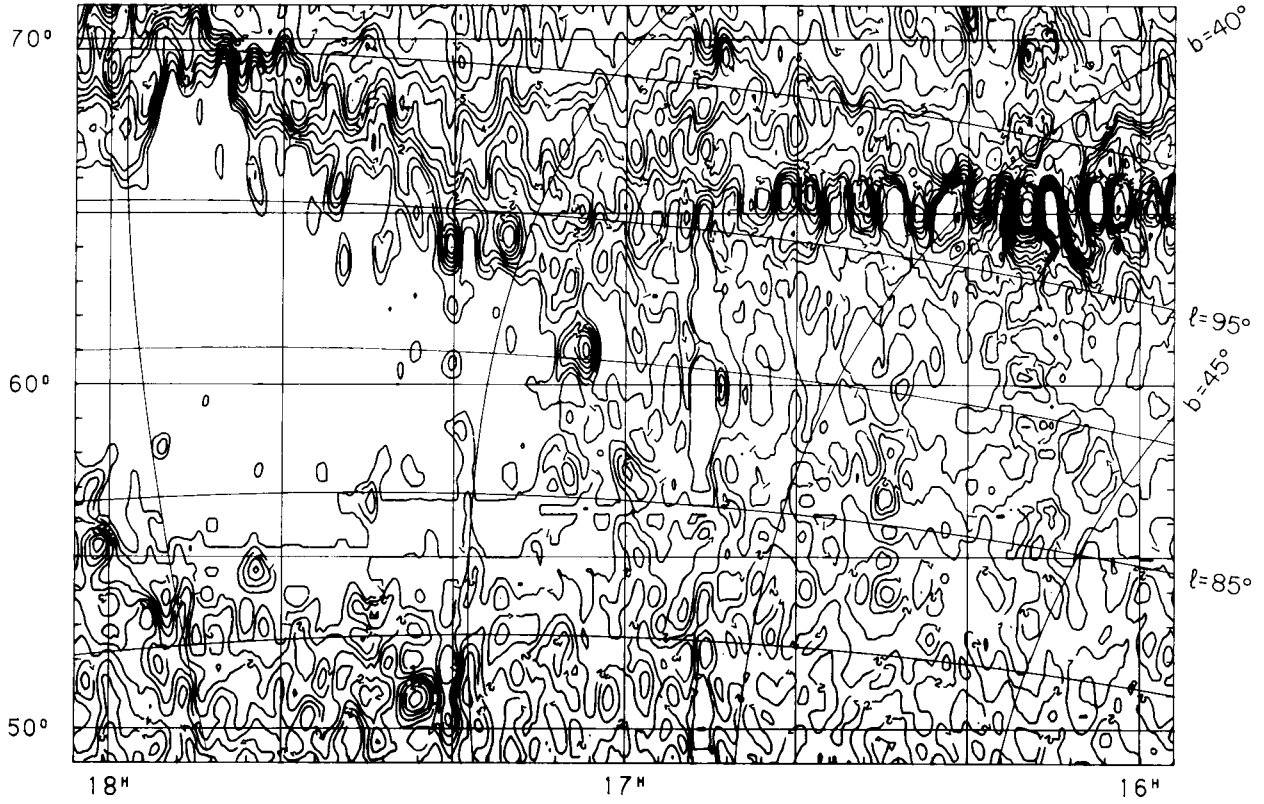
SKY AT 34.5 MHz FROM GEETEE



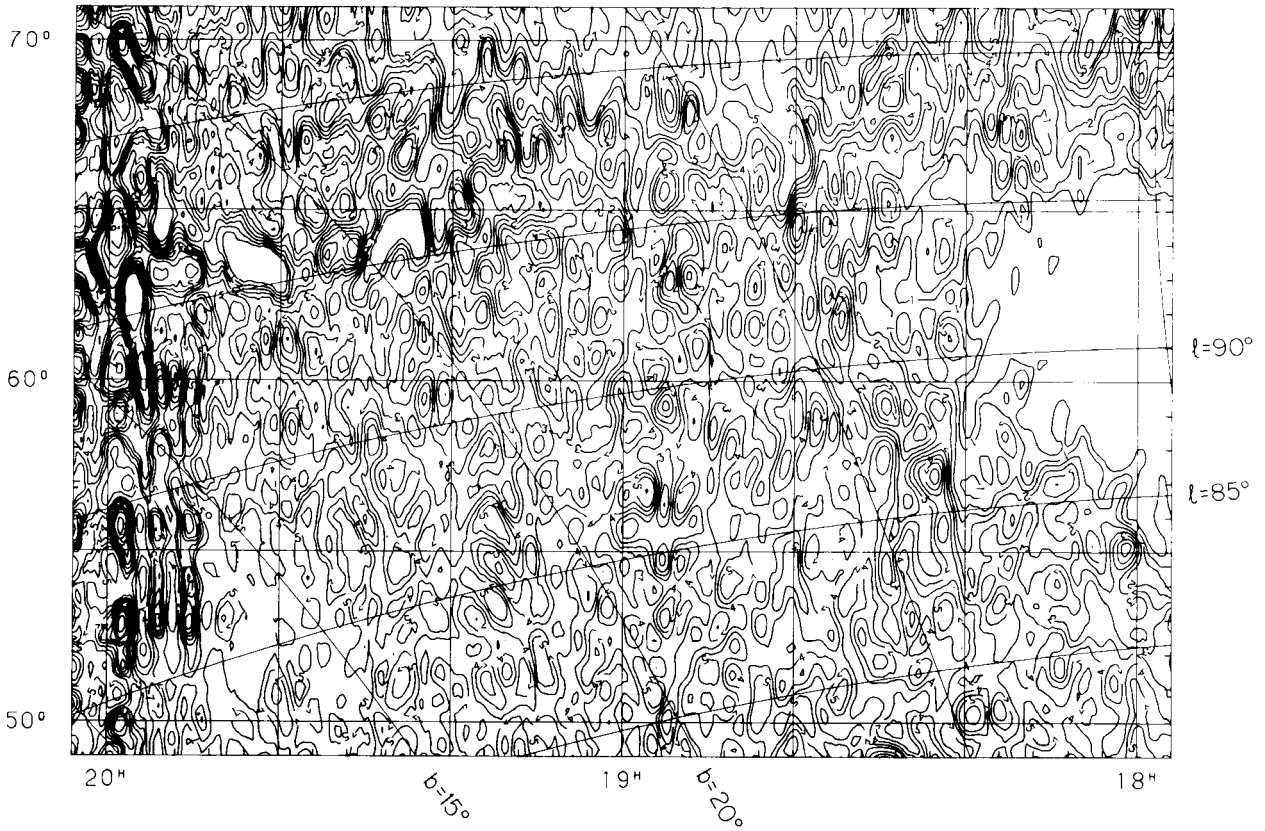
SKY AT 34.5 MHz FROM GEETEE



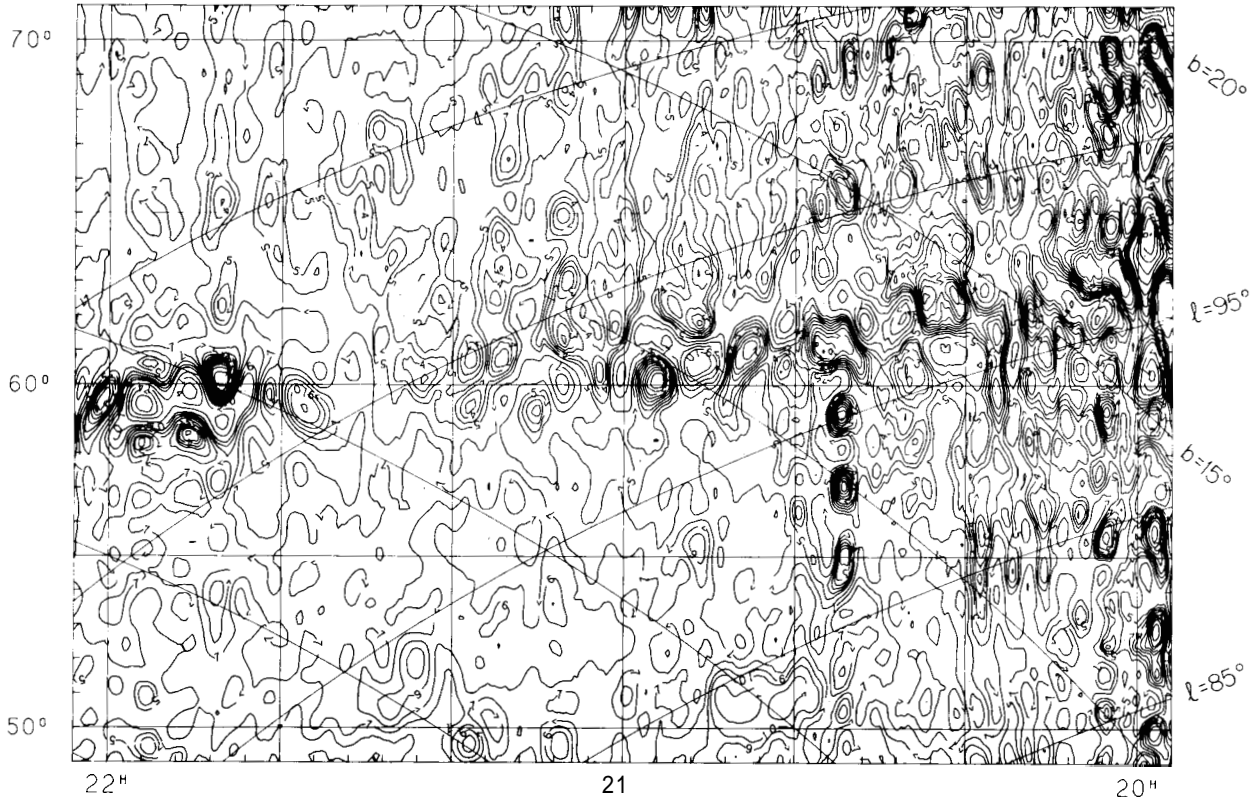
SKY AT 34.5 MHz FROM GEETEE




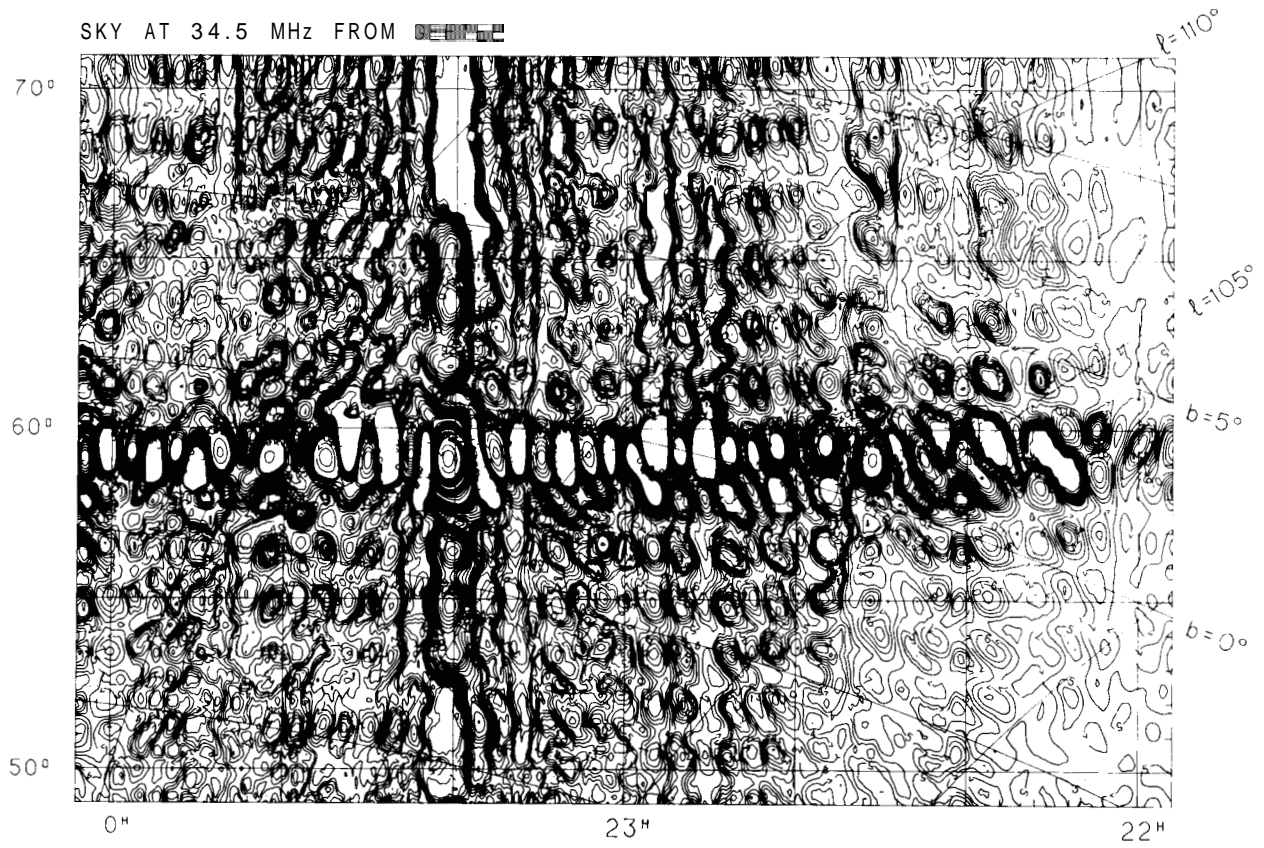
SKY AT 34.5 MHz FROM GEETEE



SKY AT 34.5 MHz FROM GEETEE



SKY AT 34.5 MHz FROM 



REFERENCES

- Baars, J.W.M., Genzel, R., Pauliny-Toth, I.I.K., **Witzel**, A. 1977, *Astr. Astrophys.*, 61, 99.
- Berkhuijsen, E.M.** 1971, *Astr. Astrophys.*, 14, 359.
- Berkhuijsen, E.M., Haslam, C.G.T., Salter, C.J.** 1971, *Astron. Astrophys.*, 14, 252.
- Haslam, C.G.T., Salter, C.J., Stoffel, H., Wilson, W.E.** 1982, *Astron. Astrophys. Suppl. Ser.*, 47, 1.
- Jones, B.B., **Finlay**, E.A. 1974, *Aust. J. Phys.*, 27, 687.
- Large, M.I., Quigley, M.J.S., Haslam, C.G.T.** 1962, *Mon. Not. R. Astr. Soc.*, 124, 405.
- Milogradov-Turin, J., Smith, F.G.** 1973, *Mon. Not. R. Astr. Soc.*, 161, 269.
- Quigley, M.J.S., Haslam, C.G.T.** 1965, *Nature*, 208, 741.
- Sofue, Y., Reich, W., Reich, P.** 1988, NRO preprint no. 196.
- Shaver, P.A., Pierre, M. 1989, ESO preprint, No. 637.